DISSERTATION

THE ROLE OF PROLINE RICH 15 IN TROPHOBLAST CELL DEVELOPMENT

Submitted by

Katherine C. Gates

Department of Biomedical Sciences

In partial fulfillment of the requirements

For the Degree of Doctor of Philosophy

Colorado State University

Fort Collins, Colorado

Summer 2012

Doctoral Committee:

    Advisor: Russell V. Anthony

    Colin Clay
    Dawn L. Duval
    Thomas R. Hansen

ABSTRACT

THE ROLE OF PROLINE RICH 15 IN TROPHOBLAST CELL DEVELOPMENT

Maintenance of pregnancy in eutherian mammals requires a sophisticated and tightly regulated program of gene expression in order to develop a fully functional placenta. This transient organ mediates nutrient and gas exchange between the mother and fetus while protecting the fetus from the maternal immune system. Deviations from the normal regulation of gene expression during early pregnancy can lead to early embryonic loss as well as dysfunctional placentation, which can cause significant maternal and fetal morbidity and mortality. Proline rich 15 (PRR15) is a low molecular weight nuclear protein expressed by the trophoblast during early gestation in several mammalian species, including humans, mice, cattle, sheep, and horses. Immunohistochemistry revealed localization of PRR15 to the trophectoderm and extraembryonic endoderm of day 15 sheep conceptuses. In humans, PRR15 is localized in the nuclei of both first and second trimester trophoblast cells. Additional research has shown increased *PRR15* transcription in colorectal cancers with mutations in the adenomatous polyposis coli (Apc) protein, suggesting a link to the Wnt signaling pathway. *PRR15* mRNA concentrations increase when trophoblast cells, both sheep (oTR) and human (ACH-3P), are cultured on Matrigel, a basement membrane matrix. The expression profile in the sheep conceptus during pregnancy revealed a rise in *PRR15* mRNA concentrations during the period of conceptus elongation with a peak in expression at day 16 of gestation, followed by a decline to day 30 of gestation.

This peak coincides with a halt in elongation of the conceptus, and the initial period of apposition to the uterine luminal epithelium. Lentiviral-mediated knockdown of *PRR15* in ovine trophectoderm at the blastocyst stage led to demise of the embryo by day 15 of gestation. This provides compelling evidence that PRR15 is a critical factor during this precarious window of development when initial attachment and implantation begin.

The first aim of this research was to determine the effect of *PRR15* deficiency on trophoblast gene expression, as well as trophoblast proliferation and survival. The human first trimester trophoblast cell line, ACH-3P, was infected with control lentivirus (LL3.7) and lentivirus expressing a short hairpin (sh)RNA to target *PRR15* mRNA for degradation, resulting in a 68% decrease in *PRR15* mRNA ($p < 0.01$). Microarray analysis of these cell lines revealed differential expression of genes related to cancer, focal adhesion, and p53 signaling. We selected 21 genes for validation of mRNA levels by quantitative real-time RT-PCR, 18 (86%) of which gave results consistent with the microarray analysis, with similar direction and magnitude fold changes. This included significant up-regulation of *GDF15*, a cytokine increased in pregnancies with preeclampsia. *GDF15* mRNA concentrations were examined more extensively during early ovine gestation, which revealed that *GDF15* was low during peak *PRR15* expression, then increased significantly at day 30 when *PRR15* was nearly undetectable. Proliferation, as measured by cell metabolic activity and bromodeoxyuridine (BrdU) uptake, decreased in the PRR15-deficient cells, which was consistent with a decrease observed in cell cycle-related genes *CCND1* and

CDK6, and an increase in *CCNG2* and *CDKN1A* in the PRR15-deficient cells. *TNFSF10*, a tumor necrosis factor superfamily member known to induce apoptosis, and its receptor, *TNFRSF10b*, increased significantly in the PRR15-deficient cells, suggesting trophoblast cells may be more susceptible to apoptosis when depleted of PRR15. Assays for caspase activity and annexin V staining revealed an increased population of apoptotic cells when treated with shRNA to target PRR15. These results suggest that PRR15 is required for driving trophoblast proliferation and survival during early development of the placenta, functions that are critical to early embryonic survival and successful placentation.

The second experimental aim was to examine regions of the *PRR15* promoter that are necessary for regulating its expression in trophoblast cells and to identify the role of Wnt signaling in *PRR15* transcription. The 5'-flanking sequences from -824, -640, -424, -326, and -284 bp to +7 bp relative to the annotated transcription start site were amplified by PCR and ligated into the pGL3-Basic plasmid. These vectors were co-transfected into the first trimester human trophoblast cell line, ACH-3P, HT29 (human colorectal carcinoma), oTR, and BHK-21 (hamster kidney fibroblast) cells with a RSV-β-galactosidase vector control. In ACH-3P cells, transactivation of the luciferase reporter was maximal following transfections with the -326 construct (15.4 ± 4.8-fold). Significant promoter activity was absent in the -284, -424, and -640 constructs, but regained with the -824 construct (14.8 ± 5.8-fold). These results suggest that *cis*-acting elements within the proximal promoter of the *PRR15* gene are essential for expression in trophoblast cells, requiring the regions from -284 to -326 and -640

to -824. DNase I footprinting and electrophoretic mobility shift assays were performed to identify transcription factor binding sites within these regions. Due to the potential link to the Wnt signaling pathway, cells were treated with an inhibitor to GSK3β, the kinase responsible for phosphorylation and proteasomal degradation of β-catenin. Inhibition of GSK3β decreased *PRR15* mRNA concentrations and decreased transactivation of the luciferase reporter in all proximal promoter reporter constructs; this effect was mediated through β-catenin activity in the proximal 284 bases of the *PRR15* 5'-flanking region. Furthermore, trophoblast cell proliferation decreased after treatment with the GSK3β inhibitor. Electrophoretic mobility shift assays on the region from -98 to -68 revealed differential binding of nuclear proteins derived from ACH-3P cells grown in the presence or absence of the GSK3β inhibitor. These results reveal that canonical Wnt signaling inhibits the transcription of *PRR15*, mediated in part through the -98 to -68 region of the 5'-flanking region, and decreases proliferation in trophoblast cells. This indicates that suppression of Wnt signaling may be crucial during early trophectoderm outgrowth in order to allow significant transcriptional activation of *PRR15* and conceptus survival.

ACKNOWLEDGEMENTS

TABLE OF CONTENTS

LIST OF TABLES

LIST OF FIGURES

CHAPTER I – Introduction

Eutherian mammals have developed a unique system in which the placenta allows for prolonged intrauterine fetal growth and development. This transient yet vital organ develops from a single layer of cells on the outside of the early embryo, the trophectoderm. The placenta facilitates nutrient and waste exchange between the mother and fetus while protecting the allogeneic fetus from the maternal immune system. Though the morphology of this organ varies widely across species, these functions are conserved. The mature placenta represents an intimate and complex connection between cells of maternal and fetal origin. The development of this organ from a single layer of cells requires a tightly regulated program of gene expression from the differentiating trophectoderm. Deviations from this program during early placental development can lead to a variety of issues for both the mother and the developing embryo.

The most dramatic consequence of dysfunctional placental development is early embryonic loss due to failed implantation. This is a common issue in both human and animal reproduction. Increasing cases of early pregnancy loss and recurrent miscarriage cause substantial emotional hardship for couples trying to conceive. In our food animal species, early embryonic losses lead to significant costs for producers, threatening the viability of the animal agriculture industry. Though complete failures of implantation lead to embryonic loss, dysfunctional trophoblast development during early placentation may cause placental insufficiency which can lead to intrauterine growth restriction or preeclampsia. Some cases of intrauterine growth restriction and preeclampsia are attributed to

dysfunctional placentation during the first trimester; these pregnancy complications not only cause increased maternal and fetal morbidity and mortality, but also increase the risk of adult-onset diseases in these children. Placental insufficiency in agricultural species leads to increased fetal losses as well as decreased viability and growth of offspring, again increasing costs for producers. Enhancing our understanding of the regulation of implantation and early placental development will pave the way for therapeutic interventions in cases of placental insufficiency. Furthermore, increasing reproductive efficiency in our agricultural species will help to maintain an affordable and sustainable food supply in the face of a growing world population.

The focus of this research is the gene Proline rich 15 (PRR15), which appears to have a crucial function during early pregnancy. PRR15 is expressed by the trophectoderm of elongating sheep conceptuses, as well as first and second trimester human trophoblast cells. The mRNA and protein are well conserved among several mammals, suggesting a similar function across species. In the sheep, PRR15 expression increases during conceptus elongation, a period of rapid trophoblast outgrowth and proliferation. At the point of conceptus attachment, the mRNA concentration peaks and then diminishes while the trophoblast and endometrium begin to form intricate connections that will become functional placentomes. Its purpose during placental development is not known; however, deficiency of PRR15 in elongating sheep conceptuses leads to embryonic demise prior to conceptus attachment. The spatial and temporal pattern of expression and the dramatic consequence of PRR15 deficiency *in vivo*

2

suggest an essential function of PRR15 during early placental development. The aims of these experiments were two-fold. First, determine the effect of PRR15 deficiency on trophoblast gene expression and function in order to elucidate the role of PRR15 during normal placental development. Second, determine the transcription factors and signaling pathways that regulate transcription of PRR15 and lead to the strict window of expression during trophoblast elongation and attachment. Though focusing on a single gene may seem myopic, the demonstrated necessity for PRR15 during early embryonic growth suggests it plays a critical role in this developmental window. Understanding the upstream regulators of its transcription, as well as the downstream effects of its presence will shed light on pathways critical to early placental development.

CHAPTER II – Review of Literature

Placentation in the Human

Placental Dysfunction

Carrying a fetus to term requires an intimate connection between mother and fetus, which is mediated through the placenta. The period of implantation and early placental development is the most precarious time for the developing embryo. Only 50-60% of conceptions survive to twenty weeks of gestation; the majority of these early pregnancy losses are due to a failure of implantation.[1] Chromosomal abnormalities account for a portion of these spontaneous abortions, but leave a number of cases without an etiology.[2] Recurrent miscarriage, defined as three or more consecutive spontaneous miscarriages, affects 1-3% of women of reproductive age.[3] Risk factors for recurrent miscarriage include genetic and physiologic disorders that lead to deficient placental development.[4] The control of trophoblast invasion into maternal tissues is crucial for a successful pregnancy outcome. Excessive trophoblast invasion can lead to attachment of the placenta to the myometrium, termed placenta accreta, or to invasion into the uterine serosa and adjacent organs, termed placenta percreta.[5] Conversely, placental disorders such as preeclampsia and some cases of intrauterine growth restriction are attributed to insufficient trophoblast invasion.[6,7]

Preeclampsia is a complication in 4-8% of pregnancies in the United States, and up to 10% of pregnancies in the developing world.[8] The majority of cases occur in healthy nulliparous individuals, though mothers with diabetes,

chronic hypertension, or multi-fetal gestations are more likely to develop the disorder. It is a leading cause of maternal and perinatal morbidity and is associated with a 20-fold increase in perinatal mortality.[9] Up to 20% of maternal deaths in the United States are attributed to complications from preeclampsia.[10] Severe preeclampsia is often associated with intrauterine growth restriction (IUGR), which itself is a cause of significant perinatal morbidity and increases the likelihood for development of adult disease.[11] IUGR is the second leading cause of perinatal mortality and morbidity, affecting about 5% of all pregnancies.[12] The only known cure for preeclampsia is delivery of the placenta and fetus. Preterm birth (birth prior to 37 weeks gestation) accounts for more than two thirds of perinatal deaths.[13] Preterm delivery, often due to complications of preeclampsia, IUGR, or pregnancy-induced hypertension, costs the United States upwards of 26.2 billion dollars per year.[14] The rate of preeclampsia in the United States is increasing, possibly due to the rising incidence of predisposing causes such as chronic hypertension, obesity and diabetes.[15] Increasing use of assisted reproductive technologies (ART) such as *in vitro* fertilization leads to 2.7 times higher risk of preeclampsia.[16] Not only does preeclampsia increase maternal and prenatal morbidity and mortality, it is also an indicator of increased risk for future cardiovascular disease for the mother.[17] The growing rates of obesity and diabetes and the rising rate of ART call for advancing our understanding of these costly and significant diseases.

Preeclampsia is defined as the occurrence of hypertension and proteinuria during the second half of gestation. During normal placentation, trophoblast cells

invade the decidual segments of maternal spiral arteries, replacing maternal endothelium in the distal portions of the vessels, and extending into the myometrial segments.[18] The definitive cause of preeclampsia is unknown, though preeclamptic placentas at term are characterized by incomplete invasion of maternal spiral arteries by trophoblast cells. Though clinical diagnosis of preeclampsia does not occur until mid-gestation, most researchers believe the disorder originates with deranged or incomplete placentation during the first trimester.

Studying the pathogenesis of severe preeclampsia and intrauterine growth restriction presents three major challenges. First, the shallow trophoblast invasion characteristic of these disorders occurs during the first trimester, yet clinical signs are normally not apparent until after 20 weeks of gestation. Individuals destined to develop preeclampsia cannot be identified until after the critical period of trophoblast invasion and spiral artery remodeling. Identifying markers for predicting preeclampsia prior to the onset of clinical signs is the subject of much research.[19,20,21,22] Identifying growth restricted fetuses requires repeated measurements by ultrasound to determine the fetal growth curve, which is not performed in standard cases. The second major challenge is that spontaneous preeclampsia does not occur in other species, including nonhuman primates. Though growth restriction has been observed in a number of mammalian species, the mechanisms that underlie this phenotype likely vary as do placental structures across species. A number of animal models have been developed, but the capacity of these models to embody all of the changes of

human preeclampsia and IUGR is not likely, especially considering the distinctive architecture of the human placenta. Though many models demonstrate some of the key features of preeclampsia, no animal model can truly recapitulate the pathogenesis of this specifically human disease. The final challenge is the heterogeneity of these disorders, and the frequency with which they appear in conjunction with other pregnancy complications. IUGR occurs in 5-18% of pregnancies complicated by preeclampsia, and most frequently in association with early-onset disease.[23,24] Although women with obesity, diabetes, and multiple gestations are predisposed to develop preeclampsia, the majority of cases occur in healthy, nulliparous individuals. Pathologic changes specific to preeclampsia may be obscured by these complicating factors. Huppertz suggests that dysregulation of syncytiotrophoblast development leads to preeclampsia, while dysregulation of cytotrophoblast development leads to IUGR, and a combination of the two results from impaired early trophoblast development.[25] Clarifying the regulation of early trophoblast development may aid in our understanding of these disorders, and possibly reveal areas in which we can intervene clinically.

From Fertilization to Implantation

After fertilization, the trophectoderm is the first lineage to differentiate in the human embryo between the morula and blastocyst stage. The blastocyst, made up of the inner cell mass surrounded by a single layer of mononucleated trophoblast cells, hatches from the zona pellucida by day 6-7 post-conception and attaches to the uterine epithelium to initiate implantation.[26] The trophoblast

cells in contact with the endometrium proliferate and fuse to form the early syncytiotrophoblast, a multinucleated syncytium. By day 8 after conception, vacuoles form within the syncytiotrophoblast layer, which later expand and form lacunae. The lacunae are separated by columns of syncytiotrophoblast called trabeculae. Cytotrophoblast cells continue to proliferate, expand, and branch from the trabeculae, forming primary villi.[27] As early as day 12 post-conception, trophoblast cells erode maternal capillaries and release the first maternal blood cells into the lacunar space.[28] From 3-6 weeks of pregnancy, the placenta outweighs the fetus by more than five times and acts as a surrogate for various fetal organs. The fetus does not outgrow the placenta until after the first trimester as the fetal organs develop and begin to function.[29] During these initial weeks, maternal-fetal nutrient and gas exchange is at a minimum until a more dramatic remodeling of maternal vasculature occurs.

As pregnancy progresses, cytotrophoblast cells continue to proliferate in the expanding placenta. Anchoring villi are derived from the initial trabeculae and stretch across the entire trophoblast layer. Clusters of proliferative extravillous trophoblast cells form trophoblastic cell columns at the terminal ends of anchoring villi.[30,31,32,33] Spiral arterioles are plugged by clumps of extravillous trophoblast cells from 5-10 weeks of gestation, leading to a hypoxic state which promotes trophoblast proliferation.[34] From 11-14 weeks, the endovascular plugs open up, leading to a rapid increase in placental oxygen tension which triggers trophoblast differentiation.[35,36] A subpopulation of these cells differentiates into the invasive extravillous trophoblast. The type of invasion can be divided into two

categories: interstitial invasion, where trophoblast cells invade the entire endometrium and inner third of the myometrium, and endovascular invasion, where trophoblast cells invade maternal vasculature and replace maternal endothelium.[37] Endovascular trophoblast cells aid in the transformation of spiral arterioles from low flow, high resistance to high flow, low resistance vessels which support the growing fetus.

After the maternal vasculature has been remodeled, the lacunar spaces become the intervillous space. The intervillous space fills with maternal blood to bathe the syncytiotrophoblast layer, where nutrient and gas exchange occurs. The syncytiotrophoblast is also responsible for the production of hormones required for maintenance of pregnancy, such as human chorionic gonadotropin and progesterone. Maternal blood is separated from fetal blood by a layer of syncytiotrophoblast, the underlying regenerative cytotrophoblast, a basal lamina, connective tissue derived from the extraembryonic mesoderm, and the fetal endothelium.[28] The surface area for maternal-fetal exchange is maximized by multiple branching villi which protrude into the intervillous space, known as floating villi.[38] From the first trimester through the end of pregnancy, the placenta remains a dynamic and active organ. The dramatic architectural transformations, however, are by and large completed in the first trimester. The placenta grows in volume at a much slower rate than the fetus, which at birth outweighs the placenta by over seven times. The villous surface area per gram of placenta increases until term due to continuous growth and remodeling of the villous trees.[39] During the third trimester, the number of intermediate and terminal villi

increases, increasing the surface area available for maternal-fetal exchange.[40] Proper placental development during the first trimester is crucial for maintenance of pregnancy to term as well as fetal and maternal health.

Trophoblast Differentiation

All trophoblast cell subtypes arise from the trophectoderm that first differentiates in the developing embryo (Figure 1). Both the syncytiotrophoblast and the extravillous trophoblast cells are derived from a progenitor population of cytotrophoblast cells. The non-proliferative, multinucleated syncytiotrophoblast develops from the fusion of cytotrophoblast cells, and grows throughout gestation by continued fusion of the underlying cytotrophoblast layer. The syncytiotrophoblast is in direct contact with maternal blood, and is responsible for placental hormone production as well as maternal-fetal exchange and immune tolerance.[41] Extravillous trophoblast cells begin to invade the uterine stroma from the ends of anchoring villi. These cells exit the cell cycle and stop proliferating as they migrate away from the basal plate and into the maternal tissue.[42] They are responsible for the remarkable remodeling of uterine vasculature that allows increased blood flow to the growing fetus.
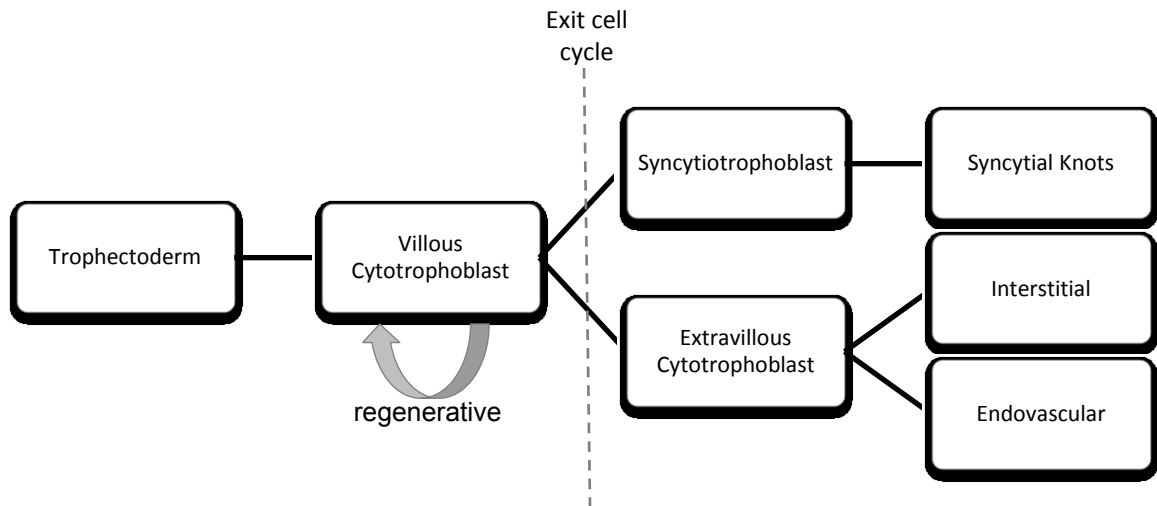
Figure II-1. Human trophoblast differentiation from trophectoderm.

Differentiation into these trophoblast subtypes is controlled by a variety of factors, including oxygen tension, growth factors, cytokines, cell-to-cell and cell-to-extracellular matrix interactions. From 8-10 weeks of gestation, oxygen tension in the placenta is low relative to endometrial levels as cytotrophoblast cell columns occlude spiral arteries. From 10-12 weeks, the spiral artery plugs open, causing a significant increase in placental partial pressure of oxygen.[43] Oxygen tension influences the expression of transcription factors such as glial cell missing factor 1 (GCM1) and Hash-2, which stimulate or inhibit, respectively, syncytial fusion.[44] These transcription factors and others initiate changes in gene expression required for trophoblast differentiation. Hypoxia inhibits trophoblast cell fusion, as assessed by staining for desmoplakin and E-cadherin, and differentiation, as measured by hCG secretion and hPL expression *in vitro*.[45] In BeWo cells, decreased cell fusion and differentiation due to hypoxia led to significant changes in protein expression.[46]

Two hypotheses exist in regards to the effect of hypoxia on differentiation into the invasive extravillous trophoblast. A large body of evidence suggests that

hypoxia promotes trophoblast proliferation, both *in vivo*, measured by mitotic index, and *in vitro* in villous explants and first trimester trophoblast cells. A smaller body of research demonstrates increased trophoblast invasion in a low oxygen environment, suggesting differentiation into the extravillous subtype.[47] The differences observed may be attributed to a range of oxygen concentrations in hypoxic conditions as well as different cellular models, such as villous explants and transformed first trimester trophoblast. The interpretation of villous explant outgrowth has been attributed to both proliferation and invasion, giving conflicting results in these types of experiments.[48,49] Immunostaining with proteins specific for proliferation or for extravillous trophoblast cells could help clarify the effect of hypoxia on this differentiation pathway.

One of the initial steps toward syncytialization is the redistribution of phosphatidylserine from the inner to the outer leaflet of the plasma membrane.[50] Treating JAR cells with monoclonal antibodies against phosphatidylserine inhibited cell fusion, suggesting that externalization of these molecules is required for cell fusion.[51] The initiation of this flip may be regulated by initiator caspases, proteases involved in apoptosis. Blocking caspase-8 activity using antisense oligonucleotides and peptide inhibitors decreased trophoblast fusion in villous explants.[52] Expression of fusogenic proteins such as syncytin-1 (HERV-W), syncytin-2 (HERV-FRD), connexin 43,[53] cadherin 11,[54] and CD98[55] is also required for trophoblast cell fusion. Galectin-1 also stimulated BeWo and villous trophoblast cell fusion.[56] The mechanism for determining which cells in the cytotrophoblast later will fuse into the growing syncytiotrophoblast and the

regulation thereof is not clear. It is evident that expression of specific fusogenic proteins and exit from the cell cycle are necessary for syncytialization. Syncytin-1 expression is decreased in placentas and cultured trophoblasts from pregnancies complicated by preeclampsia and IUGR; in addition, these trophoblasts exhibit impaired cell fusion, increased apoptosis, and decreased expression of hCG.[57] Vargas et al. observed a correlation between decreased expression of syncytin-1 and syncytin-2 and the severity of preeclampsia symptoms, with syncytin-2 being more severely impaired in preeclampsia.[58] It is clear that activation of a specific repertoire of genes is required for the process of syncytialization.

Differentiation into the invasive extravillous trophoblast requires increased expression of matrix metalloproteinases (MMPs) in order to degrade the maternal extracellular matrix. Increased expression of MMPs is commonly used as an indicator of differentiation into extravillous trophoblast cells. The precise regulation of extravillous trophoblast invasion is critical for successful placentation. Insufficient invasion can lead to placental oxidative stress and decreased nutrient exchange to the fetus, while unchecked invasion can lead to placenta accreta or choriocarcinoma. Cytokines expressed by placental stromal cells, trophoblast cells, and decidual cells influence trophoblast invasion. Treatment with hepatocyte growth factor (HGF) increased trophoblast invasion *in vitro*, while knocking out HGF in the mouse led to embryo demise due to impaired labyrinth development.[59,60] Leukemia inhibitory factor (LIF) , originating primarily from the endometrium, increases trophoblast invasion by enhancing trophoblast adhesion to the extracellular matrix, though it does not affect MMP

expression.[61] Treatment of extravillous trophoblast cells with human placental growth hormone stimulated invasiveness.[62] Treatment with forskolin and epidermal growth factor (EGF) significantly increased invasiveness and secretion of matrix metalloproteinase (MMP)-2 and MMP-9 in primary first-trimester trophoblast cells.[63] On the other hand, treatment of trophoblast cells with transforming growth factor beta (TGFβ1) promotes intercellular adhesion while decreasing invasion: expression of MMP-9 decreased with TGFβ1 treatment while E-cadherin and β-catenin were up-regulated.[64,65] Inhibitor of DNA binding proteins (Id)-2 is down-regulated as trophoblast cells differentiate into the invasive subtype; cells that constitutively express Id-2 retain characteristics of undifferentiated cells, such as cyclin B expression.[66] The regulation of trophoblast differentiation and invasion is clearly multifactorial and requires a complex repertoire of genes expressed in an ordered timeframe.

Preeclampsia is characterized by shallow cytotrophoblast invasion, and has been associated with an increased population of immature, more proliferative trophoblast cells.[67] The lack of invasion is correlated with impaired differentiation and decreased expression of markers of the invasive phenotype.[68] As cytotrophoblasts differentiate into the invasive extravillous trophoblast, the expression of proliferation markers decreases.[69,70] Low molecular weight heparin, used clinically for the prevention of pregnancy loss, enhances MMP expression and increases invasiveness of trophoblast cells.[71] In addition, heparin and IGF-II decreased trophoblast apoptosis in primary first-trimester trophoblast cells and may contribute to trophoblast survival during this timeframe.[72] Determining

additional factors and regulatory networks involved in trophoblast differentiation could aid in the treatment of placental disorders such as preeclampsia, IUGR, and recurrent miscarriage.

In vitro Models of Trophoblast Function

Manipulation of placental gene function *in vivo* is problematic, particularly in humans. Though methods for *in vivo* trophoblast-specific gene knockdown have been developed for rodents as well as ruminants, these types of experiments are not feasible in humans.[73,74,75,76] Various approaches to circumvent these issues while still providing data relevant to the true physiologic state have been developed. Methods relevant to the first trimester of human pregnancy include the use of placental villous explants, chorionic villus samples, primary trophoblast cells and immortalized trophoblast cell lines.

Founds et al. used chorionic villus (CV) samples to evaluate gene expression in normal and preeclamptic pregnancies by microarray analysis.[77,78] Forty percent of the differentially expressed genes were identified previously in susceptibility loci for preeclampsia.[79] However, of the 36 genes found to be differentially expressed, none of them matched the eight differentially expressed genes identified in a nearly identical study of preeclamptic versus normal CV samples.[80] This may be due to very small sample sizes in both studies, and the heterogeneity of the sample populations. Using CV samples to study first trimester trophoblast gene expression has several major drawbacks. First, CV sampling is not without risk, with a 0.33% rate of pregnancy loss, and is only indicated for women of advanced maternal age (>35 years).[81] Because of the

risks, obtaining the required samples for an un-biased analysis is challenging and time-consuming. Second, there is a very limited amount of tissue obtained from the procedure, the majority of which is used for prenatal genetic screening of the fetus. Third, the tissue obtained from a CV sample is a mixture of cell types, including mesenchymal and trophoblast cells. A recent study suggests the cells obtained from CV samples represent the villus mesenchymal core originating from the inner cell mass rather than from the trophectoderm.[82] Thus, gene and protein expression in CV samples may not be representative of trophoblast, and may simply reveal changes in mesenchymal cell expression. The limited sample size of this study warrants further testing of the embryonic origin of CV samples, but it illuminates an essential point about the heterogeneous cellular nature of the placenta. Although relevant to placental growth and development, fetal mesenchymal cells do not play a direct role in remodeling the maternal vasculature as do trophoblast cells.

The *in vitro* models that likely best approach the *in vivo* condition are placental villous explants and primary trophoblast cells. First-trimester placental explants are obtained from elective pregnancy terminations. The cellular architecture of the villus is maintained with the presence of fetal stromal, endothelial, and immune cells in addition to villous trophoblast cells. When cultured on collagen I or Matrigel, an extracellular matrix, explants can be used to study the effects of oxygen tension and growth factors on trophoblast proliferation and invasive capacity.[83,84] Hypoxic conditions which mimic the low blood flow prior to 10 weeks of gestation promote trophoblast proliferation in

villous explants.[85] There is some evidence for successful manipulation of gene expression in placental explants by delivery of siRNA using electroporation with a nucleofector.[86] Though they may closely mimic villous development *in vivo*, there are several disadvantages to explant culture. The observation of villous outgrowth on an extracellular matrix has been labeled as both invasion and proliferation, leading to mixed interpretations of these types of experiments. Differences in culture media, matrices or substrates, oxygen tension, and methods of collection make it difficult to accurately compare one experiment to the next. In addition, a number of placentas will not produce outgrowths[87]; these placentas may have spontaneously aborted or may have developed placental insufficiency if allowed to mature *in vivo*. The lack of early biomarkers for preeclampsia and intrauterine growth restriction makes differentiating normal from pathologic samples nearly impossible in the first trimester.

Primary trophoblast cells can be isolated from first-trimester placentas and grown in culture for a limited amount of time due to replicative senescence. When grown on plastic, these cells rapidly exit the cell cycle, syncytialize, and degenerate within 5 days,[88,89] whereas culturing on a basement membrane matrix stimulates differentiation into invasive extravillous trophoblast cells.[90] High interplacental variability and diverse isolation and culture protocols lead to wide-ranging and sometimes conflicting results from experiments with these cells.[91] Oxygen tension clearly plays a role in gene expression and behavior of primary trophoblast cells, just as in explants. While culturing primary trophoblasts in various levels of oxygenation, Oh *et al.* found that none of the conditions tested

mimicked the changes in gene expression observed in placentas from growth-restricted pregnancies, suggesting significant weaknesses in this particular model system for studying intrauterine growth restriction.[92] The methods of isolation, culture medium, and substrate have a profound impact on the differentiation of these cells in culture.[93] The principal drawbacks of both primary cells and explants are the limited time they can be cultured, the diversity of culturing and experimental conditions, and the difficulty of manipulating gene expression using RNA interference.

The use of trophoblast cell lines *in vitro* provides an alternative that can be easily manipulated and reproduced. Several trophoblast cell lines have been developed using various techniques; those commonly referenced are shown in Table 1.[94] Cytokeratin-7 (CK-7) is commonly associated with trophoblast-specific expression, and is not normally expressed in other placental or uterine cells.[95,96] HTR-8/SVneo cells are a first trimester trophoblast transformed with SV40 large T antigen using electroporation; these cells stain positive for cytokeratin and express human chorionic gonadotropin (hCG).[97] They have frequently been used for *in vitro* invasion assays, and are thought to represent extravillous trophoblast cells, though some debate this supposition. Though they express CK-7, there are mixed results as far as their expression of human leukocyte antigen G (HLA-G), discussed in more detail below. SGHPL-4 (MC4) cells were developed by transfecting primary first trimester trophoblast cells with SV40 large T antigen using poly-L-ornithine. Trophoblast origin was verified by the expression of placental lactogen, pregnancy specific protein, and hCG.[98] ACH-3P cells

represent a fusion of primary first trimester trophoblasts (12 weeks) with a human choriocarcinoma cell line (AC1-1), which is a mutant derivate of the JEG-3 choriocarcinoma.[99] ACH-3P cells have a mixed population of human leukocyte antigen G (HLA-G) negative (60%) and HLA-G positive (40%) cells, which can be separated by flow cytometry; the HLA-G negative cells represent cytotrophoblast-like cells, while the HLA-G positive cells represent a population of extravillous trophoblast-like cells.[100] Swan-71 cells are a primary first trimester trophoblast infected with human telomerase reverse transcriptase (hTERT); they express cytokeratin-7, vimentin, and secrete low levels of hCG.[101] There are mixed results as far as their positivity for HLA-G expression. HLA-G is a marker specific for extravillous trophoblast cells, often used for sorting these cells from a mixed population.[102] Several antibodies are available for HLA-G, and some may cross-react with additional members of HLA class I molecules, such as HLA-A and HLA-B which are ubiquitously expressed.[103] When the specificity of HLA-G antibodies was validated, it appears both hTR-8 and Swan-71 cells do not express HLA-G, and thus may not be representative of extravillous trophoblast.[103] TEV-1 cells are primary first-trimester cells that were transformed by lentiviral infection with human papillomavirus type 16 (HPV16) E6/E7 genes. They express cytokeratin-7 and secrete MMP-2 and MMP-9.[104] BeWo cells were established from a cerebral metastasis of a human choriocarcinoma that was maintained in a hamster cheek pouch until Pattillo and Gey developed a method for sustaining these cells in culture.[105] HLA-G transcripts are present in BeWo cells, although the protein was only detected in JEG cells, which represent a later

passage of this choriocarcinoma.[106,107] An increase in cyclic AMP caused by treatment with forskolin causes BeWo cells to syncytialize *in vitro*; these cells have become a valuable and widely used model for the regulation of syncytialization.[108]

Table II-1. Selection of human trophoblast cell lines.
Blank cells indicate that data is not available. CK-7 = cytokeratin-7, hCG = human chorionic gonadotropin, HLA-G = human leukocyte antigen G.

Name	Markers			Reference
	CK-7	hCG	HLA-G	
hTR-8 / SVneo	+	+	+/-	Graham et al. 1993 (97)
SGHPL-4	-	+		Choy & Manyonda 1998 (98)
ACH-3P	+	+	+/-	Hiden et al. 2007 (100)
Swan-71	+	+	+/-	Straszewski-Chavez et al. 2009 (101)
TEV-1	+		+	Feng et al. 2005 (104)
BeWo	+	+	-	Pattillo & Gey 1968 (105)

The ability of any of these cell lines to recapitulate the *in vivo* condition has been called into question. A microarray analysis comparing several choriocarcinoma and SV40 large T antigen-transformed cells to primary villous and extravillous cytotrophoblasts revealed distinct gene expression profiles for the different cell types.[109] In this comparison, the authors plated the extravillous cytotrophoblasts on a basement membrane matrix (Matrigel), while all other cell types were grown on plastic culture dishes. These culture conditions alone could cause a significant alteration of gene expression in any cell type, as evidence demonstrates that interaction with an extracellular matrix induces both phenotypic and gene expression changes in trophoblast cells.[110,111,112] Novakovic *et al*. showed that DNA methylation increased in immortalized cell lines as compared to primary trophoblast cells, which correlated with decreased global gene expression after transformation.[113] Unfortunately, culture substrates varied

with each cell type, which could confound any resulting changes in methylation status and gene expression. These studies demonstrate the difficulty of interpreting results of experiments with explants and trophoblast cells, with such a wide variety of techniques and cell lines available. Attempts have been made to isolate human trophoblast stem cells, with some recent success.[114] The utility of these cells in culture and the similarity of their behavior to primary cells remain to be seen.

In spite of many recent advances in trophoblast culture systems, every *in vitro* model lacks the capacity to fully mimic the complex interplay among the array of cell types interacting *in vivo*.[115] Careful scrutiny of *in vitro* studies is necessary in order to decipher the changes most relevant to the true condition. Ideally, phenotypes observed in trophoblast cell lines would be validated in primary cells; however, restricted access to these cells limits their availability for study. The combination of animal models, cell culture experiments in immortalized and primary cells, and the occasional genetic mutation identified in a population will bring us closer to understanding this complex and critical period of development.

Our current knowledge of human placental development is a result of data from sampling actual pregnancies to experiments on trophoblast cells *in vitro* to a plethora of animal models. Animal models are a valuable tool for assessing gene function *in vivo*. When it comes to placental development, understanding the similarities and differences between the model of choice and the human placenta are critical to interpreting resulting data. This transient yet essential organ

exhibits surprising diversity across all eutherian mammals. Rodents are the most commonly used model for research purposes due to the low cost of maintenance and the relative ease of genetic manipulations. As in the human placenta, the separation between maternal and fetal blood is described as hemochorial with trophoblast cells in direct contact with maternal blood.[116] The disadvantages are that they are a litter-bearing species, they are too small to catheterize for repeated sampling, fetal growth is not complete until after birth, and implantation occurs within hours after fertilization.[117,118] Certain non-human primates exhibit placentation very similar to humans, but the cost of maintenance and ethical concerns limit their use in research. Ruminants provide a larger and more easily maintained animal model in which catheters can be placed for repeated sampling during pregnancy, allowing for a more comprehensive analysis of placental and fetal physiology.[119] Though on gross examination the ruminant placenta may appear very different from the human, on a cellular level it exhibits many similarities.

Placentation in the Sheep

Embryonic Loss and Placental Dysfunction

Just as in humans, early pregnancy in the sheep is a period of significant embryonic loss. In the food animal industry, reproductive efficiency is critical to maintaining viability and profitability. Over the past 30 years, pregnancy rates have been decreasing up to 1% per year, particularly as producers select for qualities such as increased milk production in dairy cattle rather than reproductive traits.[120,121] These reproductive inefficiencies cost producers

upwards of $1 billion annually in the United States alone.[122] In cattle, early embryonic mortality, prior to day 20 of gestation, accounts for 75-80 percent of all embryonic and fetal losses.[123] Losses from days 8 to 16 range from 24% to over 30%, and up to 45% prior to day 35 of gestation.[124,125,126,127] Early embryonic losses in sheep are estimated at 17-30%, with most losses occurring prior to day 18 of gestation.[128,129,130] The vast majority, up to 80%, of these embryonic losses are attributed to aberrant placentation.[131] A "critical period" was identified in cattle from day 15 to 17 of gestation during which the majority of embryonic losses occur.[132] This coincides with the period where maternal recognition of pregnancy is required in order to prevent luteolysis, as well as the period of rapid conceptus outgrowth prior to attachment to the endometrium. In ruminants, the trophoblast produces interferon (IFN)-т which prevents the production of prostaglandin $F_{2\alpha}$ and allows for continued secretion of progesterone from the corpus luteum during pregnancy.[133] Maintenance of pregnancy and successful implantation require a continuous reciprocal interaction between the conceptus and endometrium.

In addition to significant embryonic losses, dysfunctional placentation is also observed in domestic ruminants, resulting in intrauterine growth restriction. IUGR is a significant concern in animal agriculture, and can have both genetic and environmental origins. Environmental effects include multi-fetal gestations, maternal over- or under-nutrition, and thermal stress. Consequences of IUGR include reduced meat quality, cardiovascular disease, reduced growth rates, hormonal imbalances, metabolic disorders, and increased perinatal morbidity and mortality.[134] In addition to the significance of IUGR to the food animal industry,

sheep have been widely used as a model for human IUGR; their size allows for repeated sampling during pregnancy to measure placental oxygen and nutrient transfer.[135,136] Though IUGR can have many etiologies, placental insufficiency is a frequent cause and the one most commonly studied.[137] Furthering our understanding of early implantation and placentation in the sheep will not only illuminate analogous pathways in the human, but may also shed light on how to improve reproductive efficiency and profitability of animal agriculture.

From Fertilization to Implantation

Placentas may be classified by the distribution of chorionic villi and by the layers separating the maternal and fetal blood supply. In ruminants, the placenta is cotyledonary and made up of discrete attachments called placentomes, with a fetal cotyledon and a maternal caruncle. The attachment is classified as syndesmochorial because the chorionic epithelium is intermittently exposed to maternal stroma when the endometrial epithelium transiently erodes.[116] Wooding suggests a more accurate designation of "synepitheliochorial" to emphasize the role of cell fusion in the formation of a maternal-fetal hybrid layer containing binucleate cells fused to endometrial epithelial cells.[138] Contrast this with the human placenta which is zonary, indicating a single area for maternal-fetal exchange, and hemochorial, meaning the chorionic epithelium is in direct contact with maternal blood.[116] Despite these gross phenotypic differences between the two species, the trophoblast cells themselves exhibit many similarities.

The sheep blastocyst hatches from the zona pellucida around day 7-8 after fertilization and begins a period of dramatic elongation prior to attaching to

the endometrium around day 16. Binucleate cells, also known as trophoblast giant cells, first appear on day 14;[139] these are thought to result from mitotic polyploidy, or consecutive nuclear divisions without cytokinesis.[138] By day 16, these cells represent nearly one fifth of the population of trophoblast cells.[140] Over the next week, binucleate cells migrate and fuse with uterine epithelial cells to form fetomaternal hybrid trinucleate cells in syncytial plaques which cover the uterine caruncles at day 24.[138] Binucleate cells are responsible for the synthesis and secretion of hormones into maternal circulation, including chorionic somatomammotropin hormone 1 (CSH-1 or placental lactogen) and progesterone.[141] The process of elongation requires trophoblast cell proliferation, growth, and cytoskeletal remodeling.[141,142] In porcine conceptuses, which have similar trophectoderm outgrowth prior to attachment, expression of Ki67 during the elongation phase indicated that cell division was active within the trophectoderm.[143] Clearly significant trophoblast proliferation is required for this rapid and dramatic outgrowth prior to implantation.

In order for initial conceptus adhesion to occur on day 16, the uterine luminal epithelium must be receptive to this interaction. This requires specific changes in gene expression and expression of cell surface proteins. Down-regulation of progesterone receptor in the luminal epithelium is associated with decreased expression of MUC1 and coincides with initial conceptus adhesion.[144] This large transmembrane mucin glycoprotein may block access of integrin receptors on the conceptus to their ligands on the luminal epithelium.[145] Integrin receptors and their ligands, such as osteopontin, are expressed by both the

luminal epithelium and trophoblast during the peri-implantation period, and have been shown to play a critical role during this interaction in several other species.[146] Glycosylated cell adhesion molecule 1 (GlyCAM-1) expression increases in the luminal epithelium on day 15, and is abundantly expressed at day 17 and 19, as well as in the trophoblast from days 13-19; this timeframe of expression suggests it may be involved in conceptus-endometrial interactions during initial adhesion.[146] In addition to adhesion molecules, growth factors and cytokines expressed by both the conceptus and endometrium are required for successful implantation in the sheep, just as in other species. Insulin-like growth factor I (IGF-I), epithelial growth factor, transforming growth factor (TGF) 1, 2 and 3, IL-6 and granulocyte-macrophage colony-stimulating factor (GM-CSF) expression has been demonstrated in the peri-implantation ovine conceptus and endometrium, though their specific functions have yet to be explained.[147] The potential roles of specific cytokines and growth factors in early pregnancy can be inferred from the expression patterns of these proteins *in vivo*. Fibroblast growth factor (FGF) 2 is expressed by ovine endometrium and conceptus during early pregnancy; conceptuses at days 14-19 express the receptors FGFR 1, 2, and 3, which suggests a possible function for FGF signaling during initial conceptus attachment.[148] FGF2 is involved in up-regulation of IFN-т transcription in bovine trophoblast cells, and is likely required for maternal recognition of pregnancy.[149] Properly timed signaling between the conceptus and endometrium is critical during this initial phase of adhesion and implantation.

Though ruminant placentas do not have a continuous syncytiotrophoblast layer in direct contact with maternal blood as in the human placenta, they do exhibit cell fusion during the formation of multinucleated syncytial plaques. In sheep, trinucleate cells making up syncytial plaques completely replace the uterine epithelium within the placentomes.[150] Like the syncytiotrophoblast of the human, post-mitotic binucleate cells are responsible for the synthesis and secretion of a number of hormones into maternal circulation, including placental lactogen, prolactin-related protein (PRP), pregnancy-associated glycoprotein (PAG), and C-type natriuretic peptide.[151,152] The function of these placental hormones in pregnancy is not well understood. Placental lactogen may stimulate fetal growth, modify maternal metabolism, stimulate lactogenesis, and/or stimulate placental angiogenesis.[153,154] Both ruminant BNCs and human cytotrophoblasts which fuse into the syncytiotrophoblast differentiate and exit the cell cycle while undergoing a significant change in the repertoire of expressed proteins; this requires specialized regulation of gene transcription in these cells. The specific mechanism of how a single trophoblast cell is selected for differentiation into a binucleate cell is not clear. Syncytial plaques undergo constant demise and renewal throughout gestation,[155] just as observed in the human syncytiotrophoblast. The BNC lifespan is likely controlled by apoptotic factors whose activities determine each cell's fate. Apoptotic pathways, discussed in more detail below, appear to play an important role in both human and ruminant placentation.

Additional similarities between human and sheep placentas exist in the factors which regulate trophoblast cell fusion. Evidence for the presence of endogenous retrovirus envelope elements in sheep and cattle was recently published. In cattle, endogenous retrovirus element-like transcript A (ERVE-A) has a similar sequence to human syncytin-1 and was specifically expressed in binucleate cells from day 20 increasing to day 70 of gestation.[156] Whether this transcript is translated into a protein with a role in trophoblast fusion remains to be seen. The endogenous Jaagsiekte sheep retrovirus envelope gene (enJSRVs) is expressed in the trophectoderm of the elongating ovine conceptus from day 12 of gestation. *In vivo* knockdown of the protein inhibited binucleate cell differentiation and slowed trophectoderm outgrowth.[157] Though BNCs are not a result of cell fusion[158], they fuse to the uterine luminal epithelium to form a syncytium. These studies suggest a similarity in the function of endogenous retroviruses during fusion of both human and ovine trophoblast cells.

In vivo loss- and gain-of-function studies as well as furthering our understanding of normal gene expression and regulation during the peri-implantation period can help to improve pregnancy rates in domestic ruminants as well as other species. As in the human, developing *in vitro* models for ruminant placental development is the topic of much research, given the limitations of *in vivo* studies. A selection of trophoblast cell lines established with varying methods is discussed below.

In vitro models of ruminant trophoblast

Ruminant-specific trophoblast cell lines are a relatively recent development in the study of placental function in these species. Prior to this, studying trophoblast development specific to cattle and sheep was limited to *in vivo* analysis or the use of trophoblast cells from other species. Altering placental gene expression *in vivo* has recently been reported by delivering morpholino oligonucleotides and lentiviruses to developing conceptuses.[159,75] These types of experiments will provide substantial insight into placental development. However, trophoblast cell lines allow for a more rapid and less expensive approach to studying transcriptional regulation and trophoblast differentiation, with more readily available methods for modifying gene expression.

Primary culture of bovine and ovine trophectoderm has been reported historically in the literature,[160,161,162,163] but cell lines capable of continuous culture are a more contemporary development. Origins and features of cell lines developed from ruminant trophectoderm and placenta are shown in Table I-2. CT-1 cells represent outgrowths of gestational day 10 to 11 bovine hatched blastocysts.[164] These cells have been used extensively to study the transcriptional regulation of IFN-т,[165,166,167] demonstrating the utility of ruminant-specific cell lines for increasing our understanding of biological function. BT-1 cells were developed from day 8 bovine blastocysts cultured on collagen, eliminating the need for a feeder cell layer as in the CT-1 cells.[168] These cells form BNCs in culture and express PL.[169] A custom cDNA microarray comparing BT-1 gene expression to *in vivo*-derived trophoblast cells showed more than one

third of the genes examined were differentially regulated, though trophoblast-specific genes such as IFN-т, PL, PAGs, and PRPs remained relatively constant.[170] As with any cell line cultured over time, one must use caution when interpreting the results as increasing time in culture can modify gene expression. Most recently, Bovine F3 cells were developed from cotyledons at 5 months of gestation, with trophoblast cells isolated by trypsinization and centrifugation over a Percoll gradient.[171] When treated with epidermal growth factor (EGF), proliferation and migration of F3 cells increased significantly, along with stimulating MMP-9 expression and activity.[172] EGF also promotes survival and reduces apoptosis in primary human cytotrophoblast[173] and increases outgrowth of mouse trophoblast cells in vitro[174], suggesting a similar function of this growth factor in multiple trophoblast types. F3 cells were recently used to develop a three-dimensional spheroid culture system, which may better mimic *in vivo* properties than a cell monolayer.[175]

Table II-2. Ruminant trophoblast cell lines.
PL = placental lactogen or chorionic somatomammotropin, IFN-т = interferon tau, IVF = *in vitro* fertilized

Name	Origin	Features	Reference
CT-1	d10-11 IVF bovine blastocysts plated on fibroblast feeder layer	IFN-т mRNA & protein	Talbot et al. 2000 (164)
BT-1	outgrowths from d8 IVF bovine blastocysts plated on collagen	IFN-т, PL mRNA & protein; cytokeratin; some BNCs	Shimada et al. 2001 (168)
F3	bovine cotyledon at 5 months gestation	PL only in early passages; cytokeratin later	Hambruch et al. 2010 (171)
oTr1, oTrF	d15 ovine conceptus plated on plastic (1) and collagen (F)		Farmer et al. 2008 (176)
oTR	d15 ovine conceptus		Anthony et al. 2010 (76)

In the sheep, oTr1 and oTrF cells were developed from plating elongating day 15 conceptuses on plastic and collagen-coated dishes, respectively.[176] Both

oTr1 and the bovine CT-1 cells responded to FGF2 or FGF10 treatment by increasing migration.[177] The analogous response of these two trophoblast cell lines derived from different species by different methods suggests a consistent phenotype, which supports their use for further studies on the regulation of trophoblast function. Our laboratory developed several lines of oTR cells from d15 conceptuses plated on plastic.[77] One difficulty with the oTR cells is that the magnitude of expression of specific genes is altered from what is observed in conceptuses collected from the same day of gestation. The cells seem to differentiate rapidly when cultured on plastic; culturing on a substrate such as collagen or a basement membrane matrix may bring the transcriptome closer to that observed *in vivo*. As with human trophoblast cells, oTR cells undergo a phenotypic change that corresponds to changes in gene expression when cultured on a basement membrane matrix. oTR cells aggregate and appear to invade when cultured on Matrigel, similar to what is observed in ACH-3P cells, primary first trimester human cytotrophoblast, and mouse trophoblast stem cells.[77,178,113] Though placentation in each of these species is quite distinct, the trophoblast cells appear to respond and behave very similarly in culture, strengthening the case for using them as a model. Identifying appropriate markers for ruminant uninucleate trophoblast and binucleate cells, as well as ideal culture media and substrates will help to provide a standardized system from which researchers can collect data and compare results. Reliable cell culture systems will allow for transfections, treatment with specific pathway inhibitors, and modification of gene expression using RNA interference; these

tools will help illuminate the pathways regulating trophoblast development during early pregnancy.

Ruminants, specifically sheep, provide a valuable model for placental development. Furthering our understanding of early ovine placentation may offer tools to help to improve reproductive efficiency in our food animal species. Moreover, it will provide considerable insight into analogous pathways of human pregnancy in a model system that can be manipulated and assessed during pregnancy *in vivo*. Though significant morphological differences exist between ruminant and human placentas, we still have much to learn about the particular pathways regulating trophoblast proliferation and differentiation during early implantation in both species. These pathways are likely widely conserved across eutherian mammals, making the sheep a useful model for this particular subject. Disturbances in trophoblast proliferation, survival, and differentiation cause significant morbidity and mortality in humans, as well as increased production costs in food animal species. Advancing our understanding of the genes and signals that are critical during this period will have a substantial impact on maternal and fetal health and the agricultural industry.

Apoptosis in the Placenta

Cell turnover and renewal is a necessary process in most tissues; the placenta is no exception. Apoptosis, or programmed cell death, plays an important role in placental development as the syncytiotrophoblast layer undergoes continual shedding and renewal, and cytotrophoblast cells invade and signal to maternal cells. Apoptosis is initiated via two potential pathways:

extrinsic or intrinsic. The extrinsic or death receptor pathway is mediated by members of the tumor necrosis factor death receptor family, including Fas (CD95), TNF-R1 (CD120a), and TNF-related apoptosis inducing ligand receptors 1 and 2 (TRAIL-R1, TRAIL-R2), while the intrinsic or mitochondrial pathway is initiated by cellular stresses which activate the mitochondrial pathway. Cysteine proteases, or caspases, are the effectors of apoptosis in both pathways; they are cleaved from inactive pro-caspases and activated upon initiation of programmed cell death. Caspase-8, an "initiator" caspase, is exclusive to the extrinsic pathway, but both pathways converge on the activation of caspase-3 and caspase-7, the "executioner" caspases.[179]

Controversy exists regarding the localization and quantity of apoptotic cells in the placenta throughout gestation due to the varied methods of visualizing and quantifying apoptosis. When measured by terminal deoxynucleotidyl transferase-mediated deoxyuridine triphosphate marker nick end-labeling (TUNEL), apoptosis appears to increase from the first to the third trimester.[180] When trophoblast apoptosis was assessed using the M30 antibody, which detects cleaved cytokeratin 18, an early event in apoptosis, they observed a significant decrease in apoptosis from first to second and third trimesters and a concomitant increase in Bcl2 expression, an anti-apoptotic protein.[181] These conflicting results may be explained by recent evidence suggesting that early stages of apoptosis are evident in the process of trophoblast fusion.

When differentiating into syncytiotrophoblast, cytotrophoblast cells undergo changes commonly associated with apoptosis, including externalization

33

of phosphatidylserine (PS), exit from the cell cycle, and rearrangement of cytoskeletal components.[182] Initially, it was proposed that cytotrophoblast cells begin the apoptotic cascade prior to syncytial fusion, but continuation is inhibited by anti-apoptotic proteins such as Bcl-2; then the apoptotic cascade is completed in the syncytium with the formation and shedding of syncytial knots into maternal circulation.[183] The mechanism of trophoblast apoptosis and its relationship to trophoblast fusion is widely debated. In BeWo cells, it appears that PS efflux can occur via a PKA-dependent pathway related to differentiation or a caspase-dependent pathway related to apoptosis. The authors of this study suggest that the PS flip in cytotrophoblast cells is independent of caspase activation and apoptosis.[184] Cleavage of caspase-8 was observed in a small number of first trimester villous cytotrophoblasts, but no signs of apoptosis were observed in the nuclei. Co-staining of cleaved caspase-8 with Ki-67 revealed that caspase-8 was only active in cells that had left the cell cycle, suggesting it may be involved in trophoblast fusion.[185] However, inhibiting caspase activity did not block syncytialization of BeWo cells or explant cultures, suggesting caspase activity is not required for trophoblast fusion.[186] Another recent study indicates that syncytialization of BeWo cells by treatment with cAMP is mediated in part by increased FasL expression and activation of caspase-3.[187] This also suggests a link between apoptosis and trophoblast fusion.

Mounting evidence suggests that apoptosis is increased in placentas from pregnancies complicated by preeclampsia and IUGR. Heazell et al. demonstrated increased apoptosis and decreased proliferation in term IUGR

placentas.[188] This concurred with an earlier study by Smith *et al*., although another group found no difference in proliferation or apoptosis in idiopathic IUGR placentas.[189,190] A number of studies have demonstrated increased trophoblast apoptosis in pregnancies complicated by preeclampsia.[191,192,193] In preeclamptic placentas, apoptosis and the number of syncytial knots was significantly increased, while FasL expression was significantly less; no difference was observed in trophoblast proliferation between groups.[194] A different study also demonstrated increased apoptosis in trophoblasts and a significant increase in FasL expression in the decidua from preeclamptic pregnancies, but no change in caspase-3 or p53 expression.[195] Sokolov et al. found a similar degree of apoptosis by TUNEL in normal and preeclamptic placentas, but observed a significant decrease in Fas, Caspase-3, and Caspase-8 expression, a significant increase in TRAIL expression, while Caspase-2, Caspase-9 and FasL were unchanged.[196] FasL was significantly increased in complete hydatidiform moles when compared to age-matched control placentas, although no change in trophoblast apoptosis was observed.[197] These studies point to a role for increased programmed cell death in placentas characterized by insufficient trophoblast differentiation and invasion.

Most recently, Longtine et al. found that induction of apoptosis with staurosporine in placental villous explants caused caspase-mediated apoptosis in cytotrophoblasts but not in the syncytiotrophoblast. The authors suggest that apoptotic cytotrophoblasts interdigitated in the syncytiotrophoblast may be mistaken for syncytiotrophoblast if specific markers are not used to distinguish

the two cell types.[198] They followed up this study with an analysis of apoptosis in normal, preeclamptic and IUGR pregnancies, demonstrating increased caspase-mediated apoptosis limited to the cytotrophoblast in pathologic pregnancies.[199] This brings into question the results of earlier studies demonstrating apoptosis in the syncytiotrophoblast layer, but confirms the enhanced apoptosis initially established.

The ruminant placenta also demonstrates continuous turnover and renewal of syncytial plaques throughout gestation. The precise role of apoptotic factors in regulating this has not been explained. Bovine placentomes demonstrate increasing apoptosis, as detected by positive staining for TUNEL and CASP3, from day 60 of gestation to post-partum, with a concomitant increase in the expression of the anti-apoptotic family member BCL2A1.[200] In early bovine pregnancy, FasL is highly expressed by day 18 conceptuses; there was no change in endometrial apoptosis between pregnant and non-pregnant animals, but the authors did not measure apoptosis in the conceptus.[201]

In yak placentomes, FasL is expressed in binuclear, mononuclear, and trinuclear trophoblast giant cells through gestation, while its receptor Fas was expressed in the cotyledonary villous trophoblast primarily in early pregnancy. Apoptosis in this species, also detected by TUNEL, was highest in the middle of pregnancy in both caruncular epithelium and trophoblast cells.[202] These limited data demonstrate the expression of apoptotic factors in ruminant trophoblast cells, but the function is not clear. It has been suggested that cell death also

plays a role early in gestation during the period of elongation, but this has not been confirmed as apoptosis.[203]

Another role for apoptotic factors in the developing placenta is to communicate between the trophoblast and the maternal endometrium. Trophoblast cells migrate and invade into uterine spiral arteries, eventually replacing maternal endothelium, possibly via endothelial cell apoptosis. Trophoblast secretion of MMP-9 may contribute to endothelial cell apoptosis by increasing the release of FasL.[204] James et al. demonstrated that FasL blocking antibodies significantly inhibited trophoblast-induced endothelial cell apoptosis, confirming that Fas/FasL interactions were involved.[205] First-trimester trophoblast cells express membrane-bound TRAIL, which can induce smooth muscle cell apoptosis.[206] Evidence for *in vivo* vascular smooth muscle cell apoptosis during spiral artery remodeling is conflicting. Bulmer et al. did not observe apoptosis in vascular smooth muscle cells in placentas from 8-20 weeks of gestation, but did identify apoptotic trophoblasts and leukocytes by double immunostaining.[207] They suggest that extravillous trophoblast cells stimulate smooth muscle cell migration away from spiral artery walls, rather than causing apoptosis.[208] In contrast, TUNEL staining of placentas at 8-20 weeks of gestation along with immunostaining for markers of smooth muscle cells and endothelial cells identified a proportion of apoptotic nuclei in both cell types during spiral artery remodeling.[209] Whether apoptosis in maternal smooth muscle cells and endothelial cells plays a role in spiral artery remodeling remains to be seen. Apoptosis-inducing ligands secreted by trophoblast cells may bind to neighboring

trophoblast cells or bind to receptors on maternal endothelial or smooth muscle cells. Determining the definitive role of these ligands in the placenta will require additional *in vivo* analyses as well as *in vitro* analyses with trophoblast cells and co-culture systems of trophoblast cells with endometrial and smooth muscle cells.

Signaling Pathways in the Placenta

Growth factors and cytokines play an essential role in the development of the placenta and the modulation of maternal hemodynamics during pregnancy. Autocrine, paracrine and endocrine signaling allow for the coordinated and controlled growth of trophoblast cells into the fully-formed placenta. Two pathways with demonstrated effects on placental development include the transforming growth factor β superfamily of ligands and receptors and the Wnt signaling pathway.

Transforming growth factor β (TGFβ), produced in the uterine decidua and to a lesser extent the trophoblast, is a key repressor of extravillous trophoblast proliferation and invasiveness.[210] At the blastocyst stage, the actions of TGFβ appear to be pro-proliferative rather than inhibitory. Pre-implantation embryos express TGFβ receptors[211] and exogenous TGF-β stimulates blastocyst proliferation and development and increases blastocyst cell numbers.[212,213,214] TGFβ secreted by the blastocyst induces apoptosis of uterine epithelial cells, perhaps aiding in implantation.[215] After initial implantation, it appears the effects of TGFβ isoforms on proliferating and invading cytotrophoblast cells are antagonistic. Neutralization of endogenous TGFβ1, 2 and 3 increased the

invasive capacity of extravillous trophoblasts while exogenous administration of these growth factors inhibited invasion; this effect was mediated through a decreased secretion of matrix metalloproteinase 9 (MMP9) and urokinase plasminogen activator.[216] MMP9 may also be involved in activation of latent stores of TGFβ through proteolytic cleavage.[217] In contrast to studies on human cells, treatment of rat placental stem cells (HRP-1) with TGFβ1, 2 and 3 significantly increased invasion; TGFβ3 administration significantly decreased apoptosis in RCHO-1 cells, a rat choriocarcinoma cell line, but had no effect on invasiveness.[218] The differing effects of TGFβ on these cells may be explained by the differing placental physiology between humans and rodents.[219] The majority of data indicate TGFβ isoforms inhibit the proliferative and invasive capacity of trophoblast cells, which is reflected in the expression pattern of these cytokines during dysfunctional placentation.

The TGFβ family of proteins is also implicated in pathologic pregnancies. TGFβ1 was significantly up-regulated in the serum of preeclamptic women as compared to normotensive controls, as well as in CV samples from women destined to develop preeclampsia.[220,221,222] In addition, TGFβ3 expression increased in preeclamptic placentas and blocking endogenous TGFβ activity stimulated extravillous trophoblast cell sprouting from villous explants.[223] The elevation of TGFβ3 appears to be partially mediated by a parallel increase in hypoxia-inducible factor 1α (HIF1α) in preeclamptic placentas.[224,225] Endoglin, a high affinity co-receptor for TGFβ1 and TGFβ3 (but not β2), appears to be required for the inhibitory effect of TGFβ on trophoblast differentiation.[226] A

soluble form of endoglin (sEng) exists in circulation and increases in the serum of women with preeclampsia as well as normotensive IUGR, indicating it may be a circulating marker for placental insufficiency.[227,228] Decreased expression of transmembrane endoglin resulted in increased invasiveness and motility of hTR8/SVneo cells.[229]

Growth differentiation factor 15 (GDF15) is a non-canonical member of the TGFβ superfamily of cytokines. It is up-regulated in decidual cells and facilitates decidualization in vitro.[230] As with other TGFβ superfamily members, it appears to be inhibitory to trophoblast invasion, causing anti-proliferative and pro-apoptotic effects *in vitro*.[231,232] GDF15 may have systemic and intrauterine immunosuppressive or anti-inflammatory actions due to high circulating concentrations during pregnancy.[231] Its expression is confined to cytotrophoblast and decidual stromal cells, and does not appear in the syncytiotrophoblast.[233] Although GDF15 knockout mice produce viable and fertile offspring,[234] it is possible that an alternative TGFβ superfamily member increases to compensate for the loss of GDF15, as is the case with activin βB knockout mouse, where activin βA is elevated.[235] Furthermore, GDF15 may play a more important role in the modulation of maternal hemodynamics in human pregnancy than in the rodent. As with other TGFβ family members, GDF15 is elevated in the placenta and in maternal serum from preeclamptic pregnancies.[236] TGFβ cytokines may play a causative role in placental insufficiency or they may be a downstream consequence of poor placental development.

Wnt signaling plays an important role in vertebrate development, as well as the progression of cancer and degenerative diseases. The multi-gene families of Wnt ligands and Frizzled (Fzd) receptors provide for a diverse array of interactions, with 19 Wnt genes and 10 Fzd receptors known in the human genome.[237,238] The canonical Wnt signaling pathway involves activation of β-catenin, which translocates to the nucleus to activate transcription of Wnt target genes in complex with T-cell factor/lymphoid enhancer factor (TCF/LEF) family proteins. In the absence of Wnt ligand, β-catenin is phosphorylated and targeted to the proteasome for destruction by a complex comprising axin, adenomatous polyposis coli (APC), glycogen synthase kinase 3β (GSK3β) and casein kinase I (CKI).[239] Non-canonical Wnt signaling can be divided into two phenotypic categories: the planar-cell-polarity (PCP) pathway and the Wnt/Ca^{++} pathway. The PCP pathway is involved in epithelial cell polarity and motility through the control of actin remodeling via activation of the GTPases Rho and Rac. The Wnt/Ca^{++} pathway is characterized by Wnt-Fzd activation of phospholipase C (PLC) and a subsequent increase in cytoplasmic calcium concentrations. The latter pathway modulates cellular adhesion and cytoskeletal rearrangements.[240] To further complicate the canonical Wnt signaling pathway, β-catenin binds to a number of other nuclear proteins in addition to the TCF/LEF family, including androgen receptor, estrogen receptor, and cyclic AMP response element binding protein (CREB).[241] The complexity of Wnt signaling is demonstrated by the array of proteins mediating these cascades and the diverse cellular responses to Wnt signals. The known functions of Wnt signaling in cell motility, cytoskeletal

remodeling, and proliferation support a function for this pathway in the developing placenta.

The role of Wnt signaling in placental development and trophoblast differentiation remains to be elucidated. In the placenta, several Wnt ligands and Fzd receptors are expressed in both human and ovine trophectoderm. Wnt2, Wnt2B and Wnt4 were detected in ovine trophectoderm, as well as Fzd6/8, GSK3β, β-catenin, and Fzd co-receptor low density lipoprotein receptor-related proteins 5/6 (LRP5/6).[242] Expression of Wnt7A in the luminal epithelium is induced by IFN-т between days 12 and 16 of pregnancy.[243] Wnt7A activates the canonical Wnt signaling pathway in ovine trophoblast cells and may regulate gene expression, proliferation, or differentiation into binucleate cells.[245,244] It may also have autocrine actions on the luminal epithelium to influence uterine receptivity. In the human, Sonderegger et al. found 14 of the 19 known Wnt ligands expressed in first trimester placenta, as well as 8 of the 10 Fzd receptors. Expression of Wnt1, Wnt7b, Wnt10a, and Wnt10b was high in first trimester samples, but mostly absent from term placentas.[245] This differential expression suggests a functional role for these Wnt ligands in early trophoblast proliferation or differentiation. TCF3 and TCF4 are highly expressed in first trimester placenta and extravillous trophoblasts. Treatment with Wnt3a increased nuclear β-catenin staining as well as canonical Wnt/TCF luciferase reporter activity in human trophoblast cells, suggesting increased transcriptional activation by β-catenin-TCF complexes. Concurrently, invasion and migration of trophoblast cells increased upon Wnt3a treatment, and this increase disappeared with the addition

of Dickkopf 1 (Dkk1), an extracellular inhibitor of Wnt signaling.[246] The expression pattern *in vivo* and effects of Wnt ligands *in vitro* demonstrates a probable function for this signaling pathway in early placental development.

Successful navigation of early pregnancy in eutherian mammals requires coordinated communication and interaction between the uterus and the developing placenta. Properly timed and controlled expression of growth factors, cytokines, transcription factors, and other regulatory proteins in the endometrium and trophoblast will determine the pregnancy outcome. Though the pathways regulating placentation have many redundancies in order to favor the propagation of each species, certain factors are critical for placental development and embryonic survival. One such protein that is conserved across mammals as well as more primitive vertebrates is the small nuclear protein proline rich 15.

Proline Rich 15

Proline rich 15 (PRR15) is a small, well-conserved nuclear protein originally identified in murine intestinal epithelium.[247] In situ hybridization analysis on sections of small and large intestine and testis showed that *PRR15* (*G90*) transcripts were present primarily in post-mitotic cells.[247] Further studies of its expression during mouse embryonic development were consistent with this, showing a correlation between *PRR15* expression and the absence of proliferation.[248] A recent finding that stimulation of proliferation of rat pancreatic islet β and acinar cells led to significant down-regulation of *PRR15* further suggests that it could play a role in differentiation or cell cycle arrest.[249] However, Meunier *et al.* observed *PRR15* expression in mouse gastrointestinal tumors

caused by mutations in the *Apc* gene, as well as in several human colorectal cancers and suggested that PRR15 is linked to the Wnt signaling pathway.[250] In Apc mutants, the complex which binds and phosphorylates β-catenin cannot form, resulting in accumulation of β-catenin and activation of Wnt target genes. Though only supported by *in situ* hybridization analysis, these data suggest that Wnt signaling could activate transcription of *PRR15*.

Glover and Seidel[251] independently identified *PRR15* in elongating bovine embryos by mRNA differential display analysis. In silico analysis of this cDNA confirmed an open reading frame encoding a 126 amino acid protein with four putative protein kinase C (PKC) phosphorylation sites, two casein kinase II phosphorylation sites and a nuclear targeting sequence.[251] The expression profile in the sheep conceptus during pregnancy revealed a peak in expression at day 16 of gestation,[75] which coincides with a halt in elongation of the conceptus, and the period of apposition to the uterine epithelium.[252] Immunohistochemistry localized PRR15 to the trophectoderm and extraembryonic endoderm of day 15 sheep conceptuses, suggesting a role in early placental development. Lentiviral-mediated knockdown of *PRR15* in ovine trophectoderm at the blastocyst stage led to demise of the embryo by gestational day 15.[75] This provides compelling evidence that PRR15 is a critical factor during this window of development where proliferation gives way to differentiation of trophoblast cells.

In humans, PRR15 immunolocalized to the nuclei of both first and second trimester placental sections, predominantly in cytotrophoblast cells.[253] *PRR15* mRNA expression increased when trophoblast cells, both sheep (oTR) and

human (ACH3P), were cultured on Matrigel, a basement membrane matrix. During this time, cells cluster together and appear to invade into the extracellular matrix.[76] First trimester cytotrophoblasts grown on an extracellular matrix differentiate into an invasive phenotype, characterized by the same phenotypic changes observed in our trophoblast cell lines.[179] It is generally believed that proliferation ceases once trophoblasts differentiate into the invasive extravillous subtype. These data support the hypothesis that PRR15 could function in trophoblast differentiation or regulation of the cell cycle.

In view of the fact that PRR15 expression increases upon induction of the invasive, more differentiated phenotype, it could be involved in the pathogenesis of placental disorders demonstrating disturbed trophoblast growth. Lentiviral-mediated delivery of shRNA provided robust evidence for the necessity of PRR15 during early embryonic development in the sheep. PRR15 does not contain any known DNA binding motifs, and may not have a direct effect on gene transcription. Due to its nuclear localization, it may act as a co-activator or co-repressor of transcription or influence mRNA processing. Understanding the effect of PRR15 on trophoblast gene expression will help to illuminate the function it may play in placental development.

CHAPTER III – Effect of PRR15-deficiency on Trophoblast Proliferation and Survival

Introduction

Maintenance of early pregnancy in eutherian mammals requires an intricate coordination of events between the embryo and endometrium in order to develop a fully functional placenta. The period of early pregnancy when the embryo begins to attach, adhere to and invade into the endometrium is the most precarious time for the developing embryo. In humans, it is estimated that nearly half of all conceptions are lost, with the majority of these losses occurring during early pregnancy.[254,255] Additionally, common disorders of pregnancy, such as early-onset preeclampsia and intrauterine growth restriction, originate with defective placentation during the first trimester.[256] Ruminants experience early embryonic losses similar to humans, with 30% loss during the period of conceptus elongation prior to gestational day 16.[125] Appropriate proliferation, differentiation, and turnover of trophoblast cells are required for normal placental development, while aberrations in the normal program of gene expression may trigger these disorders of early pregnancy.

The trophectoderm is the first lineage to differentiate in the developing embryo, and is the source of the established placenta.[257] During human implantation, cytotrophoblast cells begin to differentiate into invasive extravillous cytotrophoblasts, which invade the maternal decidua, and villous cytotrophoblasts, which fuse to form the multinucleated syncytium.[258,259] Ruminant and porcine conceptuses undergo a period of rapid elongation just

prior to attachment to the endometrium.[260,261] This process of elongation results from a combination of both proliferation and cellular remodeling.[262] A balance of cell turnover and renewal allows for appropriate and controlled growth of the placenta. Trophoblast apoptosis is increased in pregnancies complicated by IUGR and preeclampsia, suggesting a disruption in the normal balance of cell death and proliferation in these placentas.[263] In all mammalian species, a coordinated expression of transcription factors, cell cycle regulators, growth factors, and other genes is essential to proper placental development.

Proline rich 15 (PRR15) is a small, well-conserved nuclear protein originally identified in murine intestinal epithelium.[247] In situ hybridization analysis on sections of small and large intestine and testis showed that *PRR15* (*G90*) transcripts were present primarily in post-mitotic cells.[247] Further studies of its expression during mouse embryonic development were consistent with this interpretation, showing a correlation between *PRR15* expression and the absence of proliferation.[248] Stimulating proliferation of rat pancreatic islet β and acinar cells led to significant down-regulation of *PRR15*, further suggesting that it plays a role in differentiation or cell cycle arrest.[249] However, Meunier et al. observed *PRR15* expression in mouse gastrointestinal tumors caused by mutations in the *Apc* gene, as well as in several human colorectal cancers and suggested that PRR15 is linked to the Wnt signaling pathway.[250]

Glover and Seidel[251] independently identified *PRR15* in elongating bovine embryos by mRNA differential display analysis. *In silico* analysis of this cDNA predicted an open reading frame encoding a 126 amino acid protein with four

putative protein kinase C (PKC) phosphorylation sites, two casein kinase II phosphorylation sites and a nuclear targeting sequence.[251] The expression profile in the sheep conceptus during pregnancy revealed a peak in expression at day 16 of gestation.[75] This coincides with a halt in elongation of the conceptus, and the period of apposition to the uterine epithelium.[264] Immunohistochemistry localized PRR15 to the trophectoderm and extraembryonic endoderm of day 15 sheep conceptuses.[75] In humans, PRR15 is immunolocalized to the nuclei of both first and second trimester placental sections, predominantly in cytotrophoblast cells.[254] Lentiviral-mediated knockdown of *PRR15* in ovine trophectoderm at the blastocyst stage led to demise of the embryo by gestational day 15.[75] This provides compelling evidence that PRR15 is a critical factor during this window of development where proliferation gives way to differentiation of the trophoblast cells.

Our objective was to determine the impact of diminished PRR15 expression on trophoblast gene expression as well as trophoblast proliferation and apoptosis.

Materials and Methods

Cell Culture and Lentiviral Infection

ACH-3P cells, a human first trimester trophoblast cell line generated from fusion of AC1-1 cells with primary first trimester trophoblasts, were used to generate cell lines for the following experiments.[100] ACH-3P cells were grown in Ham's F-12 medium supplemented with 10% fetal bovine serum in a 37°C incubator at 5% CO_2. The lentiviral vector pLL3.7[265] was used to create stable

cell lines by transfection as well as to generate lentivirus for infection, described below. This vector contains a multiple cloning site for introducing shRNA cassettes downstream of the mouse RNA polymerase III U6 promoter, as well as enhanced green fluorescent protein (EGFP) driven by the cytomegalovirus promoter. For both infection and transfection, the control cell lines contained the LL3.7 vector with no shRNA cassette. To target the PRR15 mRNA for degradation, an shRNA homologous to human PRR15 was inserted into the pLL3.7 vector (TGGAAATCGCTCACCAACATTTCAAGAGACTGTTGGTGAGCGATTTCCTTTTTT). This vector was used previously[75] as a negative control during the in vivo infections of sheep conceptuses, as it contains 3-bp mismatches to the ovine PRR15 mRNA and specifically targeted human *PRR15* rather than ovine. The transfected and infected cells are referred to as "control" or "PRR15-shRNA" from this point forward.

Lentiviral particles were generated as described previously.[75] Briefly, 293FT cells were grown to confluence in a 15-cm tissue culture plate in high glucose DMEM medium supplemented with 10% fetal bovine serum. For each 15-cm plate, Polyfect (180 µl, Qiagen, Valencia, CA) was added to the following lentiviral and packaging vectors in serum-free DMEM to a total volume of 675 µl: pLL3.7 lentiviral construct (8.82 µg, control LL3.7 or PRR15-shRNA), pRΔ8.74 (6.66 µg; *gag/pol* elements), and pMD2.G (2.70 µg; *env* elements). The Polyfect-DNA mixture was added to 293FT cells along with 15 ml complete medium. After 4-6 hours of incubation in the transfection reagent, the medium was aspirated, cells were washed in PBS, and fresh complete medium was added. Two days

after transfection, cell culture supernatants were collected and ultracentrifuged over a 20% sucrose cushion at 47,000x*g* for 2 hours at 4°C. After ultracentrifugation, lentiviral pellets were resuspended in Ham's F-12 supplemented with 10% fetal bovine serum, and stored in aliquots at -80°C. Aliquots of lentiviral particles were titered as described previously.[75]

ACH-3P cells were infected in three replicate experiments with either control LL3.7 or PRR15-shRNA lentivirus at a multiplicity of infection of 100 viral particles per cell in 30-mm tissue culture dishes. To create stable lines, ACH-3P cells were co-transfected with either the control LL3.7 or PRR15-shRNA vector and pcDNA3.1 (Invitrogen, Carlsbad, CA) in a 20:1 ratio using Superfect (Qiagen), following the manufacturer's protocol. The pcDNA3.1 vector contains a neomycin-resistance gene, allowing for selection of transfected cells. Transfected cells were selected by treatment with 400 µg/ml neomycin (G418) for three weeks. The concentration of PRR15 mRNA in transfected and infected cells was assessed by quantitative real-time reverse transcriptase PCR, as described below.

RNA Isolation and Microarray Analysis

Total cellular RNA was isolated from cells using the RNeasy Mini Kit (Qiagen) according to the manufacturer's protocol. RNA quality, measured by the 260/280 nm absorbance ratio, and concentration were assessed using a NanoDrop 1000 Spectrophotometer (Thermo Scientific, Wilmington, DE). Samples were stored at -80˚C until use. RNA from three replicate infections with control and PRR15-shRNA lentivirus was submitted to the Colorado State

50

University Genomics and Proteomics Core for processing and hybridization to the GeneChip Human Genome U133 Plus 2.0 Array (Affymetrix). The raw data intensity files were read into ArrayTrack for analysis (http://www.fda.gov/ScienceResearch/BioinformaticsTools/Arraytrack/default.htm). Data were normalized by scaling to the geometric mean of the intensities of each chip. Genes that were flagged in more than three samples due to intensities too low to be reliable were excluded from the analysis. Control and PRR15-shRNA groups were compared by Welch's t-test on log base 2 expression values (Appendix – Supplemental Table 1 presents differentially expressed genes with *p*<0.05 in Welch's t-test). Pathway analysis on differentially expressed genes (*p*<0.05, 1.3-fold) was conducted using the Kyoto Encyclopedia of Genes and Genomes (http://www.genome.jp/kegg/) pathway maps.[266] Fisher's exact test was used to determine pathways that were significantly altered (*p*<0.05) by depletion of *PRR15*.

Quantitative Real-Time PCR

cDNA was generated from 1 µg of total cellular RNA by reverse transcription at 55°C for 50 min using oligo(dT) primers (Superscript III; Invitrogen), following the manufacturer's protocol. Each cDNA sample was treated with 5 units of RNase H (Fermentas, Burlington, ON) for 20 min at 37°C. Quantitative real-time RT-PCR (qPCR) was performed as described previously[75] except the samples were analyzed on a Lightcycler 480 (Roche Applied Science, Indianapolis, USA) in a 10 µl reaction volume. All primer sets were designed using Oligo software (Molecular Biology Insights, Cascade, CO) to amplify an

intron-spanning product; forward and reverse primers for each gene are shown in Supplemental Table 2 (Appendix), along with conditions for qPCR. A PCR product for each gene was generated using cDNA from ACH-3P cells as a template and cloned into the PCR-Script Amp SK(+) vector (Agilent Technologies, Santa Clara, CA). Each PCR product was sequenced to verify amplification of the correct mRNA (Colorado State University Proteomics and Metabolomics Facility). A standard curve was generated from 1×10^{2} to 1×10^{-6} pg using a PCR product amplified from the sequenced plasmid for each gene, and used to measure amplification efficiency. The starting quantity (picograms) of each mRNA was normalized to the starting quantity of ribosomal protein S15, after verifying that the *rpS15* mRNA concentration did not change with treatment ($p>0.50$). Control and PRR15-shRNA treatments were compared by Students t-test, with $p<0.05$ selected as significant. For analysis of *GDF15* mRNA in ovine conceptuses, total cellular RNA from ovine conceptuses (collected and isolated as described previously[75]) was reverse transcribed as described above and analyzed by qPCR. *GDF15* mRNA concentrations were normalized to ovine *GAPDH* mRNA concentrations. Normalized data were subjected to analysis of variance and comparisons between days of gestation were made using Tukey's honestly significant difference test in SAS software (SAS Institute, Cary, NC).

Proliferation Assay

Stably transfected ACH-3P cells were plated in a 96-well plate with 5000 cells per well and three replicates per treatment. Proliferation was measured using the Cell Counting Kit 8 (Enzo Life Sciences, Farmingdale, NY). Ten µl of

WST-8 [2-(2-methoxy-4-nitrophenyl)-3-(4-nitrophenyl)-5-(2,4-disulfophenyl)-2H-tetrazolium, monosodium salt] was added to each well and incubated for 3 hours, then absorbance at 450 nm was measured using a BioRad Model 680 Microplate Reader (Hercules, CA). Measurements were made 3, 24, 48, and 72 hours after plating cells. Concurrently, BrdU uptake was measured by ELISA, following the manufacturer's protocol (Calbiochem, Darmstadt, Germany). Briefly, 5000 cells were plated in a 96-well plate the day prior to labeling, with three replicates per group. BrdU label (diluted 1:10,000) was added to media for 20 hours prior to ELISA. Cell media was removed and cells were fixed in provided fixative/denaturing solution for 30 minutes at room temperature. Cells were incubated in anti-BrdU antibody diluted 1:100 in antibody dilution buffer for one hour, washed three times in wash buffer, followed by incubation with peroxidase goat anti-mouse IgG HRP conjugate diluted 1:1000 in conjugate diluent for 30 minutes. The plate was washed three times, then 100 µl substrate solution (tetra-methylbenzidine solution) was added for 15 minutes in the dark, followed by stop solution (2.5N H_2SO_4). Absorbance was measured on a spectrophotometric microplate reader (BioRad) at dual wavelengths of 450-595 nm. Absorbances in control and PRR15-shRNA cells were compared by Student's t-test, with $p<0.05$ considered statistically significant.

Caspase Assays

Caspase 3/7 and 8 activity was measured using the Caspase-Glo Reagent (Promega, Madison, WI) in stably transfected ACH-3P cells following the manufacturer's protocol. Briefly, cells (30,000 per well for Caspase 3/7 and

60,000 per well for caspase 8) were plated in triplicate in a white-walled clear-bottom 96-well plate (Costar). Caspase-Glo Reagent was added and incubated at room temperature for 30 minutes. Luminescence was measured on a BioTek Microplate Reader (Winooski, VT) with integration for 10 seconds. The amount of protein in each well was quantified by a Bradford assay, and used to normalize luminescence values. Groups were compared by Student's t-test, with $p<0.05$ considered statistically significant.

Flow Cytometry for Annexin V

The FlowCellect Annexin Red Kit (Millipore) was used to quantify apoptosis in stably transfected ACH-3P cells. Cells were collected by detaching with EDTA (15mM in PBS, pH 7.4) and resuspending in 1X Assay Buffer HSC. Annexin V CF647 Working Solution was added to each sample and incubated for 15 minutes in a 37°C CO_2 incubator. Cells were washed in 1X Assay Buffer, then incubated with 7AAD reagent in the dark for 5 minutes. Samples were analyzed by flow cytometry on a MoFlo flow cytometer (Dako Colorado Inc, Carpinteria, CA) at the Colorado State University Proteomics and Metabolomics Facility. The 7AAD signal was measured on a detector with a 630/30 Band pass filter and the CF647 Annexin V signal was measured on a detector with a 670/20 Band pass filter, with compensation used between the two dyes. Data were analyzed using Summit Software (Dako Colorado Inc). Cell counts for control versus PRR15-shRNA were compared by a Student's t-test, with $p<0.05$ considered statistically significant.

Results and Discussion

Microarray and qPCR Analyses

Transfection and infection of ACH-3P cells with an shRNA to target PRR15 resulted in a comparable decrease in *PRR15* mRNA concentrations for both methods. Lentiviral infection led to a 68% decrease in *PRR15* mRNA ($p<0.01$, Figure III-1A), while stably transfected cells exhibited a 69% reduction ($p<0.01$, Figure III-1B). In the microarray comparison of control to PRR15-shRNA cells, 1375 genes were differentially expressed with a $p<0.05$ and greater than 1.3-fold change (Figure III-2A). Pathway analysis was conducted on these differentially expressed genes using KEGG pathway maps. From the 1375 input genes, 285 genes were found in 155 total pathway maps. Fisher's exact test revealed significant changes in pathways related to proliferation, cancer, and focal adhesion (Figure III-2B). Specifically, colorectal cancer, p53 signaling, and focal adhesion were the pathways most affected by *PRR15* deficiency.
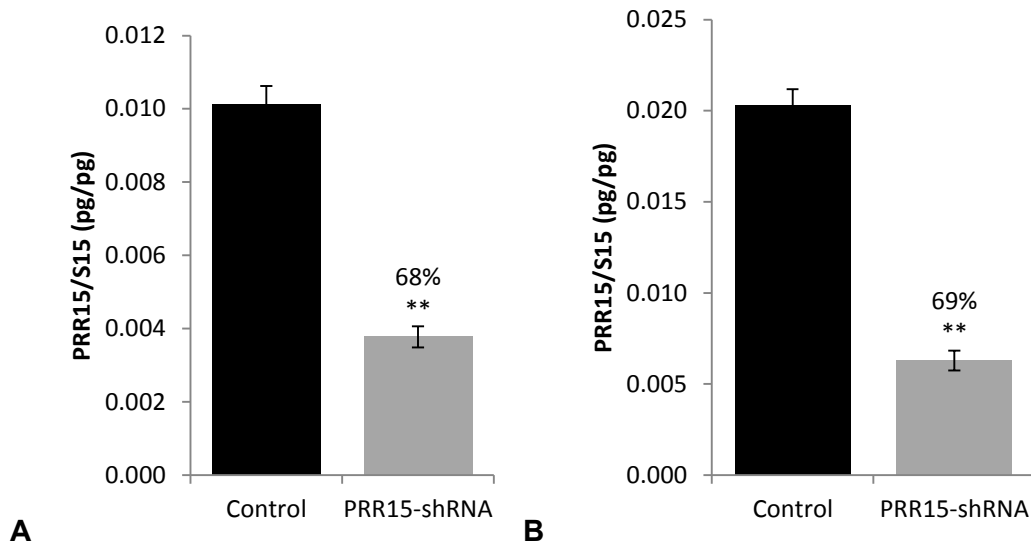
Figure III-1. qPCR for *PRR15* in ACH-3P cells transfected and infected with shRNA.

PRR15 mRNA concentration decreased significantly in the presence of an shRNA to target the mRNA for degradation. qPCR for PRR15 normalized to ribosomal protein S15 in (A) cells infected with lentiviral particles or (B) cells transfected with vectors with or without shRNA. LL3.7 indicates cells infected or transfected with control lentilox vector; shRNA indicates cells infected or transfected with virus/vector containing PRR15-targeting shRNA. ** indicates $p < 0.01$ in Student's t-test.
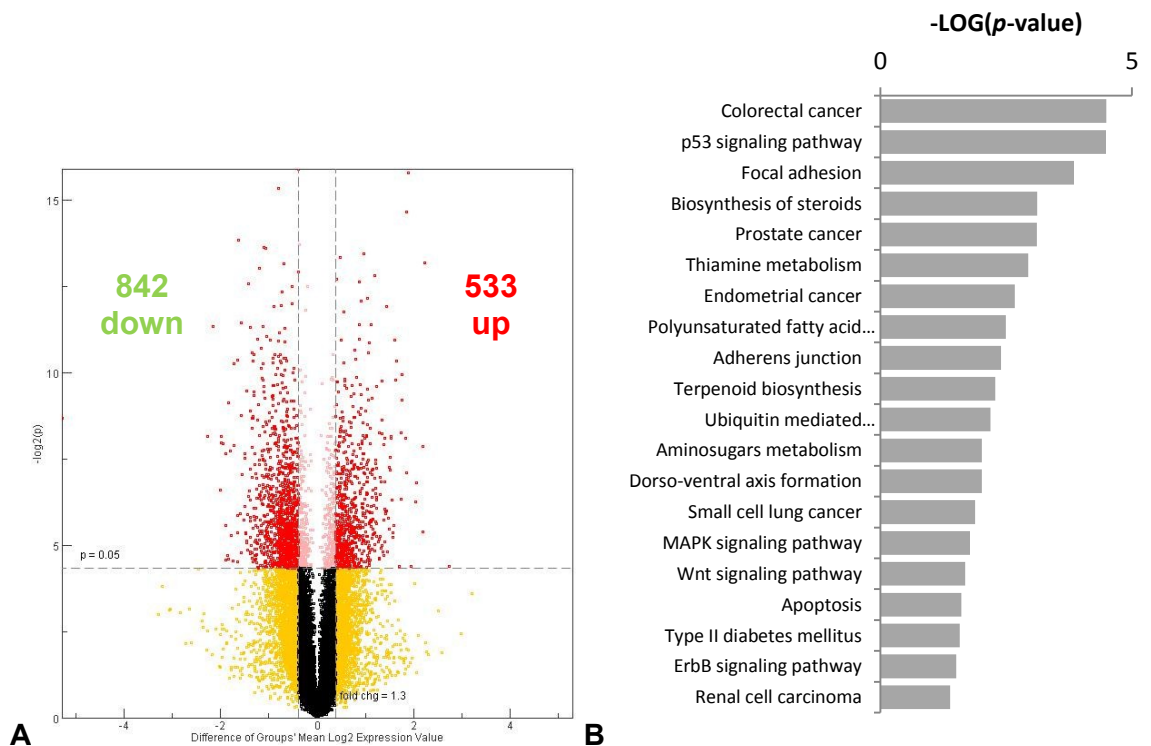
Figure III-2. Volcano plot and pathway analysis from PRR15 microarray.
(A) Volcano plot showing changes in all probe sets measured in microarray analysis of control compared to PRR15-shRNA ACH-3P cells. (B) KEGG pathway analysis of 1375 differentially expressed genes with *p*<0.05 and greater than 1.3-fold change in microarray analysis comparing control to PRR15-shRNA. The *p*-value represents the results of Fisher's exact test.

From the microarray analysis, we selected genes for validation with qPCR that had the most dramatic changes in the PRR15-depleted cells or had known cellular functions potentially related to trophoblast development. Twenty-one genes were selected for validation, 18 (86%) of which gave results consistent with the microarray study. The remaining genes expressed the same trend of up- or down-regulation as in the microarray analysis, but were not statistically significant (*p*≥0.05) in the qPCR results (Table III-1). The genes that were validated by qPCR can be divided into several functional groups, with some genes present in more than one category: regulation of the cell cycle (*CCND1*,

CCNG2, *CDK6*, *CDNK1A*), cell differentiation (*JAG1*, *OVOL2*, *TWIST1*), cell survival/apoptosis (*CRYAB*, *GDF15*, *MXD1*, *MYC*, *TNFSF10*), cell migration and/or invasion (*CCDC88A*, *PTEN*, *PXN*, *TFPI2*, *TWIST1*), insulin-like growth factor (IGF) signaling (*IGF1R*, *IGFBP3*, *PTEN*, *SOCS2*), and placental function (*LIFR*, *OVOL2*).

Table III-1. Differentially expressed genes from PRR15 microarray.
Genes identified as significantly up- or down-regulated in PRR15-deficient cells by microarray analysis with validation by qPCR. For each gene, all probesets from the microarray analysis are shown.

Symbol	Name	Microarray		qRT-PCR	
		Fold	p	Fold	p
Cell Cycle Regulation					
CCND1	cyclin D1	-2.1	0.055	-2.5	0.033
		-1.4	0.052		
CCNG2	cyclin G2	+2.4	0.012	+2.1	0.002
		+3.3	0.003		
		+2.8	0.036		
CDK6	cyclin-dependent kinase 6	-1.9	0.016	-2.7	0.050
		-2.7	0.012		
		-1.9	0.015		
		-1.7	0.004		
CDKN1A	cyclin-dependent kinase inhibitor 1A (p21)	+1.9	0.014	+1.7	0.030
Cell Differentiation					
JAG1	jagged 1	+2.2	0.008	+2.0	0.001
		+2.3	0.010		
OVOL2	ovo-like 2	-2.4	0.030	-2.8	0.034
TWIST1	twist homolog 1	-1.8	0.025	-1.5	0.206
Cell Survival or Apoptosis					
CRYAB	crystallin α B	+4.6	0.009	+3.8	0.002
GDF15	growth/differentiation factor 15	+3.6	0.007	+49.0	0.0001
MXD1	MAX dimerization protein 1	+2.0	0.007	+1.7	0.025
		+2.2	0.010		
MYC	v-myc myelocytomatosis viral oncogene homolog	-1.6	0.016	-2.4	0.003
TNFSF10	tumor necrosis factor superfamily member 10 (TRAIL)	+2.8	0.069	+8.1	0.011
		+2.8	0.007		
		+3.0	0.001		
Cell Migration or Invasion					
CCDC88A	coiled-coil domain containing 88A (girdin)	-3.3	0.043	-3.1	0.047
PTEN	phosphatase and tensin homolog	-1.3	0.088	-2.6	0.054
		-1.2	0.002		
		-1.5	0.008		
		-1.4	0.023		
PXN	paxillin	-2.1	0.097	-1.4	0.017
TFPI2	tissue factor pathway inhibitor 2	-1.9	0.240	-10.5	0.0002
		-39.0	0.002		
IGF Signaling					
IGF1R	insulin-like growth factor 1 receptor	-1.4	0.300	-1.6	0.185
		-1.4	0.018		
		-2.2	0.005		
IGFBP3	insulin-like growth factor binding factor 3	-2.1	0.008	-2.0	0.019
SOCS2	suppressor of cytokine signaling 2	-2.9	0.008	-2.8	0.009
Placental Function					
LIFR	leukemia inhibitory factor receptor	-1.5	0.048	-1.7	0.033
		-2.2	0.008		
		-1.6	0.042		
		-2.3	0.025		

Differential expression of genes related to proliferation and cell cycle regulation revealed a reduction in pro-proliferative genes (*CCND1*, *CDK6*, *JAG1*, *MYC*, *TWIST1*) and an increase in anti-proliferative genes (*CCNG2*, *CDKN1A*, *MXD1*) in the PRR15-shRNA cells. Cyclin D1 (*CCND1*), cyclin G2 (*CCNG2*), cyclin-dependent kinase 6 (*CDK6*), and cyclin-dependent kinase inhibitor 1A (*CDKN1A*, also known as p21 Cip1) function as direct regulators of cell cycle progression. CCND1 and CDK6 promote progression through the G1 phase of the cell cycle,[267] while CCNG2 induces G1/S phase arrest[268] and CDKN1A can induce cell cycle arrest at the G1- or G2-phase checkpoints.[269] Decreased expression of *CCND1* and *CDK6* and an increase in *CCNG2* and *CDKN1A* in the PRR15-shRNA suggest proliferation may be diminished in PRR15-deficient cells.

The insulin-like growth factor (IGF) signaling axis also plays a role in cell proliferation: binding of IGF1 and 2 to the IGF1 receptor (IGF1R) promotes cell growth and proliferation.[270] Circulating IGFs are often bound to IGFBP3 which protects them from proteolysis and enhances IGF activity. Treatment with IGF-I and IGF-II promotes proliferation and protects cytotrophoblasts from apoptosis in first-trimester villous explants, and this effect is mediated in part through IGF1R.[271] Both *IGF1R* and *IGFBP3* were down-regulated in the PRR15-shRNA cells (1.6-fold, $p=0.185$, 2.0-fold, $p=0.019$, respectively), suggesting a decrease in IGF-axis activity and a decrease in proliferation in the PRR15-depleted cells. Conversely, suppressor of cytokine signaling 2 (*SOCS2*), a negative regulator of the IGF1 signaling pathway,[272] was also reduced in the PRR15-shRNA (1.4-fold, $p=0.009$), which conflicts with the directional changes observed in *IGF1R* and

IGFBP3. Furthermore, phosphatase and tensin homolog (*PTEN*), a well-described tumor suppressor, was significantly down-regulated in the PRR15-deficient cells. PTEN has been connected to numerous cellular functions including controlling cell migration through its dephosphorylation of phosphatidylinositol-3,4,5-trisphosphate (PIP3).[273] The reduction of *PTEN* in the PRR15-shRNA may affect cell migration in these cells rather than decreasing proliferation. Despite a few discordant results, the majority of validated genes suggested that trophoblast cell proliferation would be reduced in the PRR15-shRNA cells as compared to the control.

Proliferation decreases and apoptosis increases PRR15-deficient cells

Because the microarray revealed differentially expressed genes in pathways related to proliferation and cell survival, we opted to measure proliferation and apoptosis in PRR15-depleted trophoblast cells. ACH-3P cells transfected with the shRNA-expressing vector to target *PRR15* mRNA for degradation had significantly decreased proliferation based on the CCK-8 assay (Figure III-3A). When measured by the uptake of BrdU, the decrease in the PRR15-shRNA was not statistically significant (p=0.092), although the same trend toward decreased proliferation in the PRR15-shRNA cells was observed (Figure III-3B). The CCK-8 assay measures cell metabolic activity through the reduction of a tetrazolium salt by cellular dehydrogenases to a yellow-colored dye. The decreased absorbance observed in the PRR15-deficient cells may be due to a reduction in cellular proliferation, increased apoptosis, decreased metabolic activity, or a combination of these phenotypes. The BrdU assay

measures DNA synthesis and though it showed a decrease in the PRR15-shRNA

cells, the difference was not as dramatic, suggesting that the PRR15-deficient

cells may be more susceptible to apoptosis.

A

B
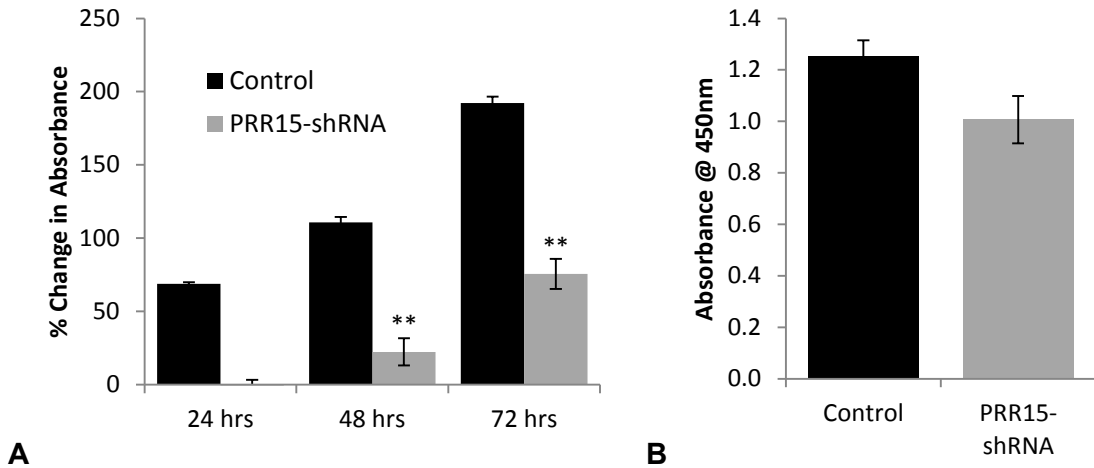
Figure III-3. Proliferation decreases in PRR15-deficient ACH-3P cells.
(A) CCK-8 assay presenting change in absorbance over time in culture of stably
transfected ACH-3P cells. (B) ELISA for BrdU uptake in stably transfected ACH-
3P cells. Control indicates cells transfected with control LL3.7 vector; PRR15-
shRNA indicates cells transfected with vector containing PRR15-targeting
shRNA. ** indicates $p<0.01$.

Apoptosis was measured by the activation of caspases involved in the

apoptotic cascade. Caspase 3/7 activity was significantly increased in the

PRR15-shRNA cells, while caspase 8 activity was unchanged (Figure III-4A).

Caspases, or cysteine-dependent aspartate-specific proteases, are enzymes that

aid in the execution of programmed cell death or apoptosis. Caspase 8 is known

as an "initiator" caspase in the extrinsic pathway of apoptosis, while caspases 3/7

are "executioner" caspases activated by both the intrinsic and extrinsic apoptotic

pathways.[274] The changes observed suggest that the PRR15-deficient cells are

more susceptible to apoptosis through the intrinsic pathway.

We confirmed the changes in apoptosis by measuring annexin V staining followed by quantification with flow cytometry. Annexin V specifically binds to phosphatidylserine on the outer surface of cells in the early stages of apoptosis; phosphatidylserine remains primarily on the inner leaflet of the plasma membrane in viable cells.[275] In order to distinguish apoptotic from dead cells, 7-AAD is used which binds to nucleic acids in late apoptotic or necrotic cells. The percentage of cells that did not absorb either the Annexin Red or 7-AAD stains decreased significantly in the PRR15-shRNA cells, while early apoptotic and late apoptotic/necrotic cells increased (Figure III-4B). These results demonstrate an increased tendency to undergo apoptosis when PRR15 mRNA concentration is decreased in ACH-3P cells.
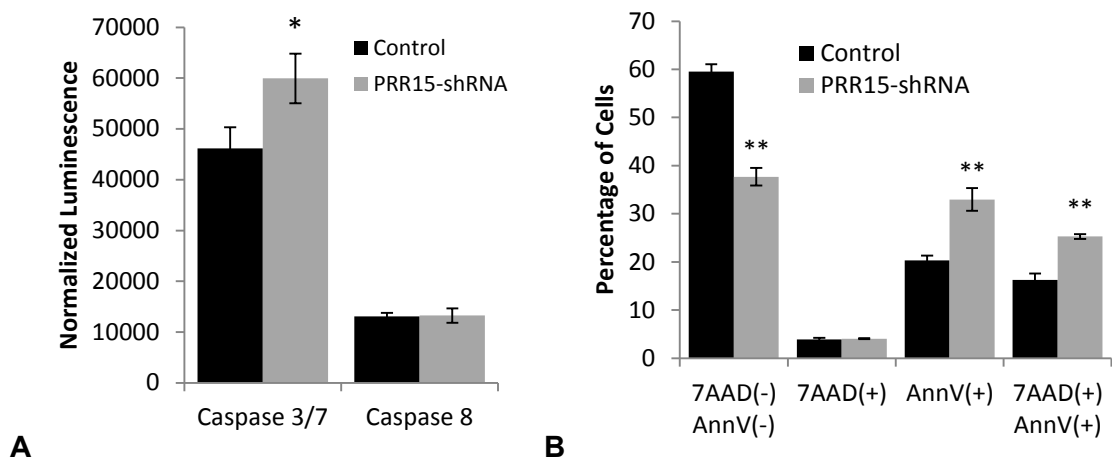
Figure III-4. Apoptosis increases in PRR15-deficient ACH-3P cells.
(A) Caspase 3/7 and 8 activity was measured using Caspase-Glo Reagent. Luminescence values were normalized to protein concentration in each well. Different letters above bars indicate $p<0.05$ in Student's t-test. (B) Annexin V staining was quantified by flow cytometry. 7AAD(-), AnnV(-) indicates cells that were not positive for either stain; 7AAD(+) indicates necrotic cells; AnnV(+) indicates early apoptotic cells; 7AAD(+), AnnV(+) indicates late apoptotic and necrotic cells. * indicates $p<0.05$, and ** indicates $p<0.01$ in Student's t-test.

In the microarray analysis, we observed differential expression of several genes related to apoptosis. *TNFSF10*, also known as *TRAIL*, is a death receptor ligand known to induce apoptosis in transformed and tumor cells;[276] *TFNSF10* was up-regulated in PRR15-deficient cells (8.1-fold, *p*=0.011). This ligand could signal to the trophoblast cells themselves, or to endometrial cells *in vivo*. *TNFRSF10b* (TRAIL-R2, DR5), a receptor for TRAIL, increased 1.5-fold (*p*=0.007) in PRR15-deficient trophoblast cells. *TNFSF10* mRNA concentration was elevated in placentas from women experiencing recurrent miscarriage, and its soluble form was elevated in maternal serum.[277] Furthermore, inhibition of IGF1R kinase activity increases melanoma cell susceptibility to TRAIL-induced apoptosis, and *IGF1R* was also down-regulated in the PRR15-shRNA.[278] These studies indicate that TRAIL could directly affect trophoblast apoptosis *in vitro* and may play a role in embryonic loss when *PRR15* was targeted for degradation *in vivo*.[75] In normal placental development, PRR15 likely protects cells from apoptosis and enhances cell survival, aiding in proper remodeling and formation of the placenta. In contrast to *TNFSF10*, *CRYAB*, a small heat shock protein that may protect cells from apoptosis,[279,280] was increased 3.8-fold (*p*=0.002) in the PRR15-shRNA. However, recent studies show that CRYAB interacts directly with p53 and is required for p53-dependent apoptosis[281] and its anti-apoptotic function is affected by its phosphorylation status.[282] Furthermore, the role of increased *CRYAB* in PRR15-depleted cells may be related to cellular functions other than apoptosis, such as acting as a chaperone for vascular endothelial growth factor A (VEGFA) during angiogenesis, a process critical for early placentation.[283]

Apoptosis, or programmed cell death, is a necessary process in normal placental development as trophoblast cells undergo constant turnover and renewal. However, apoptosis increases in placentas suffering from complications such as preeclampsia, intrauterine growth restriction, and hydatidifiorm moles.[284] In relation to the cell cycle and proliferation, evidence shows that CCND1 is decreased in placentas from IUGR and IUGR with preeclampsia[285], while CDKN1A is increased in IUGR placentas.[286] During normal trophoblast development, PRR15 may protect cells from apoptosis and promote trophoblast cell proliferation and survival.

MYC is a transcription factor and oncogene that is frequently overexpressed in cancer cells; while it drives cell proliferation, it also sensitizes cells to death receptor-mediated apoptosis.[287] In first-trimester human placentas, the extravillous trophoblast, endovascular trophoblast cells, and syncytiotrophoblast express MYC protein.[288] MXD1 is another transcriptional regulator that antagonizes MYC actions, and has anti-apoptotic effects partially through its repression of *PTEN* transcription.[289] *MYC* was down-regulated 2.4-fold (p=0.003) and *MXD1* was up-regulated 1.7-fold (p=0.025) in PRR15-depleted trophoblast cells, which is consistent with decreased proliferation in these cells but not with increased apoptosis. Jagged-1 (JAG1) is a ligand for Notch receptors which is highly expressed in first-trimester cytotrophoblasts and promotes cell proliferation.[290] It may be involved in endovascular remodeling and is decreased in cytotrophoblasts from preeclamptic placentas.[291] *JAG1* was up-regulated (2.0-fold, p=0.001) in the PRR15-shRNA cells, which is not consistent

with decreased proliferation in these cells. The control of cell cycle progression and cell survival is maintained through a delicate balance of a plethora of factors; these data suggest that PRR15-deficiency shifts the balance toward decreased proliferation and increased susceptibility to apoptosis.

A significant down-regulation of genes which function in cell migration and/or invasion was observed in the PRR15-shRNA cells (*CCDC88A*, *PTEN*, *PXN*, *TFPI2*, *TWIST1*).[292] Paxillin (PXN) is a component of focal adhesions and is highly expressed from 5 to 8 weeks of gestation in villous and extravillous trophoblast cells; expression decreases dramatically at 10-12 weeks of gestation, when placental oxygen tension increases.[293] IGF1R signaling leads to phosphorylation of paxillin (PXN) during the assembly of focal adhesions and stimulates extravillous trophoblast migration.[294,295] Girdin (CCDC88A) is a non-receptor guanine nucleotide exchange factor for Gαi which localizes to lamellipodia[296] and is required for migration and invasion of breast cancer cells.[297] *PXN* was down-regulated 1.4-fold (p=0.017) while *CCDC88A* was down-regulated 3.1-fold (p=0.047). Conversely, tissue factor pathway inhibitor 2 (*TFPI2*), a potent inhibitor of matrix metalloproteinases 2 and 9 and possible inhibitor of invasion[298] was also significantly down-regulated, which would support an increase in the invasive capacity of PRR15-deficient trophoblast cells. This protease inhibitor is normally expressed only in the syncytiotrophoblast of the human placenta, and is absent from the proliferative cytotrophoblasts and invasive extravillous trophoblasts.[299]

TWIST1 is a transcription factor involved in the epithelial-mesenchymal transition during cancer metastasis and invasion.[300] It has been suggested that during implantation, the process of trophoblast invasion into maternal tissue requires a partial epithelial-mesenchymal transition of trophoblast cells.[301] *TWIST1* is up-regulated upon conceptus attachment to the luminal epithelium in bovine pregnancies. [302] It is highly expressed in human first-trimester extravillous trophoblast and is required for trophoblast invasion.[303] *TWIST1* was down-regulated in the microarray and qPCR analyses but the decrease was not statistically significant in the qPCR validation (1.5-fold, *p*=0.206). Impaired trophoblast invasion is a well-described phenotype of severe preeclamptic and IUGR placentas, pointing towards a possible function of PRR15 in these pregnancy disorders.

Differentially expressed genes from the microarray analysis with known functions in implantation or placentation included *LIFR* and *OVOL2*. Endometrial expression of leukemia inhibitory factor (LIF) is required for implantation in mice,[304] and is decreased in women with unexplained infertility and recurrent pregnancy loss.[305,306] Its receptor, LIFR, increases significantly during the period of conceptus elongation in pigs.[307] *LIFR* mRNA was detected by *in situ* hybridization in human villous and extravillous trophoblast, while *LIF* mRNA was primarily detected in the decidua.[308] LIF promotes proliferation of trophoblast cells in culture and invasiveness of JEG3 cells.[309,310] Down-regulation of *LIFR* (1.3-fold, *p*=0.033) in the PRR15-shRNA cells could contribute to the decreased proliferation observed. OVOL2 is a zinc-finger transcription factor that directly

represses transcription of *MYC* and *NOTCH1*.[311] OVOL2 knockout mice exhibit impaired placental labyrinth development and embryonic mortality by day 12.5 of gestation.[312] Down-regulation of both *LIFR* and *OVOL2* (2.8-fold, *p*=0.034) in the PRR15-shRNA may have contributed to the embryonic loss observed in sheep when PRR15 was depleted *in vivo*.[75]

Growth/differentiation factor 15 is up-regulated in PRR15-deficient cells

Growth/differentiation factor 15 (*GDF15*, *MIC1*) was up-regulated in the microarray analysis by 3.6-fold (*p*=0.007). When evaluated with qPCR, we observed a 49-fold increase (*p*<0.01) in the PRR15-depleted cells. This suggested PRR15 may have a substantial impact on the concentration of *GDF15* mRNA. The time course of *PRR15* expression in the sheep conceptus reveals a peak in expression at day 16 of gestation, which diminishes dramatically by day 30 (Figure III-5A), as reported previously.[75] Analysis of *GDF15* mRNA concentrations in the same samples revealed low levels of *GDF15* during peak *PRR15* expression, and a striking increase in *GDF15* at day 30 of gestation (Figure III-5B). This demonstrated an inverse relationship between *PRR15* and *GDF15* mRNA levels in trophoblast cells during early pregnancy.
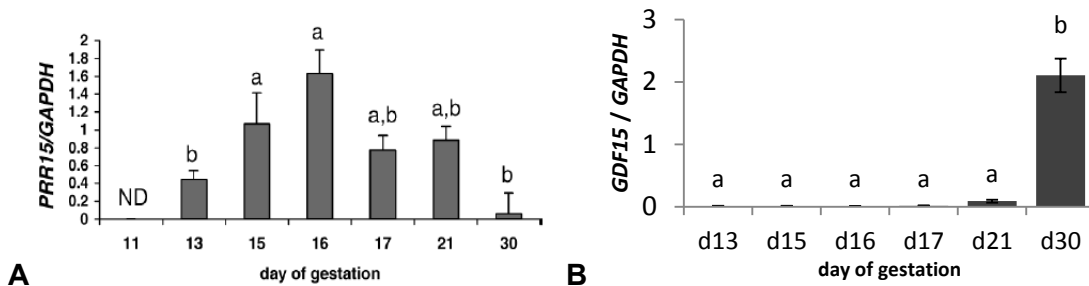
Figure III-5. *PRR15* and *GDF15* mRNA concentrations during early ovine gestation.
Profile of *PRR15* (A – reproduced from Purcell et al. 2009) and *GDF15* (B) mRNA concentrations in ovine conceptuses from days 11 to 30 of gestation, as measured by qPCR and normalized to *GAPDH*. Bars with different letters above them are statistically different ($p<0.05$).

GDF15 is a non-canonical member of the transforming growth factor β superfamily of cytokines that is significantly up-regulated during pregnancy.[230] GDF15 peaks in circulation at 12-14 weeks gestation, and again at 33-35 weeks at approximately double the initial concentrations.[230] It is expressed primarily in villous and extravillous cytotrophoblast as well as decidual stroma, but not in the syncytiotrophoblast.[313,233] Treatment of immature dendritic cells with exogenous GDF15 favored the development of an immature more tolerant phenotype, which may contribute to maternal immune tolerance to the semiallogenic conceptus.[233] During the first trimester, Tong et al. demonstrated decreased concentrations of GDF15 in maternal serum in pregnancies that ended in miscarriage.[314] Furthermore, *GDF15* placental mRNA concentrations were elevated in preeclampsia when compared to control samples from term placentas; this elevation was also observed in maternal and fetal circulation.[315,236] However, Marjono et al. detected no significant differences in serum concentrations of GDF15 associated with either labor or preeclampsia.[230] The discrepancy may be a result of how the authors defined preeclampsia in these studies or the very

limited sample size in the study by Marjono et al. Treatment of HTR8-SVneo cells with GDF15 resulted in reduced proliferation and increased apoptosis as GDF15 concentrations increased.[316] This parallels the phenotypic changes observed when we diminish PRR15 in ACH-3P cells, where *GDF15* expression increased nearly 50-fold. The function of GDF15 in early implantation and placentation is not known, though the significant up-regulation observed in the PRR15-shRNA cells may infer a contribution to pregnancy failure when *PRR15* was targeted for degradation in ovine trophectoderm.[75] Moreover, it may act as a secreted signal of placental dysfunction during early implantation

This study provides evidence that PRR15 affects gene expression of trophoblast cells and is required for trophoblast proliferation and survival. Diminished expression of *PRR15* in ACH-3P cells produced changes in the expression of genes related to cell cycle control as well as apoptosis, migration, and invasion. PRR15 may function through a variety of mechanisms in order to directly affect gene expression. Immunohistochemistry and the conserved nuclear localization signal suggest that PRR15 is primarily nuclear, although it lacks a putative DNA- or RNA-binding motif.[75] It may bind to other transcription factors to suppress or activate transcription of *GDF15* and other genes, or its effects could be post-transcriptional. Post-transcriptional gene regulation can occur through alternative splicing, modified capping and polyadenylation, restriction of nuclear export, and translational inhibition.[317] Preliminary evidence from our laboratory shows that PRR15 interacts with proteins involved in mRNA processing and transport, such as heterogeneous nuclear ribonucleoprotein

(hnRNP) A2/B1, hnRNP D0, lin28 homolog B, and nucleophosmin (Cantlon JD, Anthony RV, unpublished results). These interactions suggest that PRR15 could directly affect mRNA concentrations by modulating processing or splicing of initial transcripts, or by sequestering mRNAs in nuclear bodies. Many of the effects of PRR15 on gene expression are likely indirect via changes to upstream regulators of multiple other genes.

The microarray analysis was conducted in ACH-3P cells, a fusion of primary first-trimester trophoblast cells with a choriocarcinoma cell line.[318] The fact that these cells are transformed for continuous culture and express some degree of tumorigenic potential could affect the transcriptome.[319] Confirmation of the differentially expressed genes in a primary cell line would reinforce the validity of these results. However, primary first-trimester human trophoblast cells are difficult to obtain, and problematic to culture due to their rapid differentiation.[320,321] Limited time is allowed for altering gene expression prior to replicative senescence. Post-transcriptional regulation plays an important role in regulating a number of genes which could be involved in early placental development. This study is limited to identifying those genes regulated at the mRNA level due to the nature of a microarray analysis. Nevertheless, it sheds light on potential pathways involved in early placental development which may be critical to early embryonic survival. The demonstration of early embryonic loss when *PRR15* was targeted for degradation *in vivo*[75] supports a critical role for this protein and the pathways in which it functions for appropriate formation of the placenta during early pregnancy. Though PRR15 itself may not be a useful

biomarker due to its nuclear localization, secreted downstream proteins such as TRAIL and GDF15 could act as signals of impending embryonic loss and/or dysfunctional placentation. Furthermore, understanding the regulatory pathways involved in embryonic survival and normal placental development will aid in identifying therapeutic targets for pathologic changes. The microarray results and phenotype of PRR15-deficient cells suggest that PRR15 promotes trophoblast proliferation and enhances cell survival – roles that are critical to proper placental development during early pregnancy.

Summary

Maintenance of pregnancy in mammals requires a sophisticated and tightly regulated program of gene expression in order to develop a fully functional placenta. This transient organ mediates nutrient and gas exchange between the mother and fetus while protecting the fetus from the maternal immune system. Deviations from the normal regulation of gene expression during early pregnancy can lead to early embryonic loss as well as dysfunctional placentation, which can cause significant maternal and fetal morbidity and mortality. Proline rich 15 (PRR15) is a low molecular weight nuclear protein expressed by the trophoblast during early gestation in several mammalian species, including humans, mice, cattle, sheep, and horses. Immunohistochemistry localized PRR15 to the trophectoderm and extraembryonic endoderm of day 15 sheep conceptuses. In humans, PRR15 is localized in the nuclei of both first and second trimester trophoblast cells. *PRR15* mRNA expression increases when trophoblast cells, both sheep (oTR) and human (ACH-3P), are cultured on Matrigel, a basement

membrane matrix. The expression profile in the sheep conceptus during pregnancy revealed a rise during the period of conceptus elongation with a peak in expression at day 16 of gestation, followed by a decline to day 30 of gestation. This peak coincides with a halt in elongation of the conceptus, and the initial period of apposition to the uterine luminal epithelium. Lentiviral-mediated knockdown of *PRR15* in ovine trophectoderm at the blastocyst stage led to demise of the embryo by gestational day 15. This provides compelling evidence that PRR15 is a critical factor during this precarious window of development when initial attachment and implantation begin. The aims of these experiments were to determine the effect of *PRR15* knockdown on trophoblast gene expression, as well as trophoblast proliferation and survival. The human first trimester trophoblast cell line, ACH-3P, was infected with control lentivirus (LL3.7) and lentivirus expressing a short hairpin (sh)RNA to target *PRR15* mRNA for degradation, resulting in a 68% decrease in *PRR15* mRNA ($p<0.01$). Microarray analysis of these cell lines revealed differential expression of genes related to cancer, focal adhesion, and p53 signaling. We selected 21 genes for validation of mRNA levels by quantitative real-time RT-PCR, 18 (86%) of which gave results consistent with the microarray analysis. These changes included significant up-regulation of *GDF15*, a cytokine increased in pregnancies with preeclampsia. We evaluated *GDF15* mRNA concentrations during early ovine gestation and found that *GDF15* was low during peak *PRR15* expression, then increased significantly at day 30 when *PRR15* was nearly undetectable. Proliferation decreased in the absence of *PRR15*, which was consistent with a

decrease observed in cell cycle-related genes *CCND1* and *CDK6*, and an increase *CCNG2* and *CDKN1A* in the PRR15-deficient cells. *TNFSF10*, a tumor necrosis factor superfamily member known to induce apoptosis, and its receptor, *TNFRSF10b*, increased significantly in the PRR15-deficient cells, suggesting trophoblast cells may be more susceptible to apoptosis when depleted of *PRR15*. Assays for caspase activity and annexin V staining revealed an increased population of apoptotic cells when treated with shRNA to target *PRR15*. These results suggest that PRR15 is required for driving trophoblast proliferation and survival during early development of the placenta, functions that are critical to early embryonic survival and successful placentation.

CHAPTER IV – Transcriptional Regulation of *PRR15*

Introduction

Reproduction in mammals requires the development of the placenta: a transient yet essential organ that mediates maternal to fetal exchange while protecting the fetus from the maternal immune system. After successful fertilization, the embryo must navigate through a precarious time in development: implantation and early placentation. In humans, it is estimated that nearly half of all conceptions are lost, with the majority of these losses occurring during early pregnancy.[322,323] Additionally, pregnancy complications such as early-onset preeclampsia and intrauterine growth restriction, originate with defective placentation during the first trimester.[324] Ruminants experience similar early embryonic losses to humans, with up to 30% loss during the period of trophectoderm outgrowth and elongation.[325] Expressing the appropriate repertoire of proteins in specific spatial and temporal patterns is critical to reproductive success, while aberrations in expression can lead to pregnancy loss and placental dysfunction.

Proline rich 15 (PRR15) is a small, well-conserved nuclear protein expressed by the trophectoderm during early pregnancy in ruminants.[75] The *PRR15* gene encodes a 126 amino acid protein with four putative protein kinase C (PKC) phosphorylation sites, two casein kinase II phosphorylation sites, and a nuclear targeting sequence.[251] The expression profile in the sheep conceptus during pregnancy revealed a peak in expression at day 16 of gestation, followed by a decline to day 30.[75] The peak of *PRR15* expression coincides with a halt in

elongation of the conceptus, and the period of apposition to the uterine epithelium.[326] Immunohistochemistry demonstrated localization of PRR15 to the trophectoderm and extraembryonic endoderm of day 15 sheep conceptuses.[75] In humans, PRR15 is immunolocalized to the nuclei of both first and second trimester placental sections, predominantly in cytotrophoblast cells.[253] Lentiviral-mediated knockdown of *PRR15* in ovine trophectoderm at the blastocyst stage led to demise of the embryo by gestational day 15,[75] indicating that PRR15 is a critical factor during implantation and early trophoblast development.

PRR15 transcripts were concurrently identified by *in situ* hybridization of small and large intestine, and were present primarily in cells that lie in the transitional zone of intestinal villi.[248] This zone represents a population of cells which have migrated out of the proliferative crypts, and continue to differentiate as they migrate toward the villous tips.[327] Meunier et al. observed *PRR15* expression in mouse gastrointestinal tumors caused by mutations in the *Apc* gene, as well as in several human colorectal cancers and suggested that PRR15 is linked to the Wnt signaling pathway.[251]

Wnt signaling is a conserved pathway involved in development and is frequently altered in cancer. In the absence of Wnt binding to its extracellular receptor, β-catenin is phosphorylated by glycogen synthase kinase 3β (GSK3β) in a destruction complex with adenomatous polyposis coli (Apc), axin, and casein kinase I, and is targeted for proteasomal degradation. When Wnt ligands are present, the destruction complex is inactive; β-catenin accumulates within the cytoplasm and translocates to the nucleus where it interacts with T cell

factor/lymphoid enhancer factor (TCF-LEF) transcription factors to activate transcription of Wnt target genes.[328] This pathway is known as the "canonical" Wnt signaling cascade, while the "non-canonical" pathway regulates cell polarity and cell division independent of β-catenin.[329] Mutations in Apc are commonly found in cancers, leading to accumulation of β-catenin and transcription of Wnt target genes. Given the increased expression of *PRR15* observed in Apc mutants, it is feasible that *PRR15* is a Wnt target gene.

Transcriptional regulation is the first step in determining the amount of protein a cell will produce in different conditions or developmental stages. Spatial and temporal regulation of gene transcription is primarily determined by the 5'-flanking region or promoter, which contains *cis*-acting regulatory elements that interact with transcription factors. Binding of specific transcription factors can either enhance or reduce recruitment of RNA polymerase II and transcription of the gene of interest. The pattern of PRR15 expression during early gestation[75] suggests it is under complex positive and negative transcriptional regulation, in order to be strictly expressed in specific developmental periods and cell types. Given the lethal effect of its absence,[75] we aimed to examine regions of the *PRR15* promoter necessary for regulating its expression in trophoblast cells and to localize putative transcription factor binding sites. We also examined the role of the Wnt signaling pathway on the transcription of *PRR15*.

Materials and Methods

Cell Culture

ACH-3P cells, a fusion of human first-trimester trophoblasts with a choriocarcinoma cell line,[100] were cultured as described previously (Chapter III). oTR-19 cells were generated by collecting day 15 ovine conceptuses to generate trophoblast cell lines as described.[330] Estrus was detected in mature ewes in the presence of a vasectomized ram. At estrus, day 0, ewes were mated to intact rams. On day 15 after mating, the uterus was flushed with sterile PBS to collect the conceptuses. These were minced and plated on plastic culture dishes in DMEM/F12 medium supplemented with 10% fetal bovine serum, 2 mM glutamine, 700 nM insulin, 1 mM pyruvate, and 0.1 mM non-essential amino acids. Cells were maintained for no more than 20 passages. HT29 cells, derived from a human colorectal carcinoma, and BHK21 cells, hamster kidney fibroblasts, cells were obtained from American Type Culture Collection (Manassas, VA) and grown in McCoy's 5A Medium Modified or Eagle's Minimum Essential Medium, respectively, supplemented with 10% FBS.

Promoter Deletion Constructs and Transfections

Genomic DNA from human blood was isolated using the Wizard® Genomic DNA Purification Kit (Promega, Madison, WI). The 5'-flanking sequence from -824 to +7 bp relative to the annotated transcription start site of the human *PRR15* gene (Accession NM_175887, National Center for Biotechnology Information) was amplified by PCR using human genomic DNA as a template and cloned into PCR-Script Amp SK(+) (Agilent Technologies). Deletion

constructs from -640, -424, -326, and -284 bp to the transcription start site were generated by PCR using the full-length construct as a template, and cloned into PCR-Script Amp SK(+). All vectors were sequenced to determine authenticity and the direction of insertion, then sub-cloned and ligated into pGL3-Basic (Promega). Reporter vectors were sequenced to verify the correct direction of insertion of the promoter cassette.

Transient transfections were performed as described by Jeckel et al. with some modifications.[331] ACH-3P, oTR-19, HT29, and BHK21 cells were co-transfected with the reporter vectors and a RSV-β-galactosidase vector as a transfection control in a 20:1 ratio using Superfect (Qiagen), following the manufacturer's protocol. The day prior to transfection, 2×10^5 cells per well were seeded on 6-well plates. In a total volume of 300 µl, 5.7 µg reporter vector and 0.3 µg RSV-β-galactosidase vector were added to serum-free medium for transfection of three replicate wells. The DNA mixture was incubated with 30 µl Superfect reagent at room temperature for 10 minutes, then split among three wells in 600 µl complete medium per well. Transfection complexes were removed after three hours and replaced with fresh complete medium.

Two days after transfection, cells were washed three times in PBS and lysed in 200 µl lysis buffer (25 mM glycyl-glycine, pH 7.8; 1.0% Triton X-100, 10 mM $MgSO_4$, and 1.0 mM dithiothreitol). For luciferase activity, 20 µl of cell lysate was added to 100 µl luciferin; luminescence was measured after a two second delay with 10 second integration. Luminescence was measured on a TD 20/20 Luminometer (Turner Designs, Sunnyvale, CA). For β-galactosidase activity, the

Galacto-Light Plus system (Applied Biosystems, Carlsbad, CA) was used. Cell extract (10 μl) was added to reaction buffer (200 μl) and incubated for one hour at room temperature. Accelerator II (300 μl) was added and luminescence integrated over 4 seconds. Experiments were repeated on three separate preparations of reporter plasmids. Activity of each reporter vector was compared to the empty vector control (pGL3 Basic) in a Dunnett's t-test after normalizing to β-galactosidase activity.

GSK3β Inhibitor, β-catenin Plasmids, and Quantitative Real-time PCR

The GSK3β inhibitor SB216763 (Sigma-Aldrich, St. Louis, MO) was used to generate active β-catenin/TCF-LEF signaling in treated cells. ACH-3P cells were serum-starved (0.5% FBS) for two hours, then treated with either 10 μM SB216763 dissolved in DMSO or DMSO alone as a vehicle control for 24 hours prior to assay. For reporter activity in the presence of SB216763, transfections were performed as described above. For analysis of *PRR15* mRNA concentrations, total cellular RNA was collected using the RNeasy Mini Kit (Qiagen). Reverse transcription and quantitative real-time PCR (qPCR) was performed as described previously (Chapter III). Concentrations of *PRR15* mRNA were normalized to the mRNA concentration of ribosomal protein S15. Proliferation of ACH-3P cells in the presence or absence of SB216763 was measured using the Cell-Counting Kit 8 (Enzo Life Sciences) as previously described (Chapter III). All samples were run in triplicate and experiments were repeated three independent times. DMSO- and SB216763-treated groups were compared by a Student's t-test, with $p < 0.05$ considered statistically different.

In order to determine the role of β-catenin in *PRR15* promoter activity, ACH-3P cells were transfected with constitutively active β-catenin or shRNA targeting β-catenin mRNA for degradation. The pMXs-beta-catenin-S33Y plasmid (Addgene, Cambridge, MA) harbors a point mutation (S33Y) resulting in expression of a constitutively active form of β-catenin.[332] pLKO.1-puro-shRNA-beta-catenin (Addgene) is a plasmid that expresses a shRNA directed against β-catenin mRNA.[333] Transfections were performed as described above with some modifications. The -824 reporter plasmid was co-transfected in a 1:1 ratio with pBlueScript as a negative control and treated with DMSO or SB216763 as previously described. Additional samples were co-transfected in a 1:1 ratio with the -824 reporter plasmid and the plasmid expressing a shRNA to target β-catenin mRNA for degradation or the plasmid expressing constitutively active β-catenin (S33Y). Transactivation of the luciferase reporter was measured as described above. Luciferase activity of each sample was compared to the DMSO control in a Student's t-test, with $p<0.05$ considered statistically significant.

Nuclear Extraction

ACH-3P and HT29 cells were dislodged from subconfluent culture dishes using trypsin (0.25% with 0.5 mM EDTA), washed in PBS, and pelleted. Nuclear protein was extracted using a modified Dignam method.[334] Cells were resuspended in three volumes of hypotonic buffer (10 mM HEPES, 1.5 mM MgCl2, 10 mM KCl, 0.5 mM DTT, 0.2 mM PMSF) and allowed to swell on ice for 10 minutes. The cells were homogenized in a Dounce homogenizer and nuclei were pelleted by centrifugation at 3300xg for 30 minutes. The nuclear pellet was

resuspended in ½ volume low salt buffer (0.15 M NaCl, 0.1 mM EDTA, 20 mM TrisHCl, 0.5 mM DTT, 0.2 mM PMSF), followed by slowly adding ½ volume of high salt buffer (same as low salt with 1 M NaCl). Nuclei were extracted by gentle shaking on ice for 30 minutes, then pelleted by centrifugation at 25,000xg for 30 minutes. The nuclear extract was dialyzed overnight in 10,000 molecular weight cutoff (MWCO) Slide-A-Lyzer dialysis cassettes (Thermo Scientific) against dialysis buffer (20 mM HEPES, 0.2 mM EDTA, 0.5 mM DTT, and 0.2 mM PMSF). Following dialysis, the extract was concentrated by centrifugation over a 3,000 MWCO Amicon centrifugal filter (Millipore) and protein concentration was determined by Bradford assay. Glycerol (20%) was added as a cryoprotectant prior to aliquoting and storing at -80°C until use. ACH-3P cells for EMSA were treated with DMSO or GSK3β inhibitor (SB216763) for 24 hours prior to collection of nuclear extract.

DNase I Footprinting

Non-radiochemical DNase I footprinting was performed as described in Zianni et al. with some modifications.[335] DNA fragments for footprinting were prepared by PCR of three overlapping constructs from the *PRR15* proximal promoter (-855 to -510, -562 to -268, -286 to +7) using the plasmid containing the full proximal promoter as a template. Each forward primer was labeled on the 5'-end with 6-FAM (Integrated DNA Technologies, Coralville, IA). The PCR was performed in 50 µl reactions as follows: 95°C for 5 minutes, followed by 40 cycles of 95°C for 1 minute, 55°C for 1 minute, and 72°C for 1 minute, followed by 72°C for 10 minutes. Reactions were electrophoresed through a 1% agarose gel to

verify size, then purified using QiaQuick PCR Purification columns (Qiagen). Concentration was assessed with a NanoDrop 1000 spectrophotometer (Thermo Scientific).

Nuclear extracts or bovine serum albumin (100 µg) were incubated in binding buffer (12 mM Tris-HCl (pH 7.9), 1 mM $MgCl_2$, 1 mM $CaCl_2$, 5 mM NaCl, 0.1 mM DTT, 5% glycerol, 1 µg herring sperm DNA) in 50 µl total volume on ice for 10 minutes. FAM-labeled probe (250 ng) was added, and incubated at 30°C for 30 minutes. RNase-free DNase I (Thermo Scientific) was added and reactions were incubated at 30°C for varying times, which were optimized for each promoter fragment. To terminate digestion, EDTA (50mM, pH 7.4) was added to a final concentration of 5 mM and reactions were incubated at 75°C for 10 minutes. The FAM-labeled fragments were purified with QiaQuick PCR Purification columns (Qiagen) and eluted in nuclease-free water. Analysis was performed on an ABI 3130xL Genetic Analyzer (Applied Biosystems) by adding 3 µl sample to 10 µl HiDi formamide (Applied Biosystems) and 0.3 µl GeneScan[TM]-600 LIZ size standards (Applied Biosystems). Fragmentation patterns were analyzed using PeakScanner software (Applied Biosystems).

Electrophoretic Mobility Shift Assay

Oligonucleotides were generated with a biotin label on the 5' end (Integrated DNA Technologies). Oligonucleotides were derived from the optimized TCF-LEF binding site[336,337] (sense 5'- CCCTTTGATCTTACC-3', antisense 5'-GGTAAGATCAAAGGG-3') and from the protected -98 to -68 region of the *PRR15* proximal promoter (sense 5'-

83

GCACTGCACAGCTTTTCTCCAATCAGACAC-3', antisense 5'-GTGTCTGATTGGAGAAAGCTGTGCAGTGC-3'). Complementary oligos were annealed by mixing in a 1:1 ratio to a final concentration of 1 pmol/μl in annealing buffer (10 mM Tris, 1 mM EDTA, 50 mM NaCl, pH 8.0) and heating to 95°C for 5 minutes, followed by gradually cooling to room temperature. Gel shifts were performed using the LightShift Chemiluminescent EMSA Kit (Thermo Scientific). In a total of 20 μl, 10 μg nuclear extract and 0.5 pmol biotinylated oligos were combined in 1X Binding Buffer, 50 ng/μl Poly(dI:dC), 5% glycerol, 100 mM KCl, 1 mM EDTA, and incubated at 37°C for 30 minutes. Unlabeled competing oligonucleotides were added in 200-fold molar excess to verify specificity of binding. Loading buffer (5 μl) was added to each binding reaction and samples were electrophoresed through a 5% polyacrylamide TBE gel (BioRad) at 100V for 45 to 90 minutes. DNA-protein complexes were transferred to a positively charged Biodyne B Nylon Membrane (Thermo Scientific) at 100V for one hour at 4°C. Complexes were cross-linked for one minute at 120 mJ/cm^2 using a CL-1000 Ultraviolet Crosslinker (UVP, Upland, CA). Biotinylated DNA was detected by chemiluminescence following the manufacturer's instructions. Membrane was exposed to X-ray film (Kodak, Rochester, NY) or analyzed on the ChemiDoc XRS (BioRad).

Results and Discussion

Proximal Promoter Transactivation

The homology of the 5'-flanking region of the *PRR15* gene is well-conserved between the human and the cow in the first 800 bp (75% identity), and

begins to deviate widely beyond this point. The longest construct designed encompassed this evolutionarily conserved region to -824 bases of the human *PRR15* 5'-flanking region. Progressive deletions of the proximal promoter were generated at -640, -424, -326, and -284 bp from the annotated transcriptional start site. First trimester human trophoblast cells (ACH-3P) were co-transfected with promoter deletion constructs and a RSV-β-galactosidase transfection control. Transactivation of the luciferase reporter was measured by luminescence and normalized to β-galactosidase activity (Figure IV-1A). Transfections were repeated in primary ovine trophoblast cells (oTR-19), human colorectal carcinoma (HT29), and hamster kidney fibroblast (BHK21, Figure IV-1B, C, D, respectively). ACH-3P, oTR-19, and HT29 cells normally express *PRR15* mRNA, while BHK21 cells do not normally express *PRR15*.
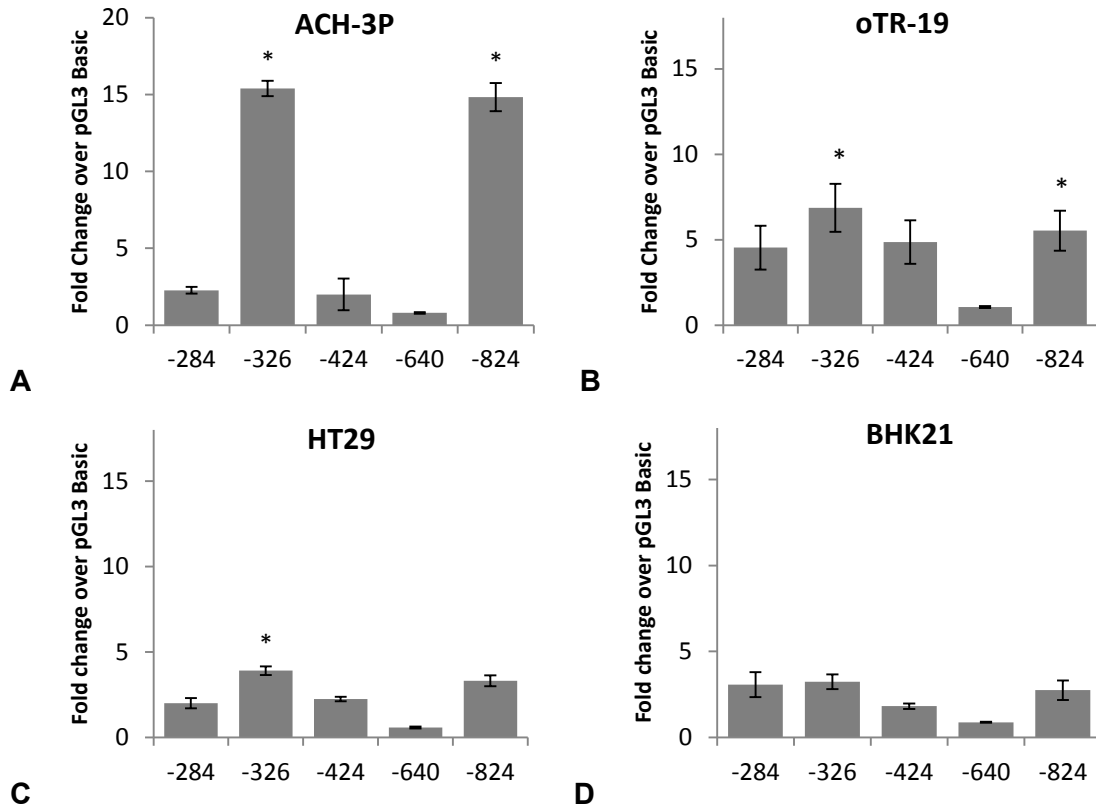
Figure IV-1. Transactivation of luciferase reporter from *PRR15* promoter deletion constructs.
(A) ACH-3P = human first trimester trophoblast, (B) oTR-19 = primary ovine trophoblast, (C) HT29 = human colorectal carcinoma, (D) BHK21 = hamster kidney fibroblast. * indicates *p*<0.05 in Dunnett's t-test when compared to empty vector control (pGL3-Basic).

Maximal transactivation of the luciferase reporter was observed in the -326 (15.4 ± 4.8-fold) and -824 (14.8 ± 5.8-fold) constructs in ACH-3P cells. Significant promoter activity was absent in the -284, -424, and -640 constructs in all cell lines. These results suggest that *cis*-acting elements within the proximal promoter of the *PRR15* gene are essential for transcription in trophoblast cells, requiring the regions from -284 to -326 and -640 to -824. We examined these regions for putative transcription factor binding sites using the Transcription Element Search System (TESS, www.cbil.upenn.edu/tess/) and identified numerous potential transcriptional activators. DNase I footprinting and

electrophoretic mobility shift assays, discussed below, were used to verify protein-DNA interactions at these sites.

ACH-3P cells exhibited the largest fold changes over the empty vector control, while none of the constructs demonstrated significant transactivation in the BHK21 cells. Though HT29 cells express relatively high levels of *PRR15* mRNA, transactivation of the luciferase reporter was not as robust as expected. This is could be due to the low transfection efficiencies we observed in these cells, or transcriptional activation of the *PRR15* gene in these cells could be imparted primarily by more distant regulatory elements. HT29 cells express a truncated form of the Apc protein[338] which results in the accumulation of β-catenin and activation of Wnt target genes. Meunier et al. observed increased *PRR15* in colorectal cancers with mutations in Apc and suggested a link between PRR15 and the Wnt signaling pathway.[251] We opted to explore the connection between Wnt signaling and *PRR15* transcription using an inhibitor of glycogen synthase kinase 3β (GSK3β). GSK3β is the kinase responsible for phosphorylation of β-catenin, which leads to degradation of β-catenin by the proteasome and a lack of Wnt target gene activation. Inhibition of this kinase is comparable to treating cells with exogenous Wnts in order to activate Wnt target genes through the accumulation and translocation of β-catenin to the nucleus.

Inhibition of GSK3β Activity and the Role of β-catenin

ACH-3P cells treated with the GSK3β inhibitor, SB216763, had significantly reduced concentrations of *PRR15* mRNA, as measured by qPCR (Figure IV-2A). In keeping with this observation, transactivation of the luciferase

reporter from the proximal -824 bases of the *PRR15* promoter was significantly decreased after cells were treated with GSK3β inhibitor, SB216763 (Figure IV-2B). When transactivation of the promoter deletion constructs was tested in the presence of GSK3β inhibitor, all constructs demonstrated a comparable reduction in luciferase activity (Figure IV-2C). This suggests that the effect of GSK3β on *PRR15* promoter activity is mediated through the most proximal 284 bp of the 5'-flanking region.
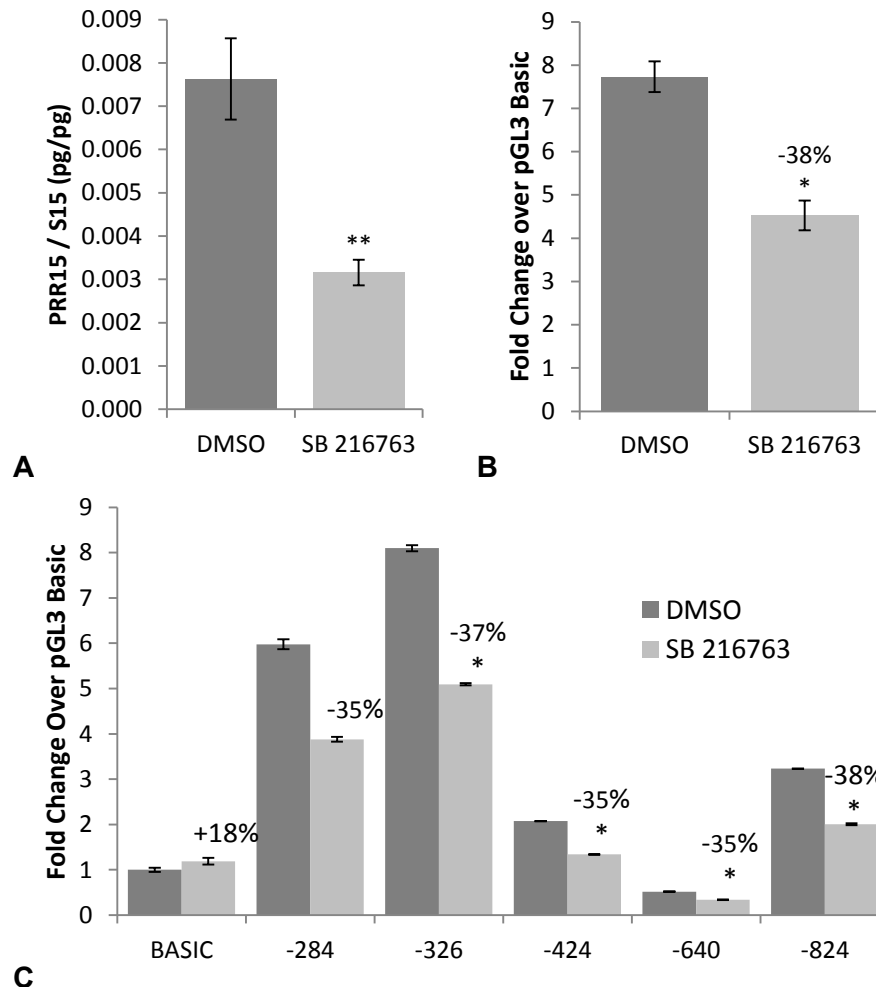
Figure IV-2. GSK3β inhibition decreases *PRR15* transcriptional activity.
(A) qPCR for *PRR15* normalized to *rpS15* in ACH-3P cells treated with GSK3β inhibitor (SB216763) or vehicle control (DMSO); (B) Fold change of normalized luciferase activity in ACH-3P cells transfected with a reporter vector containing the proximal 824 bp of the *PRR15* 5'-flanking region. Cells were treated with SB216763 or vehicle control; (C) Luciferase reporter activity of all PRR15 promoter constructs normalized to β-galactosidase in ACH-3P cells after treatment with SB216763. Numbers indicate percent change when treated with SB216763. * indicates $p<0.05$, ** indicates $p<0.01$ when compared to vehicle control in Student's t-test.

In order to verify that β-catenin was involved in the transcriptional repression of *PRR15*, ACH-3P cells were co-transfected with the -824 reporter construct as well as vectors expressing either shRNA to target β-catenin (β-cat shRNA) or constitutively active β-catenin (S33Y). Expression of the β-catenin

shRNA did not affect transactivation of the luciferase reporter from the proximal -

824 bp of the promoter (Figure IV-3). Over-expression of constitutively active β-

catenin resulted in a reduction in luciferase activity comparable to that observed

after treatment with the GSK3β inhibitor (SB216763). These results infer that the

effect of GSK3β inhibition on *PRR15* transcriptional activity is in fact mediated

through β-catenin activity.
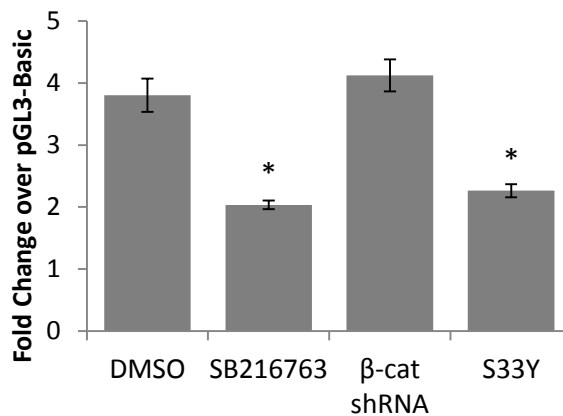
Figure IV-3. Constitutive activity of β-catenin reduces *PRR15* promoter activity. ACH-3P cells were co-transfected with the -824 reporter plasmid and plasmids expressing either shRNA to target β-catenin (β-cat shRNA) or constitutively active β-catenin (S33Y). All samples were compared to the DMSO control by a Student's t-test, with * indicating *p*<0.05.

The fact that *PRR15* transcriptional activity decreases upon inhibition of

GSK3β is counter to what we predicted based on the results of Meunier et al.[251]

Their data suggested increased *PRR15* mRNA concentrations in colorectal

tumors with mutations in the Apc protein, but these data were limited to *in situ*

hybridization analysis. The characteristic action of Wnt signaling is transcriptional

activation of target genes through the interaction of β-catenin with TCF-LEF

transcription factors. Here, we demonstrate decreased transcriptional activity of

the *PRR15* gene in response to GSK3β inhibition, which simulates active Wnt

signaling. Furthermore, expression of constitutively active β-catenin causes a comparable decrease in promoter activity. In the absence of β-catenin, TCF-LEF transcription factors typically bind to target regions and can repress transcription; during active Wnt signaling, nuclear β-catenin complexes with TCF-LEFs to activate transcription.[339] Transcriptional repression by β-catenin-TCF-LEF complexes is uncharacteristic but not unprecedented; Jamora et al. observed reduced transcription of E-cadherin as a result of β-catenin activation of Lef1 transcription complexes.[340] Our data infer that active Wnt signaling through β-catenin represses transcription of *PRR15* in trophoblast cells.

Because we observed a decrease in proliferation in PRR15-deficient cells (Chapter III), we measured proliferation of ACH-3P cells after treatment with the GSK3β inhibitor. Proliferation decreased ($p<0.01$) when ACH-3P cells were treated with SB216763 after 96 hours (Figure IV-4), which is consistent with the reduced proliferation of the PRR15-depleted cells. Constitutive activation of Wnt signaling is a characteristic event in several types of cancer,[341] resulting in activation of pro-proliferative genes such as c-MYC and cyclin D1.[342,343] In contrast to the stimulation of proliferation observed in cancers, activation of canonical Wnt signaling was shown to induce invasive differentiation in primary first-trimester human trophoblast cells;[344,345] this differentiated state is associated with a lack of proliferation. It appears that in trophoblast cells, canonical Wnt signaling may regulate more genes promoting differentiation and invasion rather than proliferation.
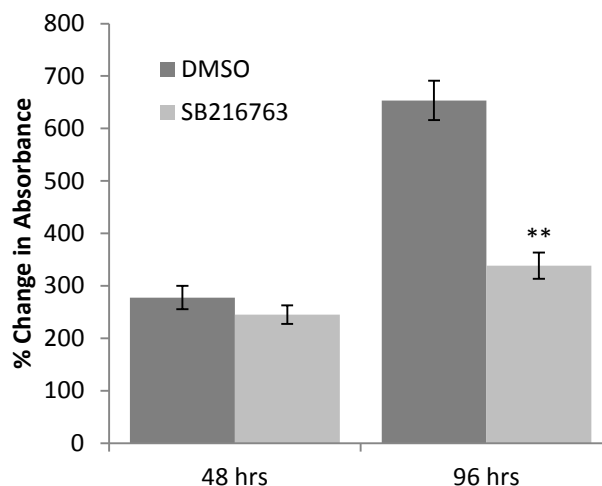
Figure IV-4. Proliferation decreases in ACH3P cells when treated with GSK3β inhibitor.
ACH-3P cells were treated with GSK3β inhibitor (SB216763) or vehicle control (DMSO) for 24 hours. Cell metabolic activity was measure by CCK-8 assay 48 and 96 hours after treatment. ** indicates $p<0.01$ in Students t-test.

DNase I Footprinting of PRR15 5'-flanking region

We used DNase I footprinting to identify protected regions of the *PRR15* proximal promoter that may bind to transcriptional activators or repressors. The -824 promoter was divided into three over-lapping constructs which were amplified by PCR with a 6-FAM-labeled forward primer. These products were incubated with nuclear extract, digested with DNase I, and analyzed by capillary electrophoresis in an automated DNA sequencer following the protocol of Zianni et al.[335] Traces from reactions incubated with nuclear extract or BSA as a negative control were overlaid to identify regions in which the peak heights were lower for the samples incubated with nuclear extract, indicating regions that were protected from DNase I digestion (Figure IV-5).
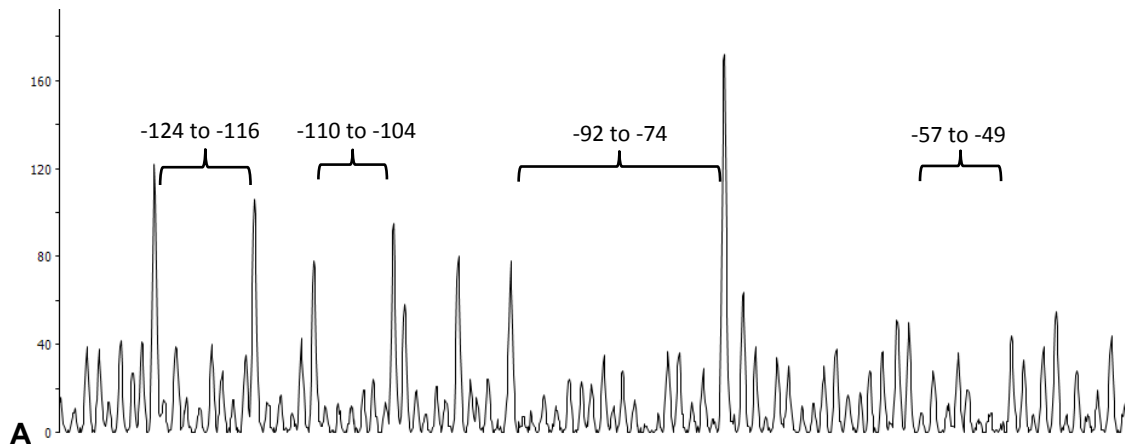
Figure IV-5. DNase I Footprinting of *PRR15* proximal promoter.
Representative trace from fragment analysis from DNase I footprinting of FAM-labeled probe incubated with ACH-3P nuclear extract. Brackets delineate protected regions. Graph shows the region from -135 to -35 of the *PRR15* 5'-flanking region.

Protected regions, or footprints, were identified throughout the *PRR15* proximal promoter. These regions were searched for putative transcription factor binding sites using TESS (Table IV-1). The most distal probe from -510 to -855 bp did not reveal any discernible protected regions. This is not expected, because the reporter activity demonstrated significant transactivation when the region from -640 to -824 was added to the construct, suggesting transcriptional activators are binding in this region. The base composition of this probe may affect DNase I digestion, making certain regions of the probe less accessible to digestion in the samples incubated with BSA. This could mask any difference between samples incubated with BSA or nuclear extract.

Table IV-1. Protected regions of the *PRR15* proximal promoter.

Region	Putative Transcription Factor Binding Sites
-453 to -435	POU3F2
-414 to -396	GT-IIBα, LEF/TCF, HSTF, YY1
-237 to -217	Yi, GAL4, Hb, YY1, POU3F2, POU1F1a
-196 to -176	T-Ag, LEF/TCF
-144 to -131	
-110 to -104	
-92 to -74	Sp1, LEF/TCF, GT-IIBα, HSTF, NF-1, AP-1, CBF
-57 to -49	
-32 to -19	GATA-1, CACCC-binding factor, PuF

DNase I footprinting identified protected regions of the *PRR15* proximal promoter that included binding sites for TCF-LEF, YY1, Sp1, and AP-1. TCF-LEF transcription factors are mediators of Wnt signaling, and may be involved in transcriptional repression of the *PRR15* gene. Yin Yang 1 (YY1) is widely expressed and can activate or repress transcription; it is expressed in the early murine trophectoderm and when disrupted, causes embryonic lethality shortly after implantation.[346] Specificity protein 1 (Sp1) can also act as an activator or repressor of transcription, and is involved in regulation of murine trophoblast cell differentiation.[347] It is involved in activating or enhancing expression of several genes crucial to trophoblast development, such as syncytin-1,[348] placental lactogen,[349] and matrix metalloproteinase 2 (MMP-2).[350] In bovine trophoblast, its expression is low during conceptus elongation (gestational days 15-18) but increases significantly after implantation at gestational day 25.[351] Activator protein 1 (AP-1) is a family of transcription factors that bind as a dimer consisting of Jun, Fos, and Fra proteins to a consensus DNA element.[352] AP-1 transcription factors have been implicated in trophoblast invasion[353,354] and are expressed primarily in human extravillous trophoblast as well as elongating bovine

trophectoderm.[355,356] C-fos, a component of the AP-1 transcription factor, mRNA and protein were detected in high amounts in ovine conceptuses prior to attachment and decreased after attachment to the uterine epithelium.[357] Lack of JunB in mice causes embryonic lethality due to impaired placental labyrinth development.[358] These studies demonstrate a central function for AP-1 transcription factors during early placentation. The specific factors binding to the *PRR15* proximal promoter remain to be determined.

Electrophoretic Mobility Shift Assay

Electrophoretic mobility shift assays were performed using oligonucleotides designed with the consensus TCF-LEF binding site, as well as oligonucleotides specific to the *PRR15* 5'-flanking region from -98 to -68. The TCF-LEF oligonucleotides demonstrated a shift only when incubated with nuclear extract from ACH-3P cells treated with the GSK3β inhibitor (SB216763, Figure IV-6A). Addition of 200-fold molar excess of unlabeled oligonucleotides was able to effectively inhibit binding, suggesting a specific protein-DNA interaction. This infers that nuclear β-catenin is required in order to observe a specific protein-DNA interaction for the TCF-LEF consensus sequence. When analyzing the -98 to -68 oligonucleotides, we observed a shift for both the DMSO- and SB216763-treated nuclear extract that were both inhibited by the addition of 200-fold molar excess unlabeled oligonucleotides (Figure IV-6B). Intriguingly, the migration of this shift changed in the two different extracts, migrating more rapidly in the SB216763-treated extract. These results suggest that the composition of the

protein or protein complex binding to the -98 to -68 oligonucleotides changes after treatment of ACH-3P cells with the GSK3β inhibitor.
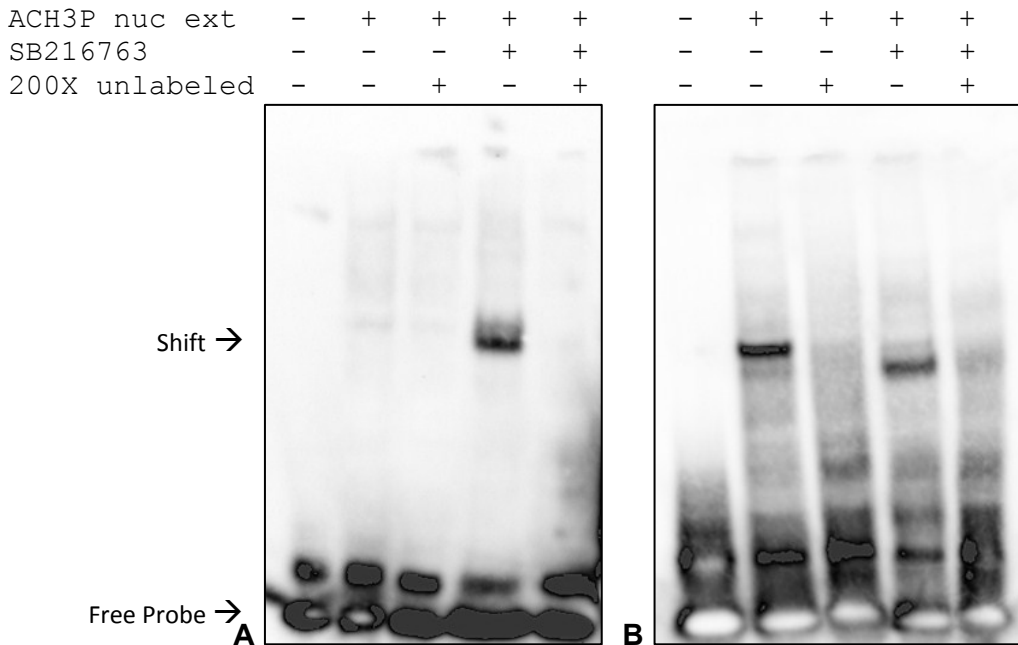
Figure IV-6. Electrophoretic mobility shift assay.
(A) Biotinylated oligonucleotides containing the consensus TCF-LEF binding site were incubated in the presence of ACH-3P nuclear extract treated with vehicle or GSK3β inhibitor (SB216763) and electrophoresed through a 5% polyacrylamide gel. A 200-fold molar excess of unlabeled oligonucleotides was added in lanes 3 and 5. (B) Biotinylated oligonucleotides from -98 to -68 of the *PRR15* proximal promoter were incubated in the presence of ACH-3P nuclear extract treated with vehicle or GSK3β inhibitor (SB216763) and electrophoresed through a 5% polyacrylamide gel. A 200-fold molar excess of unlabeled oligonucleotides was added in lanes 3 and 5.

The -98 to -68 oligonucleotides contain additional putative transcription factor binding sites other than TCF-LEF, including activator protein 1 (AP-1), Sp1, and CCAAT-binding factor (CBF). These factors may compete with TCF-LEF transcription factors for binding to this region of the *PRR15* promoter. Special AT-rich binding protein 1 (SATB1), a DNA-binding protein, was shown to compete with TCFs for binding to β-catenin and thus affect TCF-mediated transcription.[359] These two factors do not bind to the same target sequence on

DNA, but both interact with β-catenin to influence the transcription of target genes. In our experiments, the protein-DNA interaction observed in the -98 to -68 oligonucleotides could be due to a number of transcriptional regulators; antibodies specific to these factors will help to identify the protein binding this region. The protein(s) binding in the DMSO-treated reactions are likely activating *PRR15* transcription, while the protein(s) derived from the SB216763-treated extract may be repressing transcription of *PRR15* through the interaction with this region.

Transcriptional activity of *PRR15* in response to canonical Wnt signaling in trophoblast cells appears to be contrary to the typical activation by β-catenin-TCF-LEF complexes; *PRR15* mRNA concentrations and promoter activity decrease in conditions with augmented β-catenin activity. Furthermore, inhibition of GSK3β causes a reduction in trophoblast cell proliferation in culture. We observed a similar reduction in proliferation after depleting cells of *PRR15* using RNAi (Chapter III); these data support the hypothesis that PRR15 may promote trophoblast cell proliferation. During conceptus elongation, *PRR15* mRNA concentrations rise and peak at the point of initial conceptus attachment, followed by a decline to day 30 of gestation.[75] These data infer that canonical Wnt signaling may play a role in repressing transcription of *PRR15* prior to and following this period of dramatic trophectoderm outgrowth. During outgrowth, it appears PRR15 is required for normal trophoblast proliferation and survival (Chapter III). The transcriptional activators and repressors responsible for its up- and down-regulation during placental development remain to be specifically

identified. Understanding the pathways which regulate *PRR15* transcription will reveal pathways that may be affected during early embryonic loss and dysfunctional placentation.

Summary

Proline-rich 15 (PRR15) is a low molecular weight nuclear protein expressed by the trophoblast during early gestation in several mammalian species, including humans, mice, cattle, sheep, and horses. Immunohistochemistry localized PRR15 to the trophectoderm and extraembryonic endoderm of day 15 sheep conceptuses. In humans, PRR15 was immunolocalized to the nuclei of both first and second trimester trophoblast cells. *PRR15* mRNA expression increases when trophoblast cells, both sheep (oTR) and human (ACH-3P), are cultured on Matrigel, a basement membrane matrix. The expression profile in the sheep conceptus during pregnancy revealed a peak in expression at day 16 of gestation. This coincides with a halt in elongation of the conceptus, and the period of apposition to the uterine epithelium. Additional research has shown increased *PRR15* transcription in colorectal cancers with mutations in the Apc protein, suggesting a link to the Wnt signaling pathway. Lentiviral-mediated knockdown of *PRR15* in ovine trophectoderm at the blastocyst stage led to demise of the embryo by gestational day 15. This provides compelling evidence that PRR15 is a critical factor during this window of development where proliferation gives way to differentiation of the trophoblast cells. The aims of these experiments were to examine regions of the *PRR15* promoter necessary for regulating its expression in trophoblast cells and to

identify the role of Wnt signaling in *PRR15* transcription. The 5'-flanking sequences from -824, -640, -424, -326, and -284 bp to +7 bp relative to the transcription start site were amplified by PCR and ligated into pGL3-Basic. These vectors were co-transfected into the first trimester human trophoblast cell line, ACH-3P, HT29 (human colorectal carcinoma), oTR, and BHK-21 (hamster kidney fibroblast) with a RSV-β-galactosidase vector control. In ACH-3P cells, transactivation of the luciferase reporter was maximal with the -326 construct (15.4 ± 4.8-fold). Significant promoter activity was absent in the -284, -424, and -640 constructs, but regained with the -824 construct (14.8 ± 5.8-fold). These results suggest that *cis*-acting elements within the proximal promoter of the *PRR15* gene are essential for expression in trophoblast cells, requiring the regions from -284 to -326 and -640 to -824. DNase I footprinting and electrophoretic mobility shift assays were used to identify transcription factor binding sites within these regions. Due to the potential link to the Wnt signaling pathway, cells were treated with an inhibitor to GSK3β, the kinase responsible for phosphorylation and proteasomal degradation of β-catenin. Inhibition of GSK3β decreased *PRR15* mRNA concentrations and decreased transactivation of the luciferase reporter in all proximal promoter reporter constructs; this effect was mediated through β-catenin activity. Furthermore, trophoblast cell proliferation decreased after treatment with the GSK3β inhibitor. Electrophoretic mobility shift assays on the region from -98 to -68 revealed differential binding of nuclear proteins derived from ACH-3P cells grown in the presence or absence of the GSK3β inhibitor. These results reveal that canonical Wnt signaling inhibits the

99

transcription of *PRR15*, mediated in part through the -98 to -68 region of the 5'-flanking region, and decreases proliferation in trophoblast cells. This indicates that suppression of Wnt signaling may be crucial during early trophectoderm outgrowth in order to allow significant transcriptional activation of *PRR15* and conceptus survival.

REFERENCES

1. Wilcox AJ, Weinberg CR, O'Connor JF, Baird DD, Schlatterer JP, Canfield RE, Armstrong EG, Nisula BC. Incidence of early loss of pregnancy. N Engl J Med. 1988; 319(4):189-194.

2. Simpson JL. Genes, chromosomes and reproductive failure. Fertil Steril 1980; 33(2):107-116.

3. Carrington B, Sacks G, Regan L. Recurrent miscarriage: pathophysiology and outcome. Curr Opin Obstet Gynecol 2005; 17, 591–597.

4. Toth B, Jeschke U, Rogenhofer N, Scholz C, Würfel W, Thaler CJ, Makrigiannakis A. Recurrent miscarriage: current concepts in diagnosis and treatment. J Reprod Immunol. 2010; 85(1):25-32.

5. Norwitz ER, Schust DJ, Fisher SJ. Implantation and the Survival of Early Pregnancy. N Engl J Med 2001; 345(19):1400-1408

6. Meekins JW, Pijnenborg R, Hanssens M, McFadyen IR, van Asshe A. A study of placental bed spiral arteries and trophoblast invasion in normal and severe pre-eclamptic pregnancies. Br J Obstet Gynaecol 1994;101:669-674.

7. Huppertz B. Placental pathology in pregnancy complications. Thromb Res 2011; 127 Suppl 3:S96-S99.

8. Sibai BM, Caritis SN, Thom E, Klebanoff M, McNellis D, Rocco L, Paul RH, Romero R, Witter F, Rosen M, Depp R. Prevention of preeclampsia with low-dose aspirin in healthy, nulliparous pregnant women. N Engl J Med 1993; 329(17):1213-1218.

9. Kaunitz AM, Hughes JM, Grimes DA, Smith JC, Rochat RW, Kafriseen ME. Causes of maternal mortality in the United States. Obstet Gynecol 1985; 65(5):605-612.

10. Christiansen LR, Collins KA. Pregnancy-associated deaths: a 15-year retrospective study and overall review of maternal pathphysiology. Am J For Med Pathol 2006; 27(1):11-19.

11. Varvarigou AA. Intrauterine growth restriction as a potential risk factor for disease onset in adulthood. J Ped Endocrin Metab 2010; 23(3):215-224.

12. Bernstein I, Gabbe SG. Intrauterine growth restriction. In: Gabbe SG, Niebyl JR, Simpson JL, Annas GJ, et al., editors, Obstetrics: normal and problem pregnancies, 3rd ed., New York: Churchill Livingstone; 1996. pp. 863-886.

13. Arulkumaran S, Bennett PR. Pathophysiology of Preterm Birth. In: Polin RA, Fox WW, Abman SH (eds), Fetal and Neonatal Physiology, vol 1, 2nd ed., Philadelphia: Elsevier Saunders; 2011.

14. Behrman RE, Butler AS. Preterm Birth: Causes, Consequences and Prevention. National Academy of Sciences 2007; 398-429. <http://www.ncbi.nlm.nih.gov/bookshelf/br.fcgi?book=nap11622&part=a20012272ddd00314>

15. Berg CJ, Mackay AP, Qin C, Callaghan WM. Overview of maternal morbidity during hospitalization for labor and delivery in the United States: 1993–1997 and 2001–2005. Obstet Gynecol 2009; 113:1075-1081.

16. Shevell T, Malone FD, Vidaver J, Porter TF, Luthy DA, Comstock CH, Hankins GD, Eddleman K, Dolan S, Dugoff L, Craigo S, Timor IE, Carr SR, Wolfe HM, Bianchi DW, D'Alton ME. Assisted reproductive technology and pregnancy outcome. Obstet Gynecol 2005; 106(5):1039-1045.

17. Bellamy L, Casas JP, Hingorani AD, Williams DJ. Pre-eclampsia and risk of cardiovascular disease and cancer in later life: systematic review and meta-analysis. Brit Med J 2007; 335:974.

18. Lockwood CJ and Paidas MJ. Preeclampsia and hypertensive Disorders. Cherry and Merkatz's Complications of Pregnancy 2000; 5th Edition. Lippincott Williams & Wilkins, Philadelphia 207-229.

19. Carty DM, Delles C, Dominizcak AF. Novel biomarkers for predicting preeclampsia. Trends Cardio Med 2008; 18(5-24):186-194.

20. Grill S, Rusterholz C, Zanetti-Dallenbach R, Tercanli S, Holzgreve W, Hahn S, Lapaire O. Potential markers of preeclampsia – a review. Reprod Biol Endocr 2009; 7:70.

21. Hertig A, Liere P. New markers in preeclampsia. Int J Clin Chem 2010; 411(21-22):1591-1595.

22. Kenny LC, Broadhurst DI, Dunn W, Brown M, North RA, McCowan L, Roberts C, Cooper GJS, Bell DB, Baker PN. Robust early pregnancy prediction of later preeclampsia using metabolomic biomarkers. Hypertension 2010; 56:741-749.

23. Sibai BM. Diagnosis and management of gestational hypertension and preeclampsia. Obstet Gynec 2003; 102:181-192.

24. Phillips JK, Janowiak M, Badger GJ, Bernstein IM. Evidence for distinct preterm and term phenotypes of preeclampsia. J Mat Fet Neonat Med 2010; 23(7):622-626.

25. Huppertz B. Placental pathology in pregnancy complications. Thromb Res 2011; 127 Suppl 3:S96-9.

26. Huppertz B. The anatomy of the normal placenta. J Clin Pathol 2008; 61:1296-1302. doi:10.1136/jcp.2008.055277

27. Enders AC. Trophoblast differentiation during the transition from trophoblastic plate to lacunar stage of implantation in the rhesus monkey and human. Am J Anat 1989; 186:185.

28. Frank HG. Placental Development. In: Polin RA, Fox WW, Abman SH (eds), Fetal and Neonatal Physiology, vol 1, 2nd ed., Philadelphia: Elsevier Saunders; 2011.

29. Benirschke K, Kaufmann P, Baergen R. Pathology of the Human Placenta. ed 5. New York: Springer, 2006.

30. Hamilton WJ, Boyd JD. Development of the human placenta in the first three months of gestation. J Anatomy 1960; 94:297-328.

31. Okudaira Y., Hashimoto T., Hamanaka N., Yoshinare S.: Electron microscopic study on the trophoblastic cell column of human placenta. J Electron Microsc (Tokyo) 1971; 20:93.

32. Enders AC. Fine structure of anchoring villi of the human placenta. Am J Anat 1968; 122:419.

33. Enders AC, Blankenship TN, Fazleabas AT, Jones CJ. Structure of anchoring villi and the trophoblastic shell in the human, baboon and macaque placenta. Placenta 2001; 22:284.

34. Caniggia I, Winter J, Lye SJ, Post M. Oxygen and placental development during the first trimester: Implications for the pathophysiology of pre-eclampsia. Placenta 2000; 21(Suppl A):S25-S30.

35. Huppertz B, Gauster M, Orendi K, König J, Moser G. Oxygen as modulator of trophoblast invasion. J Anat 2009; 215:14-20.

36. Jauniaux E, Gulbis B, Burton GJ. Physiological implications of the materno-fetal oxygen gradient in human early pregnancy. Reprod Biomed Online 2003; 7:250-253.

37. Norwitz ER, Schust DJ, Fisher SJ. Implantation and the Survival of Early Pregnancy. N Engl J Med 2001; 345(19):1400-1408.

38. Woelkers DA. Maternal Cardiovascular Disease and Fetal Growth and Development. In: Polin RA, Fox WW, Abman SH (eds), Fetal and Neonatal Physiology, vol 1, 2nd ed., Philadelphia: Elsevier Saunders; 2011(pages?)

39. Benirschke K., Kaufmann P., Baergen R.: Pathology of the Human Placenta. ed 5. New York, Springer, 2006.

40. Benirschke K., Kaufmann P., Baergen R.: Pathology of the Human Placenta. ed 5. New York, Springer, 2006.

41. Lunghi L, Ferretti ME, Medici S, Biondi C, Vesce F. Control of human trophoblast function. Reprod Biol Endocrinol 2007; 5:6.

42. Frank HG, Kaufmann P. Nonvillous parts and trophoblast invasion. In: Benirschke K, Kaufmann P, Baergen R (eds), Pathology of the Human Placenta, 5th ed., New York: Springer; 2006 (194).

43. Rodesch F, Simon P, Donner C, Jauniaux E. Oxygen measurements in endometrial and trophoblastic tissues during early pregnancy. Obstet Gynecol. 1992; 80(2):283-285.

44. Lunghi L, Ferretti ME, Medici S, Biondi C, Vesce F. Control of human trophoblast function. Reprod Biol Endocrinol 2007; 5:6.

45. Alsat E, Wyplosz P, Malassiné A, Guibourdenche J, Porquet D, Nessmann C, Evain-Brion D. Hypoxia impairs cell fusion and differentiation process in human cytotrophoblast, in vitro. J Cell Physiol 1996; 168(2):346-353.

46. Hu R, Jin H, Zhou S, Yang P, Li X. Proteomic analysis of hypoxia-induced responses in the syncytialization of human placental cell line BeWo. Placenta 2007; 28:399-407.

47. James JL, Stone PR, Chamley LW. The regulation of trophoblast differentiation by oxygen in the first trimester of pregnancy. Hum Reprod Update 2006; 12(2):137-144.

48. Caniggia I, Mostachfi H, Winter J, Gassman M, Lye SJ, Kuliszewski M and Post M. Hypoxia inducible factor 1 mediates the biological effects of oxygen on human trophoblast differentiation through TGFbeta3. J Clin Invest 2000; 105:577–587.

49. James JL, Stone PR, Chamley LW. The effect of hypoxia on extravillous trophoblast outgrowth in a quantitative two-dimensional explant model. Placenta 2004; 25:A17.

50. Huppertz B, Borges M. Placenta trophoblast fusion. In: Chen EH (ed), Cell Fusion: Overviews and Methods, Totowa, NJ: Humana Press, 2008 (138).

51. Adler RR, Ng AK, Rote N. Monoclonal antiphosphatidylserine antibody inhibits intercellular fusion of the choriocarcinoma line JAR. Biol Reprod 1995; 53:905-910.

52. Black S, Kadyrov M, Kaufmann P, Ugele B, Emans N, Huppertz B. Syncytial fusion of human trophoblast depends on caspase 8. Cell Death Differ 2004; 11(1):90-98.

53. Frendo JL, Cronier L, Bertin G, Guibourdenche J, Vidaud M, Evain-Brion D, Malassine A. Connexin expression and gap junctional communication in human first trimester trophoblast. Mol Hum Reprod 2003; 8:1005-1013.

54. Getsios S, MacCalman CD. Cadherin-11 modulates the terminal differentiation and fusion of human trophoblastic cells in vitro. Dev Biol 2002; 257:41-54.

55. Kudo Y, Boyd CA. RNA interference-induced reduction in CD98 expression suppresses cell fusion during syncytialization of human placental BeWo cells. FEBS Lett 2004; 577:473-477.

56. Fischer I, Redel S, Hofmann S, Kuhn C, Friese K, Walzel H, Jeschke U. Stimulation of syncytium formation in vitro in human trophoblast cells by galectin-1. Placenta 2010; 31:825-832.

57. Langbein M, Strick R, Strissel PL, Vogt N, Parsch H, Beckmann MW, Schild RL. Impaired cytotrophoblast cell-cell fusion is associated with reduced syncytin and increased apoptosis in patients with placenta dysfunction. Mol Reprod Dev 2008; 75:175-183.

58. Vargas A, Toufaily C, LeBellego F, Rassart E, Lafond J, Barbeau B. Reduced expression of both syncytin 1 and syncytin 2 correlates with severity of preeclampsia. Reprod Sci 2011; 18(11):1085-1091.

59. Kauma SW, Bae-Jump V, Walsh SW. Hepatocyte growth factor stimulates trophoblast invasion: a potential mechanism for abnormal placentation in preeclampsia. J Clin Endocrinol Metab 1999; 84:4092-4096.

60. Uehara Y, Minowa O, Mori C, Shiota K, Kuno J, Noda T, Kitamura N. Placental defect and embryonic lethality in mice lacking hepatocyte growth factor / scatter factor. Nature 1995; 373:702-705.

61. Tapia A, Salamonsen LA, Manuelpillai U, Dimitriadis E. Leukemia inhibitory factor promotes human first trimester extravillous trophoblast adhesion to extracellular matrix and secretion of tissue inhibitor of mattloproteinases-1 and -1. Hum Reprod 2008; 23:1724-1732.

62. Lacroix MC, Guibourdenche J, Fournier T, Laurendeau I, Igout A, Goffin V, Pantel J, Tsatsaris V, Evain-Brion D. Stimulation of human trophoblast invasion by placental growth hormone. Endocrinology 2005; 146(5):2434-2444.

63. Staun-Ram E, Goldman S, Gabarin D, Shalev E. Expression and importance of matrix metalloproteinase 2 and 9 (MMP-2 and -9) in human trophoblast invasion. Reprod Biol Endocrinol 2004; 2:59.

64. Zhao MR, Qiu W, Li YX, Zhang ZB, Li D, Wang YL. Dual effect of transforming growth factor beta1 on cell adhesion and invasion in human placenta trophoblast cells. Reproduction 2006; 132(2):333-341.

65. Karmakar S, Das C. Modulation of ezrin and E-cadherin expression by IL-1beta and TGF-beta1 in human trophoblasts. J Reprod Immunol 2004; 64(1-2):9-29.

66. Janatpour MJ, McMaster MT, Genbacev O, Zhou Y, Dong J, Cross JC, Israel MA, Fisher SJ. Id-2 regulates critical aspects of human cytotrophoblast differentiation, invasion and migration. Development 2000; 127(3):549-558.

67. Redline RW, Patterson P (1995) Pre-eclampsia is associated with an excess of proliferative immature intermediate trophoblast. Human Pathology 26(6):594-600.

68. Lim KH, Zhou Y, Janatpour M, McMaster M, Bass K, Chun SH, Fisher SJ (1997) Human cytotrophoblast differentiation/invasion is abnormal in pre-eclampsia. American Journal of Pathology 151(6):1809-1818.

69. Janatpour MJ, Utset MF, Cross JC, Rossant J, Dong J, Israel MA, Fisher SJ (1999) A repertoire of differentially expressed transcription factors that offers insight into mechanisms of human cytotrophoblast differentiation. Developmental Genetics 25:146-157.

70. Janatpour MJ, McMaster MT, Genbacev O, Zhou Y, Dong J, Cross JC, Israel MA, Fisher SJ (2000) Id-2 regulates critical aspects of human cytotrophoblast differentiation, invasion and migration. Development 127:549-558.

71. Di Simone N, Di Nicuolo F, Sanguinetti M, Ferrazzani S, D'Alessio MC, Castellani R, Bompiani A, Caruso A. Low-molecular weight heparin induces in vitro trophoblast invasiveness: role of matrix metalloproteinases and tissue inhibitors. Placenta 2007; 28(4):298-304.

72. Hills FA, Mehmet H, Sullivan MH. Insulin-like growth factor-II and heparin are anti-apoptotic survival factors in human villous cytotrophoblast. Eur J Obstet Gynecol Reprod Biol 2012; Apr 7 [Epub ahead of print].

73. Okada Y, Ueshin Y, Isotani A, Saito-Fujita T, Nakashima H, Kimura K, Mizoguchi A, Oh-hora M, Mori Y, Ogata M, Oshima R, Okabe M, et al. Complementation of placental defects and embryonic lethality by trophoblast-specific lentiviral gene transfer. Nat Biotech 2007; 25:233-237.

74. Georgiades P, Cox B, Gertsenstein M, Chawengsaksophak K, Rossant J. Trophoblast specific gene manipulation using lentivirus-based vectors. Biotechniques 2007; 42:317–324.

75. Purcell SH, Cantlon JD, Wright CD, Henkes LE, Seidel GE Jr, Anthony RV. The involvement of proline-rich 15 in early conceptus development in sheep. Biol Reprod. 2009 Dec;81(6):1112-21.

76. Anthony RV, Cantlon JD, Gates KC, Purcell SH, Clay CM. Assessing gene function in the ruminant placenta. Soc Reprod Fertil Suppl 2010;67:119-31.

77. Founds SA, Conley YP, Lyons-Weiler JF, Jeyabalan A, Hogge WA, Conrad KP. Altered global gene expression in first trimester placentas of women destined to develop preeclampsia. Placenta. 2009; 30(1):15-24.

78. Founds SA, Terhorst LA, Conrad KP, Hogge WA, Jeyabalan A, Conley YP. Gene expression in first trimester preeclampsia placenta. Biol Res Nurs. 2011; 13(2):134-139.

79. Founds SA. Bridging global gene expression candidates in first trimester placentas with susceptibility loci from linkage studies of preeclampsia. J Perinat Med 2011; 39(4):361-368.

80. Farina A, Morano D, Arcelli D, De Sanctis P, Sekizawa A, Purwosunu Y, Zucchini C, Simonazzi G, Okai T, Rizzo N. Gene expression in chorionic villous samples at 11 weeks of gestation in women who develop preeclampsia later in pregnancy: implications for screening. Prenat Diagn 2009; 29(11):1038-1044.

81. Evans MI, Andriole S (2008) Chorionic villus sampling and amniocentesis in 2008. Curr Opin Obstet Gynecol 20(2):164-168.

82. Yong PJ, McFadden DE, Robinson WP. Developmental origin of chorionic villus cultures from spontaneous abortion and chorionic villus sampling. J Obstet Gynaecol Can 2011; 33(5):449-452.

83. Genbacev O, Zhou Y, Ludlow JW, Fisher SJ. Regulation of human placental development by oxygen tension. Science 1997; 277: 1669-1672.

84. Miller RK, Genbacev O, Turner MA, Aplin JD, Caniggia I, Huppertz B. Human placental explants in culture: approaches and assessments. Placenta 2005; 26:439-448.

85. Huppertz B, Kingdom J, Caniggia I, Desoye G, Black S, Korr H, et al. Hypoxia favours necrotic versus apoptotic shedding of placental syncytiotrophoblast into the maternal circulation. Placenta 2003; 24:181-190.

86. Forbes K, Desforges M, Garside R, Aplin JD, Westwood M. Methods for siRNA-mediated reduction of mRNA and protein expression in human placental explants, isolated primary trophoblast cells and cell lines. Placenta 2009; 30:124-129.

87. Miller RK, Genbacev O, Turner MA, Aplin JD, Caniggia I, Huppertz B. Human placental explants in culture: approaches and assessments. Placenta 2005; 26:439-448.

88. Kliman HJ, Nestler JE, Sermasi E, Sanger JM, Strauss JF. Purification, characterization, and in vitro differentiation of cytotrophoblasts from human term placentae. Endocrinology 1986; 118:1567-1582.

89. Morrish DW, Dakour J, Li H, Xiao J, Miller R, Sherburne R, Berdan RC, Guilbert LJ. In vitro cultured human term cytotrophoblast: a model for normal primary epithelial cells demonstrating a spontaneous differentiation programme that requires EGF for extensive development of syncytium. Placenta 1997; 18:577-585.

90. Tarrade A, Goffin F, Munaut C, Lai-Kuen R, Tricottet V, Foidart JM, Vidaud M, Frankenne F, Evain-Brion D. Effect of matrigel on human extravillous trophoblasts differentiation: modulation of protease pattern gene expression. Biol Reprod 2002; 67(5):1628-1637.

91. Frank HG, Morrish DW, Potgens A, Genbacev O, Kumpel B, Caniggia I. Trophoblast model systems: Cell culture models of human trophoblast: primary culture of trophoblast – a workshop report. Placenta 2001; 22:S107-S109.

92. Oh SY, Chu T, Sadovsky Y. The timing and duration of hypoxia determine gene expression in primary culture human trophoblasts. Placenta 2011; 32:1004-1009.

93. Nagamatsu T, Fujii T, Ishikawa T, Kanai T, Hyodo H, Yamashita T, Osuga Y, Momoeda M, Kozuma S, Taketani Y. A primary cell culture system for human cytotrophoblasts of proximal cytotrophoblast cell columns enabling in vitro acquisition of the extra-villous phenotype. Placenta 2004; 25:153-165.

94. Sullivan MH. Endocrine cell lines from the placenta. Mol Cell Endocrinol. 2004; 228(1-2):103-119.

95. Blaschitz A, Weiss U, Dohr G, Desoye G. Antibody reaction patterns in first trimester placenta: implications for trophoblast isolation and purity screening. Placenta 2000; 21:733-741.

96. Potgens AJ, Bolte M, Huppertz B, Kaufmann P, Frank HG. Human trophoblast contains an intracellular protein reactive with an antibody against CD133—a novel marker for trophoblast. Placenta 2001; 22:639–645.

97. Graham CH, Hawley TS, Hawley RG, MacDougall JR, Kerbel RS, Khoo N, Lala PK. Establishment and characterization of first trimester human trophoblast cells with extended lifespan. Exp Cell Res 1993; 206:204-211.

98. Choy MY, Manyonda IT. The phagocytic activity of human first trimester extravillous trophoblast. Hum Reprod. 1998; 13(1O):2941-2949.

99. Funayama H, Gaus G, Ebeling I, Takayama M, Fuzesi L, Huppertz B, Kaufmann P, Frank HG. Parent cells for the trophoblast hybridization II: AC1 and related trophoblast cell lines, a family of HGPRT-negative mutants of the choriocarcinoma cell line JEG-3. Troph Res 1997; 10:191-201.

100. Hiden U, Wadsack C, Prutsch N, Gauster M, Weiss U, Frank HG, Schmitz U, Fast-Hirsch C, Hengstschläger M, Pötgens A, Rüben A, Knöfler M, Haslinger P, Huppertz B, Bilban M, Kaufmann P, Desoye G. The first trimester human trophoblast cell line ACH-3P: a novel tool to study autocrine/paracrine regulatory loops of human trophoblast subpopulations--TNF-alpha stimulates MMP15 expression. BMC Dev Biol 2007; 7:137.

101. Straszewski-Chavez SL, Abrahams VM, Alvero AB, Aldo PB, Ma Y, Guller S, Romero R, Mor G. The isolation and characterization of a novel telomerase immortalized first trimester trophoblast cell line, Swan 71. Placenta 2009; 30(11):939-948.

102. Apps R, Gardner L, Moffett A. A critical look at HLA-G. Trends Immunol 2008; 29(7):313-321.

103. Apps R, Murphy SP, Fernando R, Gardner L, Ahad T, Moffett A. Human leucocyte antigen (HLA) expression of primary trophoblast cells and placental cell lines, determined using single antigen beads to characterize allotype specificities of anti-HLA antibodies. Immunology 2009; 127(1):26-39.

104. Feng HC, Choy MY, Deng W, Wong HL, Lau WM, Cheung AN, Ngan HY, Tsao SW. Establishment and characterization of a human first-trimester extravillous trophoblast cell line (TEV-1). J Soc Gynecol Investig 2005; 12(4):e21-e32.

105. Pattillo RA, Gey GO. The establishment of a cell line of human hormone-synthesizing trophoblastic cells in vitro. Cancer Res 1968; 28:1231-1236.

106. Risk JM, Johnson PM. Northern blot analysis of HLA-G expression by BeWo human choriocarcinoma cells. J Reprod Immunol 1990; 18:199-203.

107. Kovats S, Main EK, Librach C, Stubblebine M, Fisher SJ, DeMars R. A class I antigen, HLA-G, expressed in human trophoblasts. Science 1990; 248(4952):220-223.

108. Wice B, Menton D,Geuze H, Schwartz AL. Modulators of cyclic AMP metabolism induce syncytiotrophoblast formation in vitro. Exp Cell Res 1990; 186:306-316.

109. Bilban M, Tauber S, Haslinger P, Pollheimer J, Saleh L, Pehamberger H, Wagner O, Knöfler M. Trophoblast invasion: Assessment of cellular models using gene expression signatures. Placenta 2010; 31:989-996.

110. Hohn HP, Parker CR Jr, Boots LR, Denker HW, Höök M. Modulation of differentiation markers in human choriocarcinoma cells by extracellular matrix: on the role of a three-dimensional matrix structure. Differentiation 1992; 51(1):61-70.

111. Rajashekhar G, Loganath A, Roy AC, Chong SS, Wong YC. Extracellular matrix-dependent regulation of angiogenin expression in human placenta. J Cell Biochem 2005; 96(1):36-46.

112. Lei T, Hohn HP, Behr R, Denker HW. Influences of extracellular matrix and of conditioned media on differentiation and invasiveness of trophoblast stem cells. Placenta. 2007; 28(1):14-21.

113. Novakovic B, Gordon L, Wong NC, Moffett A, Manuelpillai U, Craig JM, Sharkey A, Saffery R. Wide-ranging DNA methylation differences of primary trophoblast cell populations and derived cell lines: implications and opportunities for understanding trophoblast function. Mol Hum Reprod. 2011; 17(6):344-353.

114. Genbacev O, Donne M, Kapidzic M, Gormley M, Lamb J, Gilmore J, Larocque N, Goldfien G, Zdravkovic T, McMaster MT, Fisher SJ. Establishment of human trophoblast progenitor cell lines from the chorion. Stem Cells 2011; 29(9):1427-1436. doi: 10.1002/stem.686.

115. James JL, Carter AM, Chamley LW. Human placentation from nidation to 5 weeks of gestation. Part II: Tools to model the crucial first days. Placenta 2012; 33(5):335-342.

116. Senger PL. Pathways to pregnancy and parturition. Pullman, USA: Current Conceptions Inc, 2nd ed., 2003.

117. Lee KY, DeMayo FJ. Animal models of implantation. Rperoduction 2004; 128:2152-2164.

118. Carter AM. Animal models of human placentation – a review. Placenta 2007; 21:S41-S47.

119. Barry JS, Anthony RV. The pregnant sheep as a model for human pregnancy. Theriogenology 2008; 69(1):55-67.

120. Beam SW, Butler WR. Energy balance effects on follicular development and first ovulation in post-partum cows. J Reprod Fertil Suppl 1999; 54:411-424.

121. Royal MD, Flint APF, Darwash AO, Webb R, Woolliams JA, Lamming GE. Declining fertility in dairy cattle: changes in traditional and endocrine parameters of fertility. Anim Sci 2000; 70:487-501.

122. Gerrits RJ, Blosser TH, Purchase HG, Terrill CE, Warwick EJ. Economics of improving reproductive efficiency in farm animals. In Beltsville Symposia in Agricultural Research, Hawk HW ed. Animal Reproduction. Allenheld, Osmun: Monclair, NJ, 1979; pp. 413-421.

123. Sreenan JM, Diskin MG. Early embryonic mortality in the cow: its relationship with progesterone concentration. Vet Rec 1983; 112(22):517-521.

124. Berg DK, van Leeuwen J, Beaumont S, Berg M, Pfeffer PL. Embryo loss in cattle between Days 7 and 16 of pregnancy. Theriogenology 2010; 73(2):250-260.

125. Diskin MG, Sreenan JM. Fertilization and embryonic mortality rates in beef heifers after artificial insemination. J Reprod Fertil 1980; 59(2):463-468.

126. Moore DA, Overton MW, Chebel RC, Truscott ML, BonDurant RH. Evaluation of factors that affect embryonic loss in dairy cattle. J Am Vet Med Assoc 2005; 226(7):1112-1118.

127. Humblot P. Use of pregnancy specific proteins and progesterone assays to monitor pregnancy and determine the timing, frequencies and sources of embryonic mortality in ruminants. Theriogenology 2001; 56:1417–1433.

128. Alosta RA, Vaughan L, Collins JD. An abattoir survey of ovine reproductive tracts in Ireland. Theriogenology. 1998; 50(3):457-464.

129. Bolet G. Timing and extent of embryonic mortality in pigs, sheep, and goats: Genetic variability. In Embryonic Mortality in Farm Animals. J. M. Sreenan, and M. G. Diskin, ed. Dordrecht, Boston, MA. 1986; pp. 12-43.

130. Dixon AB, Knights M, Winkler JL, Marsh DJ, Pate JL, Wilson ME, Dailey RA, Seidel G, Inskeep EK. Patterns of late embryonic and fetal mortality and association with several factors in sheep. J Anim Sci 2007; 85(5):1274-1284.

131. Cross JC, Werb Z, Fisher SJ. Implantation and the placenta: key pieces of the development puzzle. Science 1994; 266(5190):1508-1518.

132. Binelli M, Thatcher WW, Mattos R, Baruselli PS. Antiluteolytic strategies to improve fertility in cattle. Theriogenology 2001; 56(9):1451-1463.

133. Spencer TE, Bazer FW. Conceptus signals for establishment and maintenance of pregnancy. Reprod Biol Endocrin 2004; 2:49.

134. Wu G, Bazer FW, Wallace JM, Spencer TE. Board-invited review: intrauterine growth retardation: implications for the animal sciences. J Anim Sci. 2006; 84(9):2316-2337.

135. Barry JS, Rozance PJ, Anthony RV. An animal model of placental insufficiency-induced intrauterine growth restriction. Semin Perinatol. 2008; 32(3):225-230.

136. Wallace JM, Regnault TR, Limesand SW, Hay WW Jr, Anthony RV. Investigating the causes of low birth weight in contrasting ovine paradigms. J Physiol 2005; 565(Pt 1):19-26.

137. Regnault TR, Galan HL, Parker TA, Anthony RV. Placental development in normal and compromised pregnancies-- a review. Placenta. 2002; 23 Suppl A:S119-S129.

138. Wooding FBP. Current topic: the synepitheliochorial placenta of ruminants: binucleate cell fusions and hormone production. Placenta 1992; 13:101-113.

139. Wooding FB. Role of binucleate cells in fetomaternal cell fusion at implantation in the sheep. Am. J. Anat. 1984; 170: 233–250. doi:10.1002/AJA.1001700208

140. Spencer TE, Johnson GA, Bazer FA, Burghardt RC, Palmarini M. Pregnancy recognition and conceptus implantation in domestic ruminants: roles of progesterone, interferons, and endogenous retroviruses. Reprod Fertil Develop 2007; 19:65-78.

141. Hue I, Degrelle SA, Campion E, Renard J-P. Gene expression in elongating and gastrulating embryos from ruminants. Reprod Domest Rumin 2007; 6(1): 365-377.

142. Degrelle SA, Campion E, Cabau C, Piumi F, Reinaud P, Richard C, Renard JP, Hue I. Molecular evidence for a critical period in mural trophoblast development in bovine blastocysts. Develop Biol 2005; 288:448-460.

143. Blomberg LA, Garrett WM, Guillomot M, Miles JR, Sonstegard TS, Van Tassell CP, Zuelke KA. Transcriptome Profiling of the Tubular Porcine Conceptus Identifies the Differential Regulation of Growth and Developmentally Associated Genes. Molec Reprod Devel 2006; 73(12):1491-1502.

144. Johnson GA, Bazer FW, Jaeger LA, Ka H, Garlow JE, Pfarrer C, Spencer TE, Burghardt RC. Muc-1, integrin, and osteopontin expression during the implantation cascade in sheep. Biol Reprod 2001; 65:820-828.

145. Burghardt RC, Johnson GA, Jaeger LA, Ka H, Garlow JE, Spencer TE, Bazer FW. Integrins and extracellular matrix proteins at the maternal–fetal interface in domestic animals. Cells Tissues Organs 2002; 171:202–217.

146. Spencer TE, Johnson GA, Bazer FW, Burghardt RC. Implantation mechanisms: insights from the sheep. Reproduction 2004; 128:657-668.

147. Martal J, Chene N, Camous S, Huynh L, Lantier F, Hermier P, L'Haridon R, Charpigny G, Charlier M, Chaouat G. Recent developments and potentialities for reducing embryo mortality in ruminants: the role of IFN-t and other cytokines in early pregnancy. Reprod Fertil Dev 1997; 9:355-380.

148. Ocón-Grove OM, Cooke FN, Alvarez IM, Johnson SE, Ott TL, Ealy AD. Ovine endometrial expression of fibroblast growth factor (FGF) 2 and conceptus expression of FGF receptors during early pregnancy. Domest Anim Endocrinol 2008; 34(2):135-145.

149. Yang QE, Johnson SE, Ealy AD. Protein kinase C delta mediates fibroblast growth factor-2-induced interferon-tau expression in bovine trophoblast. Biol Reprod 2011; 84(5):933-943.

150. Wooding FBP, Morgan G, Adam CL. Structure and function of the ruminant synepitheliochorial placenta: central role of the trophoblast binucleate cell in deer. Micro Res Tech 1997; 38:88-99.

151. Hashizume K, Ushizawa K, Patel OV, Kizaki K, Imai K, Yamada O, Nakano H, Takahashi T. Gene expression and maintenance of pregnancy in bovine: roles of trophoblastic binucleate cell-specific molecules. Reprod Fertil Devel 2007; 19(3364):79-90.

152. McNeill BA, Barrell GK, Wooding FB, Prickett TC, Espiner EA. The trophoblast binucleate cell is the source of maternal circulating C-type natriuretic peptide during ovine pregnancy. Placenta 2011; 32(9):645-650.

153. Anthony RV, Liang R, Kayl EP, Pratt SL. The growth hormone/prolactin gene family in ruminant placentae. J Reprod Fertil Suppl 1995; 49:83-95.

154. Corbacho AM, Martinez De La Escalera G, Clapp C. Roles of prolactin and related members of the prolactin/growth hormone/placental lactogen family in angiogenesis. J Endocrinol 2002; 173: 219-238.

155. Wooding FBP, Hobbs T, Morgan G, Heap RB, Flint APF. Cellular dynamics of growth in sheep and goat synepitheliochorial placentomes: An autoradiographic study. J Reprod Fertil 1993; 98:275-283.

156. Koshi K, Ushizawa K, Kizaki K, Takahashi T, Hashizume K. Expression of endogenous retrovirus-like transcripts in bovine trophoblastic cells. Placenta 2011; 32(7):493-499.

157. Dunlap KA, Palmarini M, Varela M, Burghardt RC, Hayashi K, Farmer JL, Spencer TE. Endogenous retroviruses regulate periimplantation placental growth and differentiation. Proc Natl Acad Sci USA 2006; 103(39):14390-14395.

158. Hoffman LH, Wooding FBP. Giant and binucleate trophoblast cells of mammals. J Exp Zool 1993; 266:559-577.

159. Dunlap KA, Palmarini M, Varela M, Burghardt RC, Hayashi K, Farmer JL, Spencer TE. Endogenous retroviruses regulate perrimplantation placental growth and differentiation. Proc Nat Acad Sci 2006; 103:14390-14395.

160. Stringfellow DA, Gray BW, Lauerman LH, Thomson MS, Rhodes PJ, Bird RC. Monolayer culture of cells originating from a preimplantation bovine embryo. In Vitro Cell Dev Biol 1987; 23:750-754.

161. Godkin JD, Bazer FW, Roberts RM. Protein production by cultures established from Day-14-16 sheep and pig conceptuses. J Reprod Fertil. 1985; 74(2):377-382.

162. Munson L, Chandler SK, Schlafer DH. Long-term culture of bovine trophoblastic cells. J Tissue Cult Methods 1988; (11):123-128.

163. Vanselow J, Furbass R, Tiemann U. Cultured bovine trophoblast cells differentially express genes encoding key steroid synthesis enzymes. Placenta 2008; 29(6):531–538.

164. Talbot NC, Caperna TJ, Edwards JL, Garrett W, Wells KD, Ealy AD. Bovine blastocyst-derived trophectoderm and endoderm cell cultures: interferon-t and transferrin expression as respective in vitro markers. Biol Reprod 2000; 62:235-247.

165. Michael DD, Wagner SK, Ocón OM, Talbot NC, Rooke JA, Ealy AD. Granulocyte-macrophage colony-stimulating-factor increases interferon-tau protein secretion in bovine trophectoderm cells. Am J Reprod Immunol 2006; 56(1):63-67.

166. Ezashi T, Das P, Gupta R, Walker A, Roberts RM. The role of homeobox protein distal-less 3 and its interaction with ETS2 in regulating bovine interferon-tau gene expression-synergistic transcriptional activation with ETS2. Biol Reprod 2008; 79(1):115-124.

167. Bai H, Sakurai T, Kim MS, Muroi Y, Ideta A, Aoyagi Y, Nakajima H, Takahashi M, Nagaoka K, Imakawa K. Involvement of GATA transcription factors in the regulation of endogenous bovine interferon-tau gene transcription. Mol Reprod Dev 2009; 76(12):1143-1152.

168. Shimada A, Nakano H, Takahashi T, Imai K, Hashizume K. Isolation and characterization of a bovine blastocyst-derived trophoblastic cell line, BT-1: development of a culture system in the absence of a feeder layer. Placenta 2001; 22:652-662.

169. Nakano H, Shimada A, Imai K, Takezawa T, Takahashi T, Hashizume K. Bovine trophoblastic cell differentiation on collagen substrata: formation of binucleate cells expressing placental lactogen. Cell Tissue Res 2002; 307(2):225-235.

170. Ushizawa K, Takahashi T, Kaneyama K, Tokunaga T, Tsunoda Y, Hashizume K. Gene expression profiles of bovine trophoblastic cell line (BT-1) analyzed by a custom cDNA microarray. J Reprod Dev 2005; 51(2):211-220.

171. Hambruch N, Haeger J-D, Dilly M, Pfarrer . EGF stimulates proliferation in the bovine placental trophoblast cell line F3 via RAS and MAPK. Placenta 2010; 31:67-74.

172. Dilly M, Hambruch N, Haeger JD, Pfarrer C. Epidermal growth factor (EGF) induces motility and upregulates MMP-9 and TIMP-1 in bovine trophoblast cells. Mol Reprod Dev 2010; 77(7):622-629.

173. Johnstone ED, Mackova M, Das S, Payne SG, Lowen B, Sibley CP, Chan G, Guilbert LJ. Multiple anti-apoptotic pathways stimulated by EGF in cytotrophoblasts. Placenta 2005; 26(7):548-555.

174. Machida T, Taga M, Minaguchi H. Effects of epidermal growth factor and transforming growth factor alpha on the mouse trophoblast outgrowth in vitro. Eur J Endocrinol 1995; 133(6):741-746.

175. Haeger JD, Hambruch N, Dilly M, Froehlich R, Pfarrer C. Formation of bovine placental trophoblast spheroids. Cells Tissues Organs 2011; 193(4):274-284.

176. Farmer JL, Burghardt RC, Jousan FD, Hansen PJ, Bazer FW, Spencer TE. Galectin 15 (LGALS15) functions in trophectoderm migration and attachment. FASEB Journal 2008; 22:548-560.

177. Yang QE, Giassetti MI, Ealy AD. Fibroblast growth factors activate mitogen-activated protein kinase pathways to promote migration in ovine trophoblast cells. Reproduction 2011; 141(5):707-714.

178. Librach CL, Werb Z, Fitzgerald ML, Chiu K, Corwin NM, Esteves RA, Grobelny D, Galardy R, Damsky CH, Fisher SJ. 92-kD type IV collagenase mediates invasion of human cytotrophoblasts. J Cell Biol 1991; 113(2):437-449.

179. Straszewski-Chavez SL, Abrahams VM, Mor G. The role of apoptosis in the regulation of trophoblast survival and differentiation during pregnancy. Endocr Rev. 2005; 26(7):877-897.

180. Smith SC, Baker PN, Symonds EM. Placental apoptosis in normal human pregnancy. Am J Obstet Gynecol 1997; 177(1):57-65.

181. Soni S, Rath G, Prasad CP, Salhan S, Saxena S, Jain AK. Apoptosis and Bcl-2 Protein Expression in Human Placenta over the Course of Normal Pregnancy. Anat Histol Embryol 2010; 39(5):426-431.

182. Rote NS, Wei BR, Xu C, Luo L. Caspase 8 and human villous cytotrophoblast differentiation. Placenta. 2010; 31(2):89-96.

183. Huppertz B, Frank HG, Kingdom JC, Reister F, Kaufmann P. Villous cytotrophoblast regulation of the syncytial apoptotic cascade in the human placenta. Histochem Cell Biol. 1998; 110(5):495-508.

184. Das M, Xu B, Lin L, Chakrabarti S, Shivaswamy V, Rote NS. Phosphatidylserine efflux and intercellular fusion in a BeWo model of human villous cytotrophoblast. Placenta 2004; 25:396-407

185. Gauster M, Siwetz M, Huppertz B. Fusion of villous trophoblast can be visualized by localizing active caspase 8. Placenta 2009; 30:547-550.

186. Guilbert LJ, Riddell M, Winkler-Lowen B. Caspase activation is not required for villous cytotrophoblast fusion into syncytiotrophoblasts. Placenta. 2010; 31(11):982-928.

187. Chen YX, Allars M, Maiti K, Angeli GL, Abou-Seif C, Smith R, Nicholson RC. Factors affecting cytotrophoblast cell viability and differentiation: Evidence of a link between syncytialisation and apoptosis. Int J Biochem Cell Biol 2011; 43(5):821-828.

188. Heazell AE, Sharp AN, Baker PN, Crocker IP. Intra-uterine growth restriction is associated with increased apoptosis and altered expression of proteins in the p53 pathway in villous trophoblast. Apoptosis 2011; 16(2):135-144.

189. Smith SC, Baker PN, Symonds EM. Increased placental apoptosis in intrauterine growth restriction. Am J Obstet Gynecol 1997; 177:1395-1401.

190. Roje D, Tomas SZ, Prusac IK, Capkun V, Tadin I. Trophoblast apoptosis in human term placentas from pregnancies complicated with idiopathic intrauterine growth retardation. J Matern Fetal Neonatal Med 2011; 24(5):745-751.

191. DeFederico E, Genbacev O, Fisher SJ. Preeclampsia is associated with widespread apoptosis in cytotrophoblasts within the uterine wall. Am J Pathol 1999; 155(1):293-301.

192. Allaire AD, Ballenger KA, Wells SR, McMahon MJ, Lessey BA. Placental apoptosis in preeclampsia. Obstet Gynecol 2000; 96:271-276.

193. Ishihara N, Matsua H, Murakoshi H, Laoag-Fernandez JB, Samoto T, Maruo T. Increase apoptosis in the syncytiotrophoblast in human term placentas complicated by either preeclampsia or intrauterine growth retardation. Am J Obstet Gynecol 2002; 186:158-166.

194. Tomas SZ, Prusac IK, Roje D, Tadin I. Trophoblast apoptosis in placentas from pregnancies complicated by preeclampsia. Gynecol Obstet Invest. 2011;71(4):250-255.

195. Mendilcioglu I, Karaveli S, Erdogan G, Simsek M, Taskin O, Ozekinci M. Apoptosis and expression of Bcl-2, Bax, p53, caspase-3, and Fas, Fas ligand in placentas complicated by preeclampsia. Clin Exp Obstet Gynecol. 2011;38(1):38-42.

196. Sokolov DI, Kolobov AV, Lesnichija MV, Kostiouchek IN, Stepanova OI, Kvetnoy IM, Selkov SA. Regulatory mechanisms for apoptosis in placental tissue during normal pregnancy and gestosis-complicated pregnancy. Bull Exp Biol Med. 2009; 148(5):766-770.

197. Soni S, Rath G, Prasad CP, Salhan S, Jain AK, Saxena S. Fas-FasL system in molar pregnancy. Am J Reprod Immunol 2011; 65(5):512-520. doi: 10.1111/j.1600-0897.2010.00926.x.

198. Longtine MS, Chen B, Odibo AO, Zhong Y, Nelson DM. Caspase-mediated apoptosis of trophoblasts in term human placental villi is restricted to cytotrophoblasts and absent from the multinucleated syncytiotrophoblast. Reproduction 2012;143(1):107-121.

199. Longtine MS, Chen B, Odibo AO, Zhong Y, Nelson DM. Villous trophoblast apoptosis is elevated and restricted to cytotrophoblasts in pregnancies complicated by preeclampsia, IUGR, or preeclampsia with IUGR. Placenta. 2012 Feb 15. [Epub ahead of print]

200. Ushizawa K, Takahashi T, Kaneyama K, Hosoe M, Hashizume K. Cloning of the bovine antiapoptotic regulator, BCL2-Related Protein A1, and its expression in trophoblastic binucleate cells of bovine placenta. Biol Reprod 2006; 74(2):344-351.

201. Groebner AE, Schulke K, Unterseer S, Reichenbach HD, Reichenbach M, Buttner M, Wolf E, Meyer HHD, Ulbrich SE. Enhanced proapoptotic gene expression of XAF1, CASP8, and TNFSF10 in the bovine endometrium during early pregnancy is not correlated with augmented apoptosis. Placenta 2010; 31:168-177.

202. JiangFeng F, Jiu YS, Wen ZZ, Ben L. The expression of Fas/FasL and apoptosis in yak placentomes. Anim Reprod Sci 2011; 128(1-4):107-116.

203. Carnegie JA, McCully ME, Robertson HA. The early development of the sheep trophoblast and the involvement of cell death. Am J Anat 1985; 174:471-488.

204. Xu J, Liu H, Wu Y, Gong X, Zhou Q, Qiao F. Proapoptotic effect of metalloproteinase 9 secreted by trophoblasts on endothelial cells. J Obstet Gynaecol Res 2011; 37(3):187-194. doi: 10.1111/j.1447-0756.2010.01334.x.

205. James JL, Whitley GS, Cartwright JE. Shear stress and spiral artery remodelling: the effects of low shear stress on trophoblast-induced endothelial cell apoptosis. Cardiovasc Res 2011; 90(1):130-139.

206. Keogh RJ, Harris LK, Freeman A, Baker PN, Aplin JD, Whitley GS, Cartwright JE. Fetal-derived trophoblast use the apoptotic cytokine tumor necrosis factor-alpha-

related apoptosis-inducing ligand to induce smooth muscle cell death. Circ Res 2007; 100(6):834-841.

207. Bulmer JN, BA Innes, GE Lash, SC Robson. Transformation of uterine spiral arteries in normal human pregnancy: no in situ evidence for apoptosis of vascular smooth muscle cells. J Soc Gyn Invest 2006; 13:181A.

208. Bulmer JN, Innes BA, Levey J, Robson SC, Lash GE. The role of vascular smooth muscle cell apoptosis and migration during uterine spiral artery remodeling in normal human pregnancy. FASEB J 2012; [Epub ahead of print]

209. Smith SD, Dunk CE, Aplin JD, Harris LK, Jones RL. Evidence for immune cell involvement in decidual spiral arteriole remodeling in early human pregnancy. Am J Pathol 2009; 174(5):1959-1971.

210. Lala PK, Lee B, Zu G, Chakraborty C. Human placental trophoblast as an in vitro model for tumor progression. Can J Physiol Pharm 2002; 80(2):142-149.

211. Jones RL, Stoikos C, Findlay JK, Salamonsen LA. TGF-β superfamily expression and actions in the endometrium and placenta. Reproduction 2006; 132:217–232.

212. Paria BC, Dey SK. Preimplantation embryo development in vitro: cooperative interactions among embryos and role of growth factors. PNAS 1990; 87:4756-4760.

213. Lim J, Bongso A, Ratnam S. Mitogenic and cytogenetic evaluation of transforming growth factor-beta on murine preimplantation embryonic development in vitro. Mol Reprod Dev 1993; 36 482-487.

214. Nowak RA, Haimovici F, Biggers JD, Erbach GT. Transforming growth factor-beta stimulates mouse blastocyst outgrowth through a mechanism involving parathyroid hormone-related protein. Biol Reprod 1999; 60:85-93.

215. Kamijo T, Rajabi MR, Mizunuma H, Ibuki Y. Biochemical evidence for autocrine/paracrine regulation of apoptosis in cultured uterine epithelial cells during mouse embryo implantation in vitro. Mol Hum Reprod 1998; 4:990-998.

216. Lash GE, Otun HA, Innes BA, Bulmer JN, Searle RF, Robson SC. Inhibition of Trophoblast Cell Invasion by TGFB1, 2, and 3 Is Associated with a Decrease in Active Proteases. Biol Reprod 2005; 73(2):374-381.

217. Yu Q, Stamenkovic I. Cell surface-localized matrix metalloproteinase-9 proteolytically activates TGF-beta and promotes tumor invasion and angiogenesis. Genes Dev 2000; 14:163-176.

218. Lafontaine L, Chaudhry P, Lafleur MJ, Van Themsche C, Soares MJ, Asselin E. Transforming growth factor Beta regulates proliferation and invasion of rat placental cell lines. Biol Reprod 2011; 84(3):553-559.

219. Lee KY, DeMayo FJ. Animal models of implantation. Reproduction 2004; 128:679-695.

220. Djurovic S, Schjetlein R, Wisloff F, Haugen G, Husby H, Berg K. Plasma concentrations of Lp(a) lipoprotein and TGF-beta1 are altered in preeclampsia. Clin Genet 1997; 52:371-376.

221. Enquobahrie DA, Williams MA, Qiu C, Woelk GB, Mahomed K. Maternal plasma transforming growth factor-beta1 concentrations in preeclamptic and normotensive pregnant Zimbabwean women. J Matern Fetal Neonatal Med 2005; 17(5):343-348.

222. Farina A, Sekizawa A, De Sanctis P, Purwosunu Y, Okai T, Cha DH, Kang JH, Vicenzi C, Tempesta A, Wibowo N, Valvassori L, Rizzo N. Gene expression in chorionic villous samples at 11 weeks' gestation from women destined to develop preeclampsia. Prenat Diagn 2008; 28(10):956-961.

223. Caniggia I, Grisaru-Gravnosky S, Kuliszewski M, Post M, Lye SJ. Inhibition of TGF-β3 restores the invasive capability of extravillous trophoblasts in preeclamptic pregnancies. J Clin Invest 1999; 103:1641-1650.

224. Caniggia I, Winter JL. Adriana and Luisa Castellucci Award Lecture 2001 Hypoxia inducible factor-1: oxygen regulation of trophoblast differentiation in normal and pre-eclamptic pregnancies – a review. Placenta 2002; 23:S47-S57.

225. Nishi H, Nakada T, Hokamura M, Osakabe Y, Itokazu O, Huang LE, Isaka K. Hypoxia-inducible factor-1 transactivates transforming growth factor-β3 in trophoblast. Endocrinology 2004; 145(9):4113-4118.

226. St-Jacques S, Forte M, Lye SJ, Letarte M. Localization of endoglin, a transforming growth factor-beta binding protein, and of CD44 and integrins in placenta during the first trimester of pregnancy. Biol Reprod 1994; 51:405-413.

227. Jeyabalan A, McGonigal S, Gilmour C, Hubel CA, Rajakumar A. Circulating and placental endoglin concentrations in pregnancies complicated by intrauterine growth restriction and preeclampsia. Placenta 2008; 29:555–563.

228. Stepan H, Kramer T, Faber `R. Maternal plasma concentrations of soluble endoglin in pregnancies with intrauterine growth restriction. J Clin Endocrinol Metab 2007; 92(7):2831-2834.

229. Mano Y, Kotani T, Shibata K, Matsumura H, Tsuda H, Sumigama S, Yamamoto E, Iwase A, Senga T, Kikkawa F. The loss of endoglin promotes the invasion of extravillous trophoblasts. Endcrinology 2011; 152(11):4386-4394.

230. Marjono AB, Brown DA, Horton KE, Wallace EM, Breit SN, Manuelpillai U. Macrophage inhibitory cytokine-1 in gestational tissues and maternal serum in normal and pre-eclamptic pregnancy. Placenta 2003; 24:100-106.

231. Li H, Dakour J, Morrish DW. PL74: A novel TGFβ family gene expressed in trophoblast and MG-63 cells and regulated by IFNɣ and EGF. Placenta 1999; 19(7):A54.

232. Morrish DW, Dakour J, Li H. Life and death in the placenta: new peptides and genes regulating human syncytiotrophoblast and extravillous cytotrophoblast lineage formation and renewal. Curr Prot Pept Sci 2001; 2:245–259.

233. Segerer SE, Rieger L, Kapp M, Dombrowski Y, Müller N, Dietl J, Kämmerer U. MIC-1 (a multifunctional modulator of dendritic cell phenotype and function) is produced by decidual stromal cells and trophoblasts. Hum Reprod 2012; 27(1):200-209.

234. Hsiao EC, Koniaris LG, Zimmers-Koniaris T, Sebald SM, Huynh TV, Lee SJ. Characterization of growth-differentiation factor 15, a transforming growth factor β superfamily member induced following liver injury. Molec Cell Biol 2000; 20(1):3742-3751.

235. Vassalli A, Matzuk MM, Gardner HA, Lee KF, Jaenisch R. Activin/inhibin beta B subunit gene disruption leads to defects in eyelid development and female reproduction. Genes Devel 1994; 8:414-427.

236. Sugulle M, Dechend R, Herse F, Weedon-Fekjaer MS, Johnsen GM, Brosnihan KB, Anton L, Luft FC, Wollert KC, Kempf T, Staff AC. Circulating and placental growth-differentiation factor 15 in preeclampsia and in pregnancy complicated by diabetes mellitus. Hypertension 2009; 54(1):106-112.

237. Kikuchi A, Yamamoto H, Sato A. Selective activation mechanisms of Wnt signaling pathways. Trends Cell Biol 2009; 19:119 -129.

238. Amerongen R, Nusse R. Towards an integrated view of Wnt signaling in development. Development 2009; 136:3205-3214.

239. MacDonald BT, Tamai K, He X. Wnt/b-catenin signaling: components, mechanisms and diseases. Dev Cell 2009; 17(1):9-26.

240. Teo JL, Kahn M. The Wnt signaling pathway in cellular proliferation and differentiation: a tale of two coactivators. Adv Drug Deliv Rev 2010; 62(12)1149-1155.

241. Le NH, Franken P, Fodde R. Tumour-stroma interactions in colorectal cancer: converging on beta-catenin activation and cancer stemness. Br J Cancer 2008; 98:1886-1893.

242. Hayashi K, Burghardt RC, Bazer FW, Spencer TE. WNTs in the ovine uterus: potential regulation of periimplantation ovine conceptus development. Endocrinology 2007; 148(7):3496-3506.

243. Kim S, Choi Y, Bazer FW, Spencer TE. Identification of genes in the ovine endometrium regulated by interferon tau independent of signal transducer and activator of transcription 1. Endocrinology 2003; 144:5203–5214. doi:10.1210/EN.2003-0665

244. Nakano H, Shimada A, Imai K, Takahashi T, Hashizume K. The cytoplasmic expression of E-cadherin and beta-catenin in bovine trophoblasts during binucleate cell differentiation. Placenta 2005; 26:393-401.

245. Sonderegger S, Husslein H, Leisser C, Knofler M. Complex expression pattern of Wnt ligands and Frizzled receptors in human placenta and its trophoblast subtypes. Placenta 2007; 21:S97-S102.

246. Pollheimer J, Loregger T, Sonderegger S, Saleh L, Bauer S, Bilban M, Czerwenka K, Husslein P, Knofler M. Activation of the canonical Wingless/T-cell factor signaling pathway promotes invasive differentiation of human trophoblast. Am J Path 2006; 168(4):1134-1147.

247. Krause R, Hemberger M, Himmelbauer H, Kalscheuer V, Fundele RH. Identification and characterization of G90, a novel mouse RNA that lacks an extensive open reading frame. Gene 1999; 232:35-42.

248. Meunier D, Peters T, Luttges A, Curfs J, Fundele R. Preferential expression of the G90 gene in post-mitotic cells during mouse embryonic development. Anat Embryol (Berl) 2003; 207:109-117.

249. Kiba T, Kintaka Y, Suzuki Y, Ishizuka N, Ishigaki Y, Inoue S. Gene expression profiling in rat pancreas after ventromedial hypothalamic lesioning. Pancreas 2010; 39(5):627-632.

250. Meunier D, Patra K, Smits R, Hagebarth A, Luttges A, Jaussi R, Wieduwilt MJ, Quintanilla-Fend L, Himmelbauer H, Fodde R, Fundele RH. Expression analysis of proline rich 15 (Prr15) in mouse and human gastrointestinal tumors. Mol Carcinog 2011; 50(1):8-15.

251. Glover MD, Seidel GE. Increased messenger RNA for allograft inflammatory factor-1, LERK-5, and a novel gene in 17.5 day relative to 15.5 day bovine embryos. Biol Reprod 2003; 69:1002-1012.

252. Guillomot M. Cellular interactions during implantation in domestic ruminants. J Reprod Fertil Supp 1995; 49:39-51.

253. Purcell SH, Cantlon JD, Winn VD, Anthony RV. Examination of periattachment factor (PRR15) in the human placenta. Reprod Sci 2008; 15(2):S206A.

254. Wilcox AJ, Weinberg CR, O'Conner JF, Baird DD, Schlatterer JP, Canfield RE, Armstrong EG, Nisula BC. Incidence of early loss of pregnancy. N Engl J Med 1988; 319:189-194.

255. Rai R, Regan L. Recurrent miscarriage. Lancet 2006; 368:601-611.

256. Egbor M, Ansari T, Morris N, Green CJ, Sibbons PD. Morphometric placental villous and vascular abnormalities in early- and late-onset preeclampsia with and without fetal growth restriction. BJOG 2006; 113:580-589.

257. Hamilton WJ, Boyd JD. Development of the human placenta in the first three months of gestation. J Anat 1960; 94:297-328.

258. Morrish DW, Dakour J, Li H. Life and death in the placenta: new peptides and genes regulating human syncytiotrophoblast and extravillous cytotrophoblast lineage formation and renewal. Curr Protein Pept Sci 2001; 2:245-259.

259. Pijnenborg R, Dixon G, Robertson WB, Brosens I. Trophoblastic invasion of human decidua from 8 to 18 weeks of pregnancy. Placenta 1980; 1:3-19.

260. Rowson LEA, Moor RM. Development of the sheep conceptus during the first fourteen days. J Anat 1966; 100(4):777-785.

261. Spencer TE, Johnson GA, Bazer FW, Burghardt RC. Implantation mechanisms: insights from the sheep. Reproduction 2004; 128(6):657-668.

262. Hue I, Degrelle SA, Campion E, Renard J-P. Gene expression in elongating and gastrulating embryos from ruminants. Reproduction in Domestic Ruminants 2007; 6(1):365-377.

263. Ishihara N, Matsua H, Murakoshi H, Laoag-Fernandez JB, Samoto T, Maruo T. Increased apoptosis in the syncytiotrophoblast in human term placentas complicated by either preeclampsia or intrauterine growth retardation. Am J Obstet Gynecol 2002; 186:158-166.

264. Guillomot M. Cellular interactions during implantation in domestic ruminants. J Reprod Fertil Suppl 1995; 49:39-51.

265. Rubinson DA, Dillon CP, Kwiatkowski AV, Sievers C, Yang L, Kopinja J, Rooney DL, Zhang M, Ihrig MM, McManus MT, Gertler FB, Scott ML, et al. A lentivirus-based system to functionally silence genes in primary mammalian cells, stem cells and transgenic mice by RNA interference. Nat Genet 2003; 33:401-406.

266. Kanehisa M, Goto S, Kawashima S, Okuno Y, Hattori M. (2004) The KEGG resource for deciphering the genome. Nucleic Acids Res 2004; 32:D277-D280.

267. Sherr CJ. D-type cyclins. Trends Biochem Sci 1995; 20(5):187-190.

268. Bennin DA, Don AS, Brake T, McKenzie JL, Rosenbaum H, Ortiz L, DePaoli-Roach AA, Horne MC. Cyclin G2 associates with protein phosphatase 2A catalytic and regulatory B' subunits in active complexes and induces nuclear aberrations and a G1/S phase cell cycle arrest. J Biol Chem 2002; 277(30):27449-27467.

269. Cazzalini O, Scovassi AI, Savio M, Stivala LA, Prosperi E. Multiple roles of the cell cycle inhibitor p21(CDKN1A) in the DNA damage response. Mutat Res 2010; 704(1-3):12-20.

270. Bruchim I, Attias Z, Werner H. Targeting the IGF1 axis in cancer proliferation. Expert Opin Ther Targets 2009; 13(10):1179-1192.

271. Forbes K, Westwood M, Baker PN, Aplin JD. Insulin-like growth factor I and II regulated the life cycle of trophoblast in the developing human placenta. Am J Physiol Cell Physiol 2008; 294:C1313-C1322.

272. Michaylira CZ, Simmons JG, Ramocki NM, Scull BP, McNaughton KK, Fuller CR, Lund PK. Suppressor of cytokine signaling-2 limits intestinal growth and enterotrophic actions of IGF-I in vivo. Am J Physiol Gastrointest Liver Physiol 2006; 291(3):G472-G481.

273. Zhang S, Yu D. PI(3)king apart PTEN's role in cancer. Clin Cancer Res 2010; 16(17):4325-4330.

274. Pop C, Salvesen GS. Human caspases: activation, specificity, and regulation. J Biol Chem 2009; 284(33):21777-21781.

275. Koopman G, Reutelingsperger CP, Kuijten GA, Keehnen RM, Pals ST, van Oers MH. Annexin V for flow cytometric detection of phosphatidylserine expression on B cells undergoing apoptosis. Blood 1994; 84(5):1415-1420.

276. Voelkel-Johnson C. TRAIL-mediated signaling in prostate, bladder and renal cancer. Nat Rev Urol 2011;8(8):417-427.

277. Rull K, Tomberg K, Kõks S, Männik J, Möls M, Sirotkina M, Värv S, Laan M. TNF-Related Apoptosis-Inducing Ligand TRAIL as a Potential Biomarker for Early Pregnancy Complications. J Clin Endocrinol Metab. 2012 Mar 14. [Epub ahead of print]

278. Karasic TB, Hei TK, Ivanov VN. Disruption of IGF-1R signaling increases TRAIL-induced apoptosis: a new potential therapy for the treatment of melanoma. Exp Cell Res 2010; 316(12):1994-2007.

279. Kase S, He S, Sonoda S, Kitamura M, Spee C, Wawrousek E, Ryan SJ, Kannan R, Hinton DR. alphaB-crystallin regulation of angiogenesis by modulation of VEGF. Blood 2010; 115(16):3398-3406.

280. Bousette N, Chugh S, Fong V, Isserlin R, Kim KH, Volchuk A, Backx PH, Liu P, Kislinger T, MacLennan DH, Emili A, Gramolini AO. Constitutively active calcineurin induces cardiac endoplasmic reticulum stress and protects against apoptosis that is mediated by alpha-crystallin-B. Proc Natl Acad Sci U S A. 2010; 107(43):18481-18486.

281. Watanabe G, Kato S, Nakata H, Ishida T, Ohuchi N, Ishioka C. alphaB-crystallin: a novel p53-target gene required for p53-dependent apoptosis. Cancer Sci 2009; 100(12):2368-2375.

282. Launay N, Tarze A, Vicart P, Lilienbaum A. Serine 59 phosphorylation of {alpha}B-crystallin down-regulates its anti-apoptotic function by binding and sequestering Bcl-2 in breast cancer cells. J Biol Chem. 2010; 285(48):37324-37332.

283. Kase S, He S, Sonoda S, Kitamura M, Spee C, Wawrousek E, Ryan SJ, Kannan R, Hinton DR. alphaB-crystallin regulation of angiogenesis by modulation of VEGF. Blood 2010; 115(16):3398-3406.

284. Sharp AN, Heazell AE, Crocker IP, Mor G. Placental apoptosis in health and disease. Am J Reprod Immunol 2010; 64(3):159-169.

285. Yung HW, Calabrese S, Hynx D, Hemmings BA, Cetin I, Charnock-Jones DS, Burton GJ. Evidence of placental translation inhibition and endoplasmic reticulum stress in the etiology of human intrauterine growth restriction. Am J Pathol 2008;173(2):451-462.

286. Heazell AE, Sharp AN, Baker PN, Crocker IP. Intra-uterine growth restriction is associated with increased apoptosis and altered expression of proteins in the p53 pathway in villous trophoblast. Apoptosis 2011;16(2):135-144.

287. Nieminen AI, Partanen JI, Klefstrom J. c-Myc blazing a trail of death: coupling of the mitochondrial and death receptor apoptosis pathways by c-Myc. Cell Cycle 2007; 6(20):2464-2472.

288. Quenby S, Brazeau C, Drakeley A, Lewis-Jones DI, Vince G. Oncogene and tumour suppressor gene products during trophoblast differentiation in the first trimester. Mol Hum Reprod 1998; 4(5):477-481.

289. Rottmann S, Speckgens S, Lüscher-Firzlaff J, Lüscher B. Inhibition of apoptosis by MAD1 is mediated by repression of the PTEN tumor suppressor gene. FASEB J 2008; 22(4):1124-1134.

290. DeFalco M, Cobellis L, Giraldi D, Mastrogiacomo A, Perna A, Colacurci N, Miele L, De Luca A. Expression and distribution of notch protein members in human placenta throughout pregnancy. Placenta 2007; 28:118-126.

291. Hunkapiller NM, Gasperowicz M, Kapidzic M, Plaks V, Maltepe E, Kitajewski J, Cross JC, Fisher SJ. A role for Notch signaling in trophoblast endovascular invasion and in the pathogenesis of pre-eclampsia. Development. 2011; 138(14):2987-2998.

292. Ghosh P, Garcia-Marcos M, Bornheimer SJ, Farquhar MG. Activation of Gαi3 triggers cell migration via regulation of GIV. J Cell Biol 2008; 182(2):381-393.

293. MacPhee DJ, Mostachfi H, Han R, Lye SJ, Post M, Caniggia I. Focal adhesion kinase is a key mediator of human trophoblast development. Lab Invest 2001; 81(11):1469-1483.

294. Kabir-Salmani M, Shiokawa S, Akimoto Y, Hasan-Nejad H, Sakai K, Nagamatsu S, Sakai K, Nakamura Y, Hosseini A, Iwashita M. Characterization of morphological and cytoskeletal changes in trophoblast cells induced by insulin-like growth factor-I. J Clin Endocrinol Metab 2002; 87(12):5751-5759.

295. Kabir-Salmani M, Shiokawa S, Akimoto Y, Sakai K, Nagamatsu S, Sakai K, Nakamura Y, Lotfi A, Kawakami H, Iwashita M. Alphavbeta3 integrin signaling

pathway is involved in insulin-like growth factor I-stimulated human extravillous trophoblast cell migration. Endocrinology 2003; 144(4):1620-1630.

296. Garcia-Marcos M, Ghosh P, Parquhar MG. GIV is a nonreceptor GEF for G alpha i with a unique motif that regulates Akt signaling. Proc Natl Acad Sci USA 2009; 106:3178-3183.

297. Jiang P, Enomoto A, Jijiwa M, Kato T, Hasegawa T, Ishida M, Sato T, Asai N, Murakumo Y, Takahashi M.An actin-binding protein Girdin regulates the motility of breast cancer cells. Cancer Res 2008; 68:1310-1318.

298. Herman MP, Sukhova GK, Kisiel W, et al: Tissue factor pathway inhibitor-2 is a novel inhibitor of matrix metalloproteinases with implications for atherosclerosis. J Clin Invest 2001; 107:1117-1126.

299. Udagawa K, Miyagi Y, Hirahara F, Miyagi E, Nagashima Y, Minaguchi H, Misugi K, Yasumitsu H, Miyazaki K. Specific expression of PP5/TFPI2 mRNA by syncytiotrophoblasts in human placenta as revealed by in situ hybridization. Placenta 1998; 19(2-3):217-223.

300. Kang Y, Massagué J. Epithelial-mesenchymal transitions: twist in development and metastasis. Cell 2004; 118:277–279

301. Thie M, Fuchs P & Denker HW. Epithelial cell polarity and embryo implantation in mammals. Int J Devel Biol 1996; 40:389–393.

302. Yamakoshi S, Bai R, Chaen T, Ideta A, Aoyagi Y, Sakurai T, Konno T, Imakawa K. Expression of mesenchymal-related genes by the bovine trophectoderm following conceptus attachment to the endometrial epithelium. Reproduction 2012; 143(3):377-387.

303. Ng YH, Zhu H, Leung PC. Twist modulates human trophoblastic cell invasion via regulation of N-cadherin. Endocrinology 2012; 153(2):925-936.

304. Stewart CL, Kaspar P, Brunet LJ, Bhatt H, Gadi I, Kontgen F, Abbondanzo SJ. Blastocyst implantation depends on maternal expression of leukaemia inhibitory factor. Nature 1992; 359:76-79.

305. Hammoda MA, Eid MA, El-Srogy HA, Mostafa MM, Hasan AM. Assessment of leukemia inhibitory factor and glycoprotein 130 expression in endometrium and uterine flushing: a possible diagnostic tool for impaired fertility. BMC Womens Health 2012; 12(1):10.

306. Chaouat G, Menu E, Delage G, et al. Immuno-endocrine interactions in early pregnancy. Hum Reprod 1995;10:55-59.

307. Yelich JV, Pomp D, Geisert RD. Ontogeny of elongation and gene expression in the early developing porcine conceptus. Biol Reprod 1997; 57(5):1256-1265.

308. Sharkey AM, King A, Clark DE, Burrows TD, Jokhi PP, Charnock-Jones DS, Loke YW, Smith SK. Localization of leukemia inhibitory factor and its receptor in human placenta throughout pregnancy. Biol Reprod 1999; 60(2):355-364.

309. Fitzgerald JS, Tsareva SA, Poehlmann TG, Berod L, Meissner A, Corvinus FM, Wiederanders B, Pritzner E, Markert UR, Friedrich K. Leukemia inhibitory factor triggers activation of signal transducer and activator of transcription 3, proliferation, invasiveness, and altered protease expression in choriocarcinoma cells. Int J Biochem Cell Biol 2005; 37(11):2284-2296.

310. Prakash GJ, Suman P, Morales Prieto DM, Markert UR, Gupta SK. Leukaemia inhibitory factor mediated proliferation of HTR-8/SVneo trophoblast cells is dependent on activation of extracellular signal-regulated kinase 1/2. Reprod Fertil Steril 2011; 23(5):714-724.

311. Wells J, Lee B, Cai AQ, Karapetyan A, Lee WJ, Rugg E, Sinha S, Nie Q, Dai X. Ovol2 suppresses cell cycling and terminal differentiation of keratinocytes by directly repressing c-Myc and Notch-1. J Biol Chem 2009; 284(42):29125-29135.

312. Unezaki S, Horai R, Sudo K, Iwakura Y, Ito S. Ovol2/Movo, a homologue of Drosophila ovo, is required for angiogenesis, heart formation and placental development in mice. Genes Cells 2007; 12(6):773-785.

313. Fairlie WD, Moore AG, Bauskin AR, Russell PK, Zhang HP, Breit SN. MIC-1 is a novel TGF-beta superfamily cytokine associated with macrophage activation. J Leukoc Biol 1999;65:2-5.

314. Tong S, Marjono B, Brown DA, Mulvey S, Breit SN, Manuelpillai U, Wallace EM. Serium concentration of macrophage inhibitory cytokine 1 (MIC 1) as a predictor of miscarriage. Lancet 2004; 363:129-130.

315. Li H, Dakour J, Guilbert LJ, Winkler-Lowen B, Lyall F, Morrish DW. PL74, a novel member of the transforming growth factor-b superfamily is overexpressed in preeclampsia and causes apoptosis in trophoblast cells. J Clin Endocrinol Metab 2005; 90(5):3045-3053.

316. Li H, Dakour J, Guilbert LJ, Winkler-Lowen B, Lyall F, Morrish DW. PL74, a novel member of the transforming growth factor-b superfamily is overexpressed in preeclampsia and causes apoptosis in trophoblast cells. J Clin Endocrinol Metab 2005; 90(5):3045-3053.

317. Glisovic T, Bachorik JL, Yong J, Dreyfuss G. RNA-binding proteins and post-transcriptional gene regulation. FEBS Letters 2008; 582:1977-1986.

318. Hiden et al. ACH3P cells

319. Hopfer U, Jacobberger JW, Gruenert DC, Eckert RL, Jat PS, Whitsett JA. Immortalization of epithelial cells. Am J Physiol 1996; 270(1 Pt 1):C1-C11.

320. Morrish DW, Dakour J, Li H, Xiao J, Miller R, Sherburne R, Berdan RC, Guilbert LJ. In vitro cultured human term cytotrophoblast: a model for normal primary

epithelial cells demonstrating a spontaneous differentiation programme that requires EGF for extensive development of syncytium. Placenta 1997; 18: 577-585.

321. Tarrade A, Goffin F, Munaut C, Lai-Kuen R, Tricottet V, Foidart JM, Vidaud M, Frankenne F, Evain-Brion D. Effect of matrigel on human extravillous trophoblasts differentiation: modulation of protease pattern gene expression. Biol Reprod 2002; 67(5):1628-1637.

322. Wilcox AJ, Weinberg CR, O'Conner JF, Baird DD, Schlatterer JP, Canfield RE, Armstrong EG, Nisula BC. Incidence of early loss of pregnancy. N Engl J Med 1988; 319:189-194.

323. Rai R, Regan L. Recurrent miscarriage. Lancet 2006; 368:601-611.

324. Egbor M, Ansari T, Morris N, Green CJ, Sibbons PD. Morphometric placental villous and vascular abnormalities in early- and late-onset preeclampsia with and without fetal growth restriction. BJOG 2006; 113:580-589.

325. Diskin MG, Sreenan JM. Fertilization and embryonic mortality rates in beef heifers after artificial insemination. J Reprod Fertil 1980; 59:352-362.

326. Guillomot M. Cellular interactions during implantation in domestic ruminants. J Reprod Fertil Suppl 1995; 49:39-51.

327. Dongen JM, Visser WJ, Daems WTh, Galjaard H. The relation between cell proliferation, differentiation and ultrastructural development in rat intestinal epithelium. Cell and tissue Research 1976; 174(2):183-199.

328. White BD, Chien AJ, Dawson DW. Dysregulation of Wnt/β-catenin signaling in gastrointestinal cancers. Gastroenterology 2012; 142(2):219-232.

329. Chien AJ, Conrad WH, Moon RT. A Wnt survival guide: from flies to human disease. J Invest Dermatol 2009; 129:1614-1627.

330. Farmer JL, Burghardt RC, Jousan FD, Hansen PJ, Bazer FW, Spencer TE. Galectin 15 (LGALS15) functions in trophectoderm migration and attachment. FASEB J 2008; 22(2):548-560.

331. Jeckel KM, Limesand SW, Anthony RV. Specificity protein-1 and -3 trans-activate the ovine placental lactogen gene promoter. Mol Cell Endocrinol 2009; 307(1-2):118-124.

332. Sadot E, Conacci-Sorrell M, Zhurinsky J, Shnizer D, Lando Z, Zharhary D, Kam Z, Ben-Ze'ev A, Geiger B. Regulation of S33/S37 phosphorylated β-catenin in normal and transformed cells. J Cell Sci 2002; 115:2771-2780.

333. Onder TT, Gupta PB, Mani SA, Yang J, Lander ES, Weinberg RA. Loss of E-cadherin promotes metastasis via multiple downstream transcriptional pathways. Cancer Res 2008; 68(10):3645-3654.

334. Dignam JD, Lebovitz RM, Roeder RG. Accurate transcription initiation by RNA polymerase II in a soluble extract from isolated mammalian nuclei. Nucleic Acids Res 1983; 11:1475-1489.

335. Zianni M, Tessanne K, Merighi M, Laguna R, Tabita FR. Identification of the DNA bases of a DNase I footprint by the use of dye primer sequencing on an automated capillary DNA analysis instrument. J Biomolec Tech 2006; 12:103-113.

336. Korinek V, Barker N, Morin PJ, van Wichen D, de Weger R, Kinzler KW, Vogelstein B, Clevers H. Consitutive transcriptional activation by a β-catenin-Tcf complex in APC-/- colon carcinoma. Science 1997; 275:1784-1787.

337. Pollheimer J, Loregger T, Sonderegger S, Saleh L, Bauer S, Bilban M, Czerwenka K, Husslein P, Knofler M. Activation of the canonical wingless/T-cell factor signaling pathway promotes invasive differentiation of human trophoblast. Am J Path 2006; 168(4):1134-1147.

338. Lloyd AL, Marshall BJ, Mee BJ. Identifying cloned Helicobacter pylori promoters by primer extension using a FAM-labeled primer and GeneScan analysis. J Micro Meth 2005; 60:291-298.

339. Morin PJ, Vogelstein B, Kinzler KW. Apoptosis and APC in colorectal tumorigenesis. Proc Natl Acad Sci USA 1996; 93(15):7950-7954.

340. Hoppler S, Kavanagh CL. Wnt signaling: variety at the core. J Cell Sci 2007; 120:385-393.

341. Jamora C, DasGupta R, Kocieniewski P, Fuchs E. Links between signal transduction, transcription and adhesion in epithelial bud development. Nature 2003; 422:317-322.

342. Korinek V, Barker N, Morin PJ, van Wichen D, de Weger R, Kinzler KW, Vogelstein B, Clevers H. Constitutive transcriptional activation by a beta-catenin-Tcf complex in APC-/- colon carcinoma. Science 1997; 275:589-600.

343. He TC, Sparks AB, Rago C, Hermeking H, Zawel L, da Costa LT, Morin PJ, Vogelstein B, Kinzler KW. Identification of c-MYC as a target of the APC pathway. Science 1998; 281:1509.

344. Tetsu O, McCormick F. Beta-catenin regulates expression of cyclin D1 in colon carcinoma cells. Nature. 1999; 398(6726):422-426.

345. Pollheimer J, Loregger T, Sonderegger S, Saleh L, Bauer S, Bilban M, Czerwenka K, Husslein P, Knöfler M. Activation of the canonical wingless/T-cell factor signaling pathway promotes invasive differentiation of human trophoblast. Am J Pathol 2006; 168(4):1134-1147.

346. Sonderegger S, Haslinger P, Sabri A, Leisser C, Otten JV, Fiala C, Knöfler M. Wingless (Wnt)-3A induces trophoblast migration and matrix metalloproteinase-2 secretion through canonical Wnt signaling and protein kinase B/AKT activation. Endocrinology 2010; 151(1):211-220

347. Donohoe ME, Zhang X, McGinnis L, Biggers J, Li E, Shi Y. Targeted disruption of mouse Yin Yang 1 transcription factor results in peri-implantation lethality. Mol Cell Biol 1999; 19: 7237-7244.

348. Takeda T, Sakata M, Isobe A, Yamamoto T, Nishimoto F, Minekawa R, Hayashi M, Okamoto Y, Desprez PY, Tasaka K, Murata Y. Involvement of Sp-1 in the regulation of the Id-1 gene during trophoblast cell differentiation. Placenta 2007; 28(2-3):192-198.

349. Cheng YH, Handwerger S. A placenta-specific enhancer of the human syncytin gene. Biol Reprod 2005; 73(3):500-509.

350. Jeckel KM, Limesand SW, Anthony RV. Specificity protein-1 and -3 trans-activate the ovine placental lactogen gene promoter. Mol Cell Endocrinol 2009; 307(1-2):118-124.

351. Staun-Ram E, Goldman S, Shalev E. p53 Mediates epidermal growth factor (EGF) induction of MMP-2 transcription and trophoblast invasion. Placenta 2009; 30(12):1029-1036.

352. Degrelle SA, Murthi P, Evain-Brion D, Fournier T, Hue I. Expression and localization of DLX3, PPARG and SP1 in bovine trophoblast during binucleated cell differentiation. Placenta 2011; 32(11):917-920.

353. Wang WM, Wu SY, Lee AY, Chiang CM. Binding site specificity and factor redundancy in activator protein-1-driven human papillomavirus chromatin-dependent transcription. J Biol Chem 2011; 286(47):40974-40986.

354. Suman P, Godbole G, Thakur R, Morales-Prieto DM, Modi DN, Markert UR, Gupta SK. AP-1 transcription factors, mucin-type molecules and MMPs regulate the IL-11 mediated invasiveness of JEG-3 and HTR-8/SVneo trophoblastic cells. PLoS One 2012; 7(1):e29745

355. Du MR, Zhou WH, Dong L, Zhu XY, He YY, Yang JY, Li DJ. Cyclosporin A promotes growth and invasiveness in vitro of human first-trimester trophoblast cells via MAPK3/MAPK1-mediated AP1 and Ca2+/calcineurin/NFAT signaling pathways. Biol Reprod 2008; 78(6):1102-1110.

356. Bamberger AM, Bamberger CM, Aupers S, Milde-Langosch K, Löning T, Makrigiannakis A. Expression pattern of the activating protein-1 family of transcription factors in the human placenta. Mol Hum Reprod 2004; 10(4):223-228.

357. Tetens F, Kliem A, Tscheudschilsuren G, Navarrete Santos A, Fischer B. Expression of proto-oncogenes in bovine preimplantation blastocysts. Anat Embryol (Berl) 2000; 201(5):349-355.

358. Xavier F, Lagarrigue S, Guillomot M, Gaillard-Sanchez I. Expression of c-fos and jun protooncogenes in ovine trophoblasts in relation to interferon-tau expression and early implantation process. Mol Reprod Dev 1997; 46(2):127-137.

359.   Schorpp-Kistner M, Wang ZQ, Angel P, Wagner EF. JunB is essential for mammalian placentation. EMBO J 1999; 18(4):934-948.

360.   Notani D, Gottimukkala KP, Jayani RS, Limaye AS, Damle MV, Mehta S, Purbey PK, Joseph J, Galande S. Global regulator SATB1 recruits beta-catenin and regulates T(H)2 differentiation in Wnt-dependent manner. PLoS Biol 2010; 8(1):e1000296.

APPENDIX

Supplemental Table 1. Differentially expressed from PRR15 microarray.
Genes with *p*<0.05 and greater than 1.3-fold change in PRR15-shRNA compared to control from microarray analysis.

Genbank Acc	GENENAME	REFSEQ	P	Fold Change grp1/grp2	Fold Change
L27624	TFPI2	NM_006528	0.0024	0.026	-38.911
BE883300	PGBD1	NM_032507	0.0035	0.207	-4.822
NM_002064	GLRX	NM_002064	0.0004	0.225	-4.452
AF333388	MT1P2	NM_001039954	0.0104	0.251	-3.990
NM_002450	MT1X	NM_005952	0.0041	0.252	-3.973
BF664545			0.0035	0.252	-3.962
T75480	KCTD6	NM_153331	0.0041	0.258	-3.871
AL162069	KRT80	NM_001081492	0.0050	0.269	-3.723
BE967019	SPRED1	NM_152594	0.0211	0.271	-3.690
AF039698	TSHZ1	NM_005786	0.0421	0.271	-3.690
BE466195	RBM25	NM_021239	0.0386	0.278	-3.593
AW051379	LOC790955	NM_001085372	0.0018	0.280	-3.575
NM_013238	DNAJC15	NM_013238	0.0417	0.282	-3.547
NM_004078	CSRP1	NM_004078	0.0048	0.287	-3.479
NM_005952	MT1X	NM_005952	0.0259	0.291	-3.438
NM_017571	CCDC88A	NM_018084	0.0429	0.300	-3.331
NM_021963	NAP1L2	NM_021963	0.0008	0.302	-3.308
N95414	ITGA2	NM_002203	0.0042	0.304	-3.285
BE222344			0.0008	0.318	-3.147
AW885748			0.0442	0.319	-3.140
C06331	LOC399818	NM_212554	0.0243	0.320	-3.121
NM_014125	POLQ	NM_199420	0.0173	0.320	-3.121
NM_001394	DUSP4	NM_001394	0.0001	0.324	-3.085
AI827906	LOC169834	NM_001101338	0.0165	0.334	-2.998
AI768894	CGN	NM_020770	0.0023	0.335	-2.982
AW069729	ACPL2	NM_001037172	0.0004	0.337	-2.966
AW963217	NUDT19	NM_001105570	0.0368	0.339	-2.952
NM_003877	SOCS2	NM_003877	0.0077	0.341	-2.937
BF593263	NKAIN4	NM_152864	0.0188	0.352	-2.838
NM_002426	MMP12	NM_002426	0.0050	0.354	-2.822
AA205660	TRIM52	NM_032765	0.0055	0.354	-2.822
NM_004328	BCS1L	NM_001079866	0.0145	0.356	-2.811
AW170571	CPNE2	NM_152727	0.0246	0.357	-2.800
AI888594	TTL	NM_153712	0.0248	0.359	-2.789
AI742551	XAGE3	NM_130776	0.0302	0.362	-2.762
AI920953			0.0014	0.363	-2.756
NM_001964	EGR1	NM_001964	0.0287	0.366	-2.731
AK001836	KLHL5	NM_001007075	0.0348	0.367	-2.724
BF593263	NKAIN4	NM_152864	0.0349	0.368	-2.719
AL832995			0.0171	0.369	-2.711
AW274756	CDK6	NM_001259	0.0118	0.375	-2.668
U79277			0.0002	0.376	-2.660
NM_013337	TIMM22	NM_013337	0.0106	0.379	-2.636
AL117589	KIF26A	NM_015656	0.0021	0.381	-2.623
BE542563	LOC728342	XM_001129097	0.0068	0.384	-2.608
AI983896			0.0356	0.384	-2.604
AA776892	LOC399818	NM_212554	0.0128	0.385	-2.599
N74530			0.0193	0.385	-2.599
AI821399			0.0270	0.385	-2.597
AI669235	ELAC1	NM_018696	0.0373	0.385	-2.596

NM_000499	CYP1A1		NM_000499	0.0179	0.386	-2.593
AK024255				0.0004	0.386	-2.591
AU155515	RPL37A		NM_000998	0.0314	0.388	-2.577
AW972359				0.0314	0.391	-2.560
AF276659	MAP1LC3C		NM_001004343	0.0404	0.391	-2.556
NM_021083	XK		NM_021083	0.0030	0.392	-2.554
AK023354	UBQLN4		NM_020131	0.0369	0.392	-2.552
AA835417				0.0024	0.392	-2.552
NM_018584	CAMK2N1		NM_018584	0.0081	0.393	-2.545
AI655015				0.0007	0.394	-2.538
BE964048	TTL		NM_153712	0.0044	0.394	-2.535
NM_003246	THBS1		NM_003246	0.0024	0.397	-2.521
BI791845				0.0441	0.398	-2.512
AI021902				0.0008	0.400	-2.499
AJ278150	AGK		NM_018238	0.0024	0.401	-2.496
NM_017542	POGK		NM_017542	0.0224	0.401	-2.491
AW193600	LOC439949		XM_001128367	0.0007	0.404	-2.478
NM_030781	COLEC12		NM_030781	0.0150	0.405	-2.470
NM_024669	ANKRD55		NM_001039935	0.0016	0.405	-2.470
W60810	TSHZ1		NM_005786	0.0015	0.406	-2.466
AI654093	LOC645431		XR_015289	0.0175	0.406	-2.462
BC042908	RRP12		NM_015179	0.0423	0.407	-2.455
AW614120	TMEM136		NM_174926	0.0050	0.408	-2.451
AF010314	ENC1		NM_003633	0.0062	0.409	-2.448
AA191336	ZNF496		NM_032752	0.0190	0.410	-2.437
NM_003979	GPRC5A		NM_003979	0.0341	0.411	-2.435
NM_013245	VPS4A		NM_013245	0.0294	0.411	-2.434
AI928241	FERMT2		NM_006832	0.0387	0.412	-2.430
AW514267	LOC202134 /// LOC653316 /// NY-REN-7		NM_001079527	0.0414	0.413	-2.424
AW975638	HK2		NM_000189	0.0213	0.413	-2.422
BG493862	TCHP		NM_032300	0.0282	0.413	-2.421
NM_005103	FEZ1		NM_005103	0.0383	0.415	-2.409
NM_000296	PKD1		NM_000296	0.0075	0.416	-2.403
NM_007240	DUSP12		NM_007240	0.0150	0.417	-2.398
AA045184	S100A16		NM_080388	0.0101	0.419	-2.388
NM_001393	ECM2		NM_001393	0.0082	0.419	-2.386
AV693653	TNRC6B		NM_001024843	0.0381	0.420	-2.383
NM_004395	DBN1		NM_004395	0.0445	0.420	-2.381
BC006148	OVOL2		NM_021220	0.0298	0.420	-2.379
NM_005953	MT2A		NM_005953	0.0123	0.421	-2.375
AI870369	ZNF553		NM_152652	0.0339	0.422	-2.368
BE795648	SSRP1		NM_003146	0.0180	0.423	-2.365
T68150	PHLDB2		NM_145753	0.0026	0.423	-2.364
AA468591	CLK4		NM_020666	0.0005	0.425	-2.355
NM_014724	ZSCAN12		NM_001039643	0.0304	0.425	-2.353
AI479440				0.0258	0.426	-2.349
AL110225	DBN1		NM_004395	0.0485	0.426	-2.348
AI884858	TUSC3		NM_006765	0.0221	0.427	-2.341
NM_002766	PRPSAP1		NM_002766	0.0019	0.430	-2.328
AW971198	GRAMD3		NM_023927	0.0500	0.430	-2.326
AW294686	TTBK2		NM_173500	0.0499	0.431	-2.318
AI613273	CHD4		NM_001273	0.0001	0.435	-2.300
NM_003146	SSRP1		NM_003146	0.0122	0.436	-2.293
NM_005416	SPRR3		NM_001097589	0.0113	0.437	-2.290
D60621	LPHN3		NM_015236	0.0237	0.438	-2.285
AI948503	ABCC4		NM_001105515	0.0035	0.438	-2.285
NM_003157	NEK4		NM_003157	0.0057	0.438	-2.283

NM_014962	BTBD3	NM_014962	0.0062	0.439	-2.277
AW206286			0.0282	0.440	-2.275
NM_014583	LMCD1	NM_014583	0.0095	0.440	-2.275
AA701657	LIFR	NM_002310	0.0251	0.441	-2.266
NM_016034	MRPS2	NM_016034	0.0472	0.443	-2.257
M34421	PSG9	NM_002784	0.0189	0.445	-2.249
AI692432	ARID2	NM_152641	0.0325	0.445	-2.247
AI741586	ZNF720	NM_001004300	0.0116	0.446	-2.244
NM_014344	FJX1	NM_014344	0.0109	0.449	-2.230
BC014479	PXK	NM_017771	0.0212	0.449	-2.227
AI261467	IKZF4	NM_022465	0.0309	0.450	-2.222
Z24725	FERMT2	NM_006832	0.0006	0.451	-2.219
AK022566	B4GALT7	NM_007255	0.0355	0.451	-2.218
NM_006596	POLQ	NM_199420	0.0126	0.451	-2.217
AK001697	RIOK2	NM_018343	0.0009	0.451	-2.217
BG291550	FYTTD1	NM_001011537	0.0011	0.452	-2.214
NM_014950	ZBTB1	NM_014950	0.0364	0.452	-2.214
AW592684	LIFR	NM_002310	0.0078	0.453	-2.208
AJ003062	TUBGCP3	NM_006322	0.0136	0.453	-2.206
AL530462	ZNF364	NM_014455	0.0237	0.454	-2.203
NM_007361	NID2	NM_007361	0.0250	0.454	-2.201
AY114106	GEMIN7	NM_001007269	0.0474	0.455	-2.196
H05812	IGF1R	NM_000875	0.0052	0.456	-2.194
NM_004124	GMFB	NM_004124	0.0047	0.457	-2.186
W22690	C1orf175 /// TTC4	NM_001039464	0.0008	0.458	-2.182
NM_022443	MLF1	NM_022443	0.0057	0.460	-2.176
BC002791	FLJ35348	NR_002800	0.0029	0.460	-2.174
AW971205			0.0004	0.460	-2.172
NM_024597	MAP7D3	NM_024597	0.0493	0.460	-2.172
H17038	FLJ25076	XM_059689	0.0011	0.461	-2.172
AI701430	MLL	NM_005933	0.0056	0.462	-2.166
NM_007038	ADAMTS5	NM_007038	0.0203	0.462	-2.165
BF060767	ADAMTS5	NM_007038	0.0099	0.462	-2.164
NM_014391	ANKRD1	NM_014391	0.0139	0.462	-2.163
AA527587	ZNF498	NM_145115	0.0094	0.463	-2.158
NM_014830	ZBTB39	NM_014830	0.0046	0.464	-2.157
NM_006322	TUBGCP3	NM_006322	0.0013	0.464	-2.155
NM_018478	DBNDD2 /// SYS1-DBNDD2	NM_001048221	0.0001	0.465	-2.151
AL050297	R3HCC1	XM_114618	0.0172	0.465	-2.151
AU145127	FBXL7	NM_012304	0.0329	0.467	-2.143
BQ944989	STRAP	NM_007178	0.0123	0.467	-2.143
AV726956	BEX5	NM_001012978	0.0335	0.467	-2.139
N62996	ZNF70	NM_021916	0.0377	0.468	-2.137
AF087573	DFFA	NM_004401	0.0080	0.469	-2.132
AA789332	VANGL1	NM_138959	0.0015	0.469	-2.130
AI983428	COL5A1	NM_000093	0.0372	0.470	-2.130
NM_001036	RYR3	NM_001036	0.0116	0.470	-2.129
AI937060	NAV1	NM_020443	0.0440	0.470	-2.129
BE856822	C3orf39	NM_032806	0.0265	0.470	-2.127
NM_000216	KAL1	NM_000216	0.0197	0.471	-2.124
AF247167	TMEM133	NM_032021	0.0058	0.471	-2.122
BG251218	RBM25	NM_021239	0.0445	0.472	-2.120
AL136932	KIAA0922	NM_015196	0.0016	0.473	-2.116
AL080170	TRIM58	NM_015431	0.0307	0.473	-2.115
AW291487	NHS	NM_198270	0.0175	0.473	-2.115
NM_024534	LOC728193	XM_001128013	0.0032	0.475	-2.104
M31159	IGFBP3	NM_000598	0.0080	0.476	-2.101

W72455	ZNF362	NM_152493	0.0068	0.476	-2.101
AA715041	MLL	NM_005933	0.0430	0.476	-2.099
BF684446	AXIN2	NM_004655	0.0237	0.477	-2.099
AA100793	LMO7	NM_005358	0.0274	0.477	-2.098
BC006118	ZKSCAN3	NM_024493	0.0479	0.477	-2.097
AF317887	CEP290	NM_025114	0.0098	0.477	-2.096
AI695695			0.0062	0.478	-2.094
NM_018238	AGK	NM_018238	0.0260	0.479	-2.087
AK021539	DSEL	NM_032160	0.0027	0.480	-2.086
NM_004494	HDGF	NM_004494	0.0001	0.480	-2.083
NM_004623	TTC4	NM_004623	0.0358	0.481	-2.081
AI684747	PXK	NM_017771	0.0493	0.482	-2.075
AF033861	ADCY3	NM_004036	0.0106	0.484	-2.066
AW044606	TTC5	NM_138376	0.0028	0.485	-2.062
BC030710	TMEM74	NM_153015	0.0076	0.485	-2.061
X79780	RAB11B	NM_004218	0.0243	0.485	-2.060
BC015881	STRA6	NM_022369	0.0239	0.486	-2.058
AK024318	USP46	NM_022832	0.0079	0.486	-2.058
AK022622	NAV1	NM_020443	0.0005	0.487	-2.055
AA020010	KLF12	NM_007249	0.0290	0.487	-2.054
NM_005756	GPR64	NM_001079858	0.0225	0.487	-2.052
AI307763	VTI1B	NM_006370	0.0170	0.489	-2.047
M29277	MCAM	NM_006500	0.0079	0.491	-2.036
NM_012342	BAMBI	NM_012342	0.0045	0.491	-2.036
AY078987	GTPBP3	NM_032620	0.0195	0.492	-2.034
BF002121			0.0252	0.492	-2.031
AI692880	GJA5	NM_005266	0.0146	0.492	-2.031
AA361361	MAP3K1	NM_005921	0.0329	0.492	-2.031
AI521273			0.0382	0.493	-2.030
AI824012	NRIP1	NM_003489	0.0041	0.493	-2.030
AK021888			0.0455	0.493	-2.028
BF513233	LOC284952	XM_001126137	0.0324	0.493	-2.027
AA214704	TNRC6B	NM_001024843	0.0094	0.494	-2.026
AI911518	GPATCH4	NM_015590	0.0241	0.494	-2.025
AW117765	PEX13	NM_002618	0.0217	0.495	-2.022
BC002671	DUSP4	NM_001394	0.0081	0.495	-2.021
BC013912	TTC26	NM_024926	0.0288	0.495	-2.021
NM_018079	SRBD1	NM_018079	0.0109	0.495	-2.021
AI200443	MAGEA5	NM_021049	0.0263	0.495	-2.020
BC002827	TPM4	NM_003290	0.0277	0.495	-2.020
NM_012460	TIMM9	NM_012460	0.0049	0.496	-2.015
BC038589			0.0123	0.497	-2.014
AK001007			0.0353	0.497	-2.011
AW002876			0.0077	0.497	-2.010
N31717	RIPK5	NM_015375	0.0208	0.498	-2.008
AW469573	FERMT2	NM_006832	0.0142	0.498	-2.008
AI183453	AARS2	NM_020745	0.0138	0.499	-2.005
W31002	ZNF498	NM_145115	0.0198	0.499	-2.004
BC038557			0.0354	0.500	-1.998
NM_014817	KIAA0644	NM_014817	0.0398	0.501	-1.998
AI130969	COL5A1	NM_000093	0.0128	0.501	-1.994
NM_018343	RIOK2	NM_018343	0.0070	0.502	-1.993
NM_022483	C5orf28	NM_022483	0.0277	0.503	-1.989
AA524029	C9orf61	NM_004816	0.0280	0.503	-1.987
BF513384			0.0096	0.504	-1.985
NM_006466	POLR3F	NM_006466	0.0144	0.504	-1.984
AA788946	COL12A1	NM_004370	0.0115	0.506	-1.976

NM_007018	CEP110		NM_007018	0.0026	0.506	-1.976
NM_021964	ZNF148		NM_021964	0.0022	0.508	-1.970
AV724192	KIAA0644		NM_014817	0.0066	0.508	-1.969
AI679268	PIK3R1		NM_181504	0.0280	0.508	-1.967
AA976778	WDR32		NM_024345	0.0045	0.509	-1.966
AI739389	SF3B1		NM_001005526	0.0312	0.510	-1.960
AL831862	TNRC6B		NM_001024843	0.0035	0.512	-1.955
AV703555				0.0101	0.513	-1.951
AI917328	WDR75		NM_032168	0.0005	0.513	-1.950
N57538	NAV1		NM_020443	0.0155	0.513	-1.949
NM_004759	MAPKAPK2		NM_004759	0.0437	0.514	-1.947
AF124145	AMFR		NM_001144	0.0054	0.514	-1.947
AI277642	CDCA7		NM_031942	0.0473	0.514	-1.945
AI471723	RBM45		NM_152945	0.0070	0.514	-1.945
NM_001784	CD97		NM_001025160	0.0158	0.514	-1.944
BF109381				0.0493	0.514	-1.944
BF446943				0.0102	0.515	-1.941
BC029425	FILIP1		NM_015687	0.0361	0.516	-1.939
AB033007	ERGIC1		NM_001031711	0.0188	0.516	-1.938
AW103422	PCBP2		NM_001098620	0.0415	0.516	-1.937
BC034621	LPGAT1		NM_014873	0.0240	0.517	-1.936
NM_014159	SETD2		NM_014159	0.0220	0.517	-1.935
AI174988				0.0189	0.518	-1.930
AF059317	RSF1		NM_016578	0.0487	0.519	-1.926
NM_018495	CALD1		NM_004342	0.0301	0.519	-1.926
NM_007066	PKIG		NM_007066	0.0192	0.519	-1.925
AU153412	OPRK1		NM_000912	0.0083	0.519	-1.925
NM_020354	ENTPD7		NM_020354	0.0294	0.520	-1.925
AI299467				0.0204	0.520	-1.924
AA580691	RBM25		NM_021239	0.0130	0.520	-1.923
AU118165	ZNF37A /// ZNF37B		NM_001007094	0.0126	0.520	-1.923
NM_000248	MITF		NM_000248	0.0101	0.520	-1.922
AI094626	OSBPL6		NM_032523	0.0385	0.521	-1.920
AB033105	KIAA1279		NM_015634	0.0030	0.523	-1.914
BE379761	STON2		NM_033104	0.0077	0.523	-1.913
NM_002402	MEST		NM_002402	0.0468	0.523	-1.913
AA765470				0.0114	0.524	-1.909
NM_016010	C8orf70		NM_016010	0.0067	0.524	-1.909
BF059479	FLJ14712		XM_001131663	0.0292	0.524	-1.909
AL512725	MIDN		NM_177401	0.0439	0.524	-1.907
AB037776	IGSF9		NM_020789	0.0016	0.524	-1.907
AI623155	TRAF3IP1		NM_015650	0.0144	0.524	-1.907
AI377688	GTF2H1		NM_005316	0.0332	0.525	-1.907
NM_022344	C17orf75		NM_022344	0.0462	0.525	-1.904
NM_001150	ANPEP		NM_001150	0.0286	0.526	-1.900
AV699825	LOC145786			0.0024	0.528	-1.895
AI525402	LPHN1		NM_001008701	0.0405	0.528	-1.894
NM_002431	MNAT1		NM_002431	0.0134	0.528	-1.894
AA504356	PCBP2		NM_001098620	0.0013	0.528	-1.894
BC005359	GMFB		NM_004124	0.0008	0.529	-1.892
AK023585	NSFL1C		NM_016143	0.0193	0.529	-1.890
NM_023008	KRI1		NM_023008	0.0420	0.529	-1.890
AB002364	ADAMTS3		NM_014243	0.0017	0.529	-1.889
NM_006227	PLTP		NM_006227	0.0422	0.530	-1.887
BE544096	UBE2Z		NM_023079	0.0096	0.530	-1.885
NM_030952	C11orf17 /// NUAK2		NM_020642	0.0145	0.532	-1.881
NM_015909	NAG		NM_015909	0.0019	0.532	-1.881

NM_016205	PDGFC	NM_016205	0.0034	0.532	-1.881
AK001574	GORASP1	NM_031899	0.0016	0.532	-1.879
NM_005414	SKIL	NM_005414	0.0116	0.532	-1.879
AW305097	OLFML1	NM_198474	0.0007	0.533	-1.878
NM_006738	AKAP13	NM_006738	0.0365	0.533	-1.877
BC000254	ACVR1B	NM_004302	0.0123	0.534	-1.874
BE676248	DEF8	NM_017702	0.0478	0.534	-1.872
BE907791	GTPBP8	NM_001008235	0.0156	0.534	-1.872
AW194766	CDK6	NM_001259	0.0154	0.535	-1.871
AW409794	FAM80B	NM_020734	0.0003	0.535	-1.869
NM_021813	BACH2	NM_021813	0.0316	0.535	-1.869
W73820	KCTD15	NM_024076	0.0163	0.537	-1.863
NM_144990	SLFNL1	NM_144990	0.0356	0.537	-1.862
AA740754	BCLAF1	NM_001077440	0.0077	0.538	-1.858
AW025928			0.0206	0.538	-1.858
BE271180			0.0187	0.539	-1.855
U79297	ANKRD46	NM_198401	0.0013	0.539	-1.855
AL578102	IL20RB	NM_144717	0.0147	0.540	-1.851
AW051349	CDK6	NM_001259	0.0160	0.540	-1.850
AK024273	COPS7B	NM_022730	0.0212	0.541	-1.850
BF197274			0.0029	0.541	-1.850
AF070571	EXT1		0.0428	0.542	-1.844
AK095622	C1orf61	NM_006365	0.0280	0.544	-1.838
AA259174	TMED5	NM_016040	0.0029	0.544	-1.837
AK094821	ATAD2B	NM_017552	0.0368	0.545	-1.836
AU144734	NASP	NM_002482	0.0247	0.545	-1.834
AA872583	SERINC2	NM_178865	0.0454	0.545	-1.834
AB028957	SATB2	NM_015265	0.0310	0.546	-1.833
AL138455	SHROOM1	NM_133456	0.0033	0.547	-1.830
AI040029	B4GALT7	NM_007255	0.0041	0.547	-1.829
NM_017745	BCOR	NM_017745	0.0260	0.547	-1.828
NM_024724	ZBTB38	NM_001080412	0.0007	0.547	-1.827
AI766311	LOC162073	NM_001034841	0.0455	0.548	-1.823
AK026220	MRPL35	NM_016622	0.0031	0.549	-1.822
AW297204	NHLRC2	NM_198514	0.0202	0.549	-1.821
BC001247	LIMA1	NM_016357	0.0040	0.550	-1.819
AW265065			0.0010	0.550	-1.818
NM_024513	FYCO1	NM_024513	0.0117	0.551	-1.815
NM_003633	ENC1	NM_003633	0.0034	0.552	-1.811
NM_024010	MTRR	NM_002454	0.0031	0.552	-1.810
U20165	BMPR2	NM_001204	0.0181	0.553	-1.810
AI219740	LSG1	NM_018385	0.0465	0.553	-1.809
N32508	GNG12	NM_018841	0.0163	0.554	-1.807
NM_005211	CSF1R	NM_005211	0.0129	0.554	-1.807
NM_017651	AHI1	NM_017651	0.0171	0.556	-1.799
AI814644	WDR22	NM_003861	0.0446	0.556	-1.798
AI917716	LOXL3	NM_032603	0.0021	0.556	-1.798
NM_018650	MARK1	NM_018650	0.0100	0.557	-1.796
NM_007173	PRSS23	NM_007173	0.0329	0.557	-1.794
AW104509	ARID2	NM_152641	0.0124	0.557	-1.794
AF117234	FLOT1	NM_005803	0.0082	0.559	-1.791
AI953362	EIF2AK4	NM_001013703	0.0304	0.560	-1.786
BF749719			0.0224	0.560	-1.786
AA905942	TEAD2	NM_003598	0.0299	0.560	-1.785
N30339	COL5A1	NM_000093	0.0107	0.561	-1.784
AB032983	PPM1H	NM_020700	0.0353	0.561	-1.783
AA207013	CLUAP1	NM_015041	0.0212	0.561	-1.782

NM_018178	GOLPH3L	NM_018178	0.0043	0.562	-1.780
BF696912	EXOC5	NM_006544	0.0140	0.562	-1.778
NM_014840	NUAK1	NM_014840	0.0068	0.564	-1.773
NM_015322	FEM1B	NM_015322	0.0308	0.565	-1.771
AI743612	FAM80B	NM_020734	0.0161	0.565	-1.771
BE083088	SSFA2	NM_006751	0.0455	0.565	-1.771
NM_004672	MAP3K6	NM_004672	0.0191	0.565	-1.770
AI796536			0.0492	0.565	-1.770
AL578583	APITD1	NM_198544	0.0305	0.565	-1.769
AF057354	MTMR1	NM_003828	0.0009	0.566	-1.767
BE963370	BCLAF1	NM_001077440	0.0176	0.566	-1.767
NM_017687	NHLRC2	NM_198514	0.0291	0.567	-1.765
AI167164	MTMR1	NM_003828	0.0053	0.567	-1.763
BM987612			0.0448	0.568	-1.761
U32645	ELF4	NM_001421	0.0013	0.569	-1.759
AW467480			0.0204	0.570	-1.756
BF526978			0.0291	0.570	-1.755
C18965			0.0404	0.570	-1.755
AW003030	SF3B1	NM_001005526	0.0137	0.570	-1.754
AF245505	MXRA5	NM_015419	0.0189	0.570	-1.754
X99268	TWIST1	NM_000474	0.0252	0.570	-1.754
AA704766	MLL	NM_005933	0.0456	0.571	-1.751
BG170743	EXOC5	NM_006544	0.0000	0.571	-1.751
AI936517	NEK1	NM_012224	0.0240	0.571	-1.750
AW117498	FOXO1	NM_002015	0.0087	0.571	-1.750
AW165979	ZNF609	NM_015042	0.0047	0.571	-1.750
BF878343	COX15	NM_004376	0.0307	0.572	-1.749
AW304871			0.0289	0.572	-1.749
NM_014478	RCP9	NM_001040647	0.0364	0.572	-1.748
NM_000633	BCL2	NM_000633	0.0474	0.573	-1.746
AW139179	FEM1B	NM_015322	0.0038	0.573	-1.744
NM_024926	TTC26	NM_024926	0.0161	0.574	-1.743
BE620457	NRP1	NM_001024628	0.0295	0.574	-1.742
BC019922	ZNF252		0.0043	0.574	-1.742
BC032757	LOC219731		0.0223	0.574	-1.742
L04282	ZNF148	NM_021964	0.0037	0.574	-1.741
AA536004	RNF169	NM_001098638	0.0076	0.575	-1.740
BF215996	MYO1B	NM_012223	0.0007	0.575	-1.739
NM_015062	PPRC1	NM_015062	0.0203	0.575	-1.739
AI807026	CBL	NM_005188	0.0438	0.575	-1.739
NM_017650	PPP1R9A	NM_017650	0.0038	0.577	-1.734
NM_024773	JMJD5	NM_024773	0.0108	0.577	-1.734
BF940043	NID1	NM_002508	0.0196	0.577	-1.733
AA977481			0.0241	0.577	-1.732
AB020719	CEP152	NM_014985	0.0348	0.578	-1.732
AF231056	ARID1A	NM_006015	0.0228	0.578	-1.731
AA551075	KCTD12	NM_138444	0.0040	0.578	-1.731
AK002174	KLHL5	NM_001007075	0.0018	0.578	-1.730
AA912476	LOC145786		0.0005	0.578	-1.730
NM_005558	LAD1	NM_005558	0.0436	0.578	-1.729
AF465843	ZAK	NM_016653	0.0062	0.578	-1.729
AI041854	SFRS15	NM_020706	0.0004	0.580	-1.725
NM_003607	CDC42BPA	NM_003607	0.0488	0.580	-1.724
AI282485	BAT1	NM_004640	0.0331	0.580	-1.723
AA777641	KIAA0157	NM_032182	0.0200	0.581	-1.722
NM_004401	DFFA	NM_004401	0.0263	0.581	-1.721
N40199	LOC729810	XM_001131395	0.0140	0.581	-1.720

N92507	HMGB1	NM_002128	0.0272	0.581	-1.720
AL033538	TTC28	XM_929318	0.0107	0.582	-1.719
AF263462	CGN	NM_020770	0.0058	0.582	-1.719
AA922068	CDK6	NM_001259	0.0035	0.582	-1.718
AW242125	USP54	NM_152586	0.0123	0.582	-1.717
AK022838			0.0317	0.583	-1.716
NM_016129	COPS4	NM_016129	0.0292	0.583	-1.716
NM_006942	SOX15	NM_006942	0.0151	0.583	-1.715
NM_007203	AKAP2 /// PALM2-AKAP2	NM_001004065	0.0303	0.583	-1.715
AB033831	PDGFC	NM_016205	0.0168	0.583	-1.715
AU146891	SMAD1	NM_001003688	0.0243	0.583	-1.714
BG054922	CCDC113	NM_014157	0.0407	0.584	-1.714
BC000822	C16orf58	NM_022744	0.0074	0.584	-1.714
AF155117	KIF21A	NM_017641	0.0164	0.584	-1.713
D42044	KIAA0090	NM_015047	0.0131	0.584	-1.713
NM_016561	BFAR	NM_016561	0.0186	0.584	-1.711
D79987	ESPL1	NM_012291	0.0243	0.584	-1.711
AI040432	TM9SF3	NM_020123	0.0067	0.585	-1.711
AV700132	SIAH1	NM_001006610	0.0364	0.585	-1.710
NM_015694	ZNF777	NM_015694	0.0280	0.585	-1.709
NM_003370	VASP	NM_001008736	0.0272	0.586	-1.708
AW055205	ARL6IP2	NM_022374	0.0483	0.586	-1.707
NM_002015	FOXO1	NM_002015	0.0073	0.586	-1.707
AI700188	ZNF30	NM_001099437	0.0214	0.586	-1.706
NM_000305	PON2	NM_000305	0.0015	0.586	-1.705
U87460	GPR37	NM_005302	0.0328	0.586	-1.705
BE878463			0.0252	0.587	-1.705
AW264082	FAM110B	NM_147189	0.0250	0.587	-1.704
BG288755			0.0184	0.587	-1.704
NM_014783	ARHGAP11A	NM_014783	0.0178	0.587	-1.704
AW264273	ZNF445	NM_181489	0.0398	0.587	-1.703
BC000761	SNAPIN	NM_012437	0.0391	0.587	-1.703
AK026898	FOXP1	NM_001012505	0.0380	0.587	-1.702
AW612461			0.0163	0.588	-1.702
U20489	PTPRO	NM_002848	0.0061	0.588	-1.702
AC004770	C11orf9	NM_013279	0.0327	0.588	-1.701
BC029890	LOC653110 /// LOC728449	XM_001128973	0.0008	0.588	-1.701
BC007934	ARMC8	NM_014154	0.0461	0.588	-1.701
BF062828	BRWD2	NM_018117	0.0477	0.588	-1.701
H43976	MORF4L2	NM_012286	0.0109	0.589	-1.699
AK026659			0.0072	0.589	-1.697
AI580162	BTBD7	NM_001002860	0.0161	0.590	-1.696
T16257	GPR37	NM_005302	0.0274	0.590	-1.696
M10943	MT1F	NM_005949	0.0343	0.590	-1.696
BF432550	MYO1B	NM_012223	0.0389	0.591	-1.693
N51597	SFRS12	NM_001077199	0.0119	0.591	-1.693
BC002836	EFCAB2	NM_032328	0.0007	0.592	-1.690
BC012090	HNRPA3	NM_194247	0.0322	0.592	-1.689
NM_018321	BXDC2	NM_018321	0.0416	0.592	-1.689
T16443	SNHG5 /// SNORD50A /// SNORD50B	NR_002743	0.0444	0.593	-1.686
BE502826			0.0095	0.593	-1.686
NM_006599	NFAT5	NM_001113178	0.0350	0.593	-1.685
AW135003			0.0188	0.594	-1.685
BG285417	SH3D19	NM_001009555	0.0156	0.594	-1.684
NM_005983	SKP2	NM_005983	0.0178	0.594	-1.684
AA037483	HIST1H2BC	NM_003526	0.0297	0.594	-1.683
AB023179	DNAJC16	NM_015291	0.0337	0.594	-1.683

AK002200	SMC4	NM_001002799	0.0112	0.595	-1.681
BF057682	C14orf131	NM_018335	0.0010	0.595	-1.680
L24521	HDGF	NM_004494	0.0122	0.596	-1.679
H97931	SPRED2	NM_181784	0.0233	0.596	-1.678
NM_024520	C2orf47	NM_024520	0.0420	0.596	-1.678
BF594371	TNRC6B	NM_001024843	0.0464	0.596	-1.678
NM_001273	CHD4	NM_001273	0.0272	0.596	-1.677
AW242920			0.0058	0.596	-1.677
NM_022838	ARMCX5	NM_022838	0.0152	0.597	-1.676
AF234161	CIZ1	NM_012127	0.0026	0.597	-1.674
NM_004523	KIF11	NM_004523	0.0124	0.598	-1.673
AI380704	BOLA3	NM_001035505	0.0350	0.598	-1.673
AK024480	LOC126917	XM_928886	0.0252	0.598	-1.673
AA535128	C11orf74	NM_138787	0.0378	0.599	-1.671
NM_002228	JUN	NM_002228	0.0150	0.599	-1.671
NM_012302	LPHN2	NM_012302	0.0236	0.599	-1.671
AW009638	LOC728377	XM_001127355	0.0202	0.599	-1.671
AI073984	IRF8	NM_002163	0.0441	0.599	-1.669
N33174			0.0351	0.600	-1.668
NM_032773	LRCH3	NM_032773	0.0200	0.600	-1.668
NM_000173	GP1BA	NM_000173	0.0261	0.600	-1.667
AV709406	TMEM125	NM_144626	0.0207	0.600	-1.667
AU149503	G3BP2	NM_012297	0.0113	0.600	-1.667
NM_025243	SLC19A3	NM_025243	0.0354	0.600	-1.667
AI628573	FGFBP3	NM_152429	0.0008	0.600	-1.666
BC017275			0.0324	0.600	-1.666
NM_018082	POLR3B	NM_018082	0.0003	0.601	-1.665
BE538424	WDR68	NM_005828	0.0226	0.601	-1.664
AF249273	BCLAF1	NM_001077440	0.0193	0.601	-1.663
AI375486	APC	NM_000038	0.0199	0.602	-1.662
AY034482	SYNCRIP	NM_006372	0.0290	0.602	-1.662
N66622			0.0197	0.602	-1.660
AL031602	MT1M	NM_176870	0.0303	0.603	-1.659
NM_001065	TNFRSF1A	NM_001065	0.0314	0.604	-1.657
AA422049	WIZ	NM_021241	0.0140	0.604	-1.656
AI375916	TCF7L2	NM_030756	0.0302	0.604	-1.656
BF576458	NCOA1	NM_003743	0.0012	0.605	-1.652
AI721172	AARS2	NM_020745	0.0328	0.605	-1.652
AW471145	PRSS23	NM_007173	0.0231	0.606	-1.651
M23254	CAPN2	NM_001748	0.0002	0.606	-1.651
AA527515	FAM86B1	NM_001083537	0.0451	0.606	-1.651
NM_025099	C17orf68	NM_025099	0.0402	0.606	-1.651
NM_005649	ZNF354A	NM_005649	0.0207	0.606	-1.651
NM_030912	TRIM8	NM_030912	0.0259	0.606	-1.650
BF436101			0.0385	0.606	-1.650
AI743109	TRIM41	NM_033549	0.0310	0.606	-1.650
AW236976	ZNF770	NM_014106	0.0113	0.606	-1.650
AI829721	LOC647859	XM_001127102	0.0131	0.606	-1.650
AI022089	CSNK2A2	NM_001896	0.0254	0.607	-1.649
BC029474			0.0337	0.607	-1.648
BI832220	C1orf53	NM_001024594	0.0382	0.607	-1.648
NM_016357	LIMA1	NM_016357	0.0065	0.607	-1.647
AI028241	DGCR8	NM_022720	0.0248	0.607	-1.647
NM_021731	C19orf28	NM_001042680	0.0089	0.608	-1.645
AF161419	ING3	NM_019071	0.0252	0.608	-1.644
U66065	GRB10	NM_001001549	0.0182	0.609	-1.643
AI498126	BTBD14B	NM_052876	0.0143	0.609	-1.643

AA121502	HEG1		NM_020733	0.0207	0.609	-1.642
AF085357	FLOT1		NM_005803	0.0230	0.610	-1.640
BC004988	FEM1A		NM_018708	0.0193	0.610	-1.639
BF242537	ALKBH8		NM_138775	0.0029	0.610	-1.638
BG250721	KLF6		NM_001008490	0.0199	0.611	-1.638
AW263497	SYTL5			0.0171	0.611	-1.638
AK025925	WDR68		NM_005828	0.0124	0.611	-1.637
W74620	HNRPD		NM_001003810	0.0393	0.612	-1.635
AL354612	TMEM48		NM_018087	0.0096	0.612	-1.635
NM_022841	RFXDC2		NM_022841	0.0156	0.612	-1.633
AI458417	LOC162073		NM_001034841	0.0341	0.613	-1.632
T79216	OTUD4		NM_001102653	0.0368	0.613	-1.632
AK000752	ERGIC1		NM_001031711	0.0322	0.613	-1.631
AI458128	CBX6		NM_014292	0.0325	0.613	-1.631
AI272805	SNX24		NM_014035	0.0420	0.613	-1.630
AA541479	MAP3K1		NM_005921	0.0075	0.614	-1.629
AW629515	VCPIP1		NM_025054	0.0018	0.614	-1.629
BG260337				0.0164	0.614	-1.628
BC010363	LINS1		NM_001040614	0.0358	0.614	-1.628
NM_004841	RASAL2		NM_004841	0.0338	0.615	-1.627
NM_003567	BCAR3		NM_003567	0.0026	0.615	-1.627
BG168471	MGLL		NM_001003794	0.0014	0.615	-1.626
AA728758	C14orf65			0.0010	0.615	-1.626
AK091107	C15orf37		NM_175898	0.0050	0.615	-1.625
NM_024658	IPO4		NM_024658	0.0066	0.616	-1.625
BF131947	WDR51B		NM_172240	0.0030	0.616	-1.624
NM_014289	CAPN6		NM_014289	0.0352	0.616	-1.624
BF439533	FLJ32810		XM_001127587	0.0189	0.616	-1.623
NM_025128	MUS81		NM_025128	0.0126	0.616	-1.623
BF196642	UBE2D2		NM_003339	0.0073	0.617	-1.622
NM_006506	RASA2		NM_006506	0.0105	0.617	-1.620
AF132818	KLF5		NM_001730	0.0001	0.618	-1.618
BG230586	SLC7A6		NM_001076785	0.0090	0.619	-1.615
R50822	LPHN3		NM_015236	0.0442	0.619	-1.615
NM_014016	SACM1L		NM_014016	0.0032	0.619	-1.614
AL567808	ZNF19 /// ZNF23		NM_006961	0.0251	0.620	-1.613
NM_004635	MAPKAPK3		NM_004635	0.0404	0.620	-1.613
NM_001982	ERBB3		NM_001005915	0.0053	0.621	-1.612
NM_012297	G3BP2		NM_012297	0.0120	0.621	-1.611
NM_002428	MMP15		NM_002428	0.0038	0.621	-1.611
NM_002310	LIFR		NM_002310	0.0417	0.621	-1.610
AF049103	SETD2		NM_014159	0.0044	0.622	-1.609
NM_018090	NECAP2		NM_018090	0.0275	0.622	-1.608
BC041094	TAF5L		NM_001025247	0.0199	0.622	-1.608
R61374	HEY1		NM_001040708	0.0108	0.622	-1.608
NM_018324	OLAH		NM_001039702	0.0486	0.622	-1.607
AF116707	KIAA1147		NM_001080392	0.0485	0.622	-1.607
AW967916				0.0017	0.622	-1.607
AK024051	LRRC41		NM_006369	0.0474	0.623	-1.606
BF184089	ZDHHC21		NM_178566	0.0256	0.623	-1.605
AI625235	C20orf199		NR_003604	0.0245	0.623	-1.604
AW576195				0.0105	0.624	-1.604
BF447954	DOCK5		NM_024940	0.0053	0.624	-1.603
AW235608	TTC9		NM_015351	0.0007	0.624	-1.602
AA706895	ADAT2		NM_182503	0.0109	0.624	-1.602
NM_018695	ERBB2IP		NM_001006600	0.0030	0.624	-1.602
AW235061	SLC1A1		NM_004170	0.0194	0.624	-1.602

AA605121			0.0212	0.625	-1.601
BF576005	FYTTD1	NM_001011537	0.0032	0.625	-1.600
AF037448	SYNCRIP	NM_006372	0.0341	0.625	-1.599
BG223334	C9orf114	NM_016390	0.0256	0.625	-1.599
AV722693	ETV6	NM_001987	0.0331	0.626	-1.598
AL038092	ZNF134	NM_003435	0.0306	0.626	-1.598
BC006236	MAG1	NM_032717	0.0034	0.626	-1.598
NM_024584	CCDC121	NM_024584	0.0462	0.627	-1.596
NM_017742	ZCCHC2	NM_017742	0.0397	0.627	-1.595
BC004995	MARVELD1	NM_031484	0.0086	0.627	-1.594
NM_004380	CREBBP	NM_001079846	0.0253	0.628	-1.594
NM_004184	WARS	NM_004184	0.0257	0.628	-1.593
AA001052	RAB12	NM_001025300	0.0095	0.628	-1.592
BE676543	ZCCHC2	NM_017742	0.0215	0.628	-1.592
NM_030672	ARHGAP28	NM_001010000	0.0426	0.628	-1.592
BF435769	LOC646214	XR_016124	0.0084	0.628	-1.591
BF064224			0.0286	0.629	-1.591
AW052119	HOMER1	NM_004272	0.0043	0.629	-1.590
BF512491			0.0331	0.629	-1.590
AF007217	TRIP11	NM_004239	0.0298	0.629	-1.589
AW294869			0.0043	0.629	-1.589
AL110209	LYPLA3	NM_012320	0.0005	0.629	-1.589
AL110131	ANKRD50	NM_020337	0.0187	0.629	-1.589
NM_016955	SEPSECS	NM_016955	0.0487	0.630	-1.588
BC031487	MGAT4A	NM_012214	0.0244	0.630	-1.588
R71157	TRIM62	NM_018207	0.0163	0.630	-1.588
BE564430			0.0009	0.630	-1.587
BF508843	KIAA0907	NM_014949	0.0322	0.630	-1.586
AI949549	FGD4	NM_139241	0.0220	0.630	-1.586
AL109658	NSFL1C	NM_016143	0.0043	0.631	-1.586
AB028980	USP24	NM_015306	0.0188	0.631	-1.586
AB011113	WDR7	NM_015285	0.0288	0.631	-1.586
AV733308	ITGA6	NM_000210	0.0228	0.631	-1.585
AB047005	MAST2	NM_015112	0.0484	0.631	-1.584
AA988769			0.0335	0.632	-1.584
U35004	MAPK8	NM_002750	0.0004	0.632	-1.583
AK026691	GUSBL2	NM_206908	0.0482	0.632	-1.583
NM_017702	DEF8	NM_017702	0.0492	0.632	-1.583
BG260069			0.0044	0.632	-1.583
BG427809	BMS1P5	NR_003611	0.0218	0.633	-1.581
AL117653	MITF	NM_000248	0.0220	0.633	-1.580
AI467947	C3orf21	NM_152531	0.0469	0.633	-1.580
NM_006717	SPIN1	NM_006717	0.0410	0.633	-1.580
AI521618	TPM1	NM_000366	0.0447	0.633	-1.579
AK027217	PDLIM5	NM_001011513	0.0493	0.633	-1.579
NM_005886	KATNB1	NM_005886	0.0067	0.633	-1.579
AA504249			0.0473	0.634	-1.579
AI016784	ZNF148	NM_021964	0.0007	0.634	-1.578
AL574660	ABCD4	NM_005050	0.0369	0.634	-1.577
NM_018087	TMEM48	NM_018087	0.0013	0.634	-1.577
AK074354	BTBD7	NM_001002860	0.0133	0.635	-1.576
NM_024772	ZMYM1	NM_024772	0.0062	0.635	-1.576
NM_002467	MYC	NM_002467	0.0159	0.635	-1.576
D87811	GATA6	NM_005257	0.0117	0.635	-1.575
BC005369	EGLN1	NM_022051	0.0344	0.636	-1.573
AI703074	TCF7L2	NM_030756	0.0309	0.636	-1.572
BE856374	USP46	NM_022832	0.0065	0.636	-1.572

U41815	NUP98	NM_005387	0.0369	0.637	-1.571
AB007830	SCARA3	NM_016240	0.0104	0.637	-1.570
AF081567	PRKRIR	NM_004705	0.0159	0.637	-1.570
NM_024790	CSPP1	NM_001077204	0.0030	0.637	-1.570
NM_003387	WIPF1	NM_001077269	0.0385	0.637	-1.569
NM_005716	GIPC1	NM_005716	0.0331	0.638	-1.569
AA417970	ZNF621	NM_001098414	0.0048	0.638	-1.568
AA609488	CHDH	NM_018397	0.0040	0.638	-1.567
BE881219	ATPAF1	NM_001042546	0.0078	0.638	-1.567
N35244	ZNF782	NM_001001662	0.0242	0.638	-1.567
BC031345			0.0398	0.638	-1.567
NM_016358	IRX4	NM_016358	0.0167	0.638	-1.566
N79601			0.0248	0.639	-1.566
AA706480	LOC286260	XM_926851	0.0288	0.639	-1.566
N21008	ZYG11B	NM_024646	0.0227	0.639	-1.565
BF574430	RAB12	NM_001025300	0.0358	0.639	-1.564
AK002110	NDUFS8	NM_002496	0.0061	0.640	-1.564
NM_032876	JUB	NM_032876	0.0368	0.640	-1.563
BE207758	ARRB1	NM_004041	0.0139	0.640	-1.563
NM_031283	TCF7L1	NM_031283	0.0431	0.640	-1.562
AK024516			0.0473	0.640	-1.562
BE000929	MSI2	NM_138962	0.0335	0.641	-1.561
AW079553			0.0098	0.641	-1.560
BQ899060			0.0453	0.641	-1.559
NM_004834	MAP4K4	NM_004834	0.0128	0.642	-1.559
NM_004353	SERPINH1	NM_001235	0.0467	0.642	-1.558
AK025567	JUB	NM_032876	0.0008	0.642	-1.557
AW102941	FARP1	NM_001001715	0.0310	0.643	-1.556
BQ433060	ZNF642	NM_198494	0.0023	0.643	-1.555
AI888256	RNF217	NM_152553	0.0026	0.643	-1.555
NM_014160	MKRN2	NM_014160	0.0223	0.644	-1.554
AI872645	DNAH5	NM_001369	0.0261	0.644	-1.554
BG036203	LOC203547	NM_001017980	0.0328	0.644	-1.554
NM_017515	SLC35F2	NM_017515	0.0018	0.644	-1.553
BC015343	LOC162073	NM_001034841	0.0380	0.645	-1.550
NM_001566	INPP4A	NM_001566	0.0320	0.645	-1.550
AA678492	C9orf100	NM_032818	0.0115	0.646	-1.549
BF696931	CCDC50	NM_174908	0.0166	0.646	-1.548
AW204088	DCP1B	NM_152640	0.0341	0.646	-1.548
AI916242	EEA1	NM_003566	0.0331	0.646	-1.547
NM_007357	COG2	NM_007357	0.0204	0.647	-1.546
BC000050	NOB1	NM_014062	0.0215	0.647	-1.545
U47635	MTMR6	NM_004685	0.0185	0.647	-1.545
AK025444	PHLDB2	NM_145753	0.0139	0.648	-1.544
BF339566	NAV1	NM_020443	0.0152	0.648	-1.543
NM_003489	NRIP1	NM_003489	0.0138	0.648	-1.542
AI660619	SLC7A6	NM_001076785	0.0346	0.649	-1.542
AA631242	RAB15	NM_198686	0.0276	0.649	-1.542
BE671084	ARHGAP26	NM_015071	0.0049	0.649	-1.541
AI743903	FLJ39051		0.0086	0.649	-1.540
AI912523	KIAA1430	NM_020827	0.0022	0.650	-1.539
BE550452	HOMER1	NM_004272	0.0055	0.650	-1.539
AA129776	SUOX	NM_000456	0.0254	0.650	-1.538
AA278233	LOC286052		0.0246	0.650	-1.538
BC000915	PDLIM1	NM_020992	0.0045	0.650	-1.538
NM_006584	CCT6B	NM_006584	0.0275	0.650	-1.538
NM_003878	GGH	NM_003878	0.0067	0.651	-1.537

AW138594	KLHL9	NM_018847	0.0350	0.651	-1.536
NM_024834	C10orf119	NM_024834	0.0156	0.651	-1.536
BF213575	EPS15	NM_001981	0.0264	0.651	-1.536
BC000251	GSK3B	NM_002093	0.0200	0.651	-1.536
AW500220	KCTD20	NM_173562	0.0106	0.651	-1.536
NM_012201	GLG1	NM_012201	0.0383	0.651	-1.535
AW029619	CKAP4	NM_006825	0.0184	0.652	-1.534
BE927772	SFRS3	NM_003017	0.0304	0.652	-1.533
AI652633			0.0414	0.652	-1.533
BE379393	C6orf132	XM_371820	0.0479	0.652	-1.533
D21851	LARS2	NM_015340	0.0188	0.652	-1.533
AL832682	PARVA	NM_018222	0.0020	0.653	-1.532
BF438203	ZXDC	NM_001040653	0.0499	0.653	-1.532
NM_000188	HK1	NM_000188	0.0348	0.653	-1.531
AA531337	CRIPAK	NM_175918	0.0324	0.654	-1.530
BC001327	IFRD2	NM_006764	0.0163	0.654	-1.530
AI743880			0.0235	0.654	-1.529
R85437	VANGL1	NM_138959	0.0044	0.654	-1.528
BC013077			0.0015	0.655	-1.528
BC040723	AFAP1L1	NM_152406	0.0216	0.655	-1.528
BC004490	FOS	NM_005252	0.0239	0.655	-1.527
AL562733	ERAL1	NM_005702	0.0341	0.655	-1.527
N58163	WDR32	NM_024345	0.0078	0.655	-1.526
BE879367	AKAP2 /// PALM2-AKAP2	NM_001004065	0.0256	0.655	-1.526
AI652645	IQSEC1	NM_014869	0.0135	0.656	-1.525
AI184512	THEM4	NM_053055	0.0167	0.656	-1.525
BU683415	KLF6	NM_001008490	0.0154	0.656	-1.524
NM_024121	TMEM185B	NR_000034	0.0092	0.657	-1.523
AI742039	OGT	NM_181672	0.0455	0.657	-1.522
AA582932	RAB15	NM_198686	0.0309	0.657	-1.522
AU157304	C3orf59	NM_178496	0.0044	0.658	-1.520
BF001312	EEF2K	NM_013302	0.0173	0.658	-1.520
BE501789	NSL1	NM_001042549	0.0253	0.658	-1.520
BE858180	PEG10	NM_001040152	0.0024	0.659	-1.519
AW952547	MDH1	NM_005917	0.0422	0.659	-1.519
AW593330			0.0038	0.659	-1.518
AA960804	LOC728613	NR_003713	0.0150	0.659	-1.518
AA481141	VAV2	NM_003371	0.0365	0.659	-1.517
NM_018117	BRWD2	NM_018117	0.0114	0.659	-1.517
AI769569	MAML2	NM_032427	0.0130	0.660	-1.516
BE552097	PWWP2A	NM_052927	0.0491	0.660	-1.516
AA148301	COMMD7	NM_001099339	0.0273	0.660	-1.516
AL046979	TNS1	NM_022648	0.0096	0.660	-1.515
AA829836	C9orf126	NM_173690	0.0123	0.660	-1.515
BC005821	PTEN	NM_000314	0.0076	0.660	-1.514
NM_012179	FBXO7	NM_001033024	0.0329	0.661	-1.514
NM_004125	GNG10 /// LOC552891	NM_001017998	0.0261	0.661	-1.513
AV704797	KIAA1549	NM_020910	0.0460	0.661	-1.513
T58129	HUNK	NM_014586	0.0330	0.662	-1.511
NM_015623	TANC2	NM_025185	0.0279	0.662	-1.511
NM_004034	ANXA7	NM_001156	0.0260	0.662	-1.511
NM_004865	TBPL1	NM_004865	0.0124	0.663	-1.509
BG286920	RSF1	NM_016578	0.0270	0.663	-1.509
AF119841	PECR	NM_018441	0.0219	0.663	-1.508
BE049621	LUC7L	NM_018032	0.0456	0.663	-1.507
AL117352	EGLN1	NM_022051	0.0300	0.664	-1.507
AA234096	MGC16121	XM_001128419	0.0406	0.664	-1.507

AK023513	SNAPC4	NM_003086	0.0417	0.664	-1.507
BG540494	AKAP2 /// PALM2-AKAP2	NM_001004065	0.0063	0.664	-1.506
AI623211	LOC645166	XM_001129441	0.0498	0.664	-1.506
AW593801			0.0466	0.664	-1.506
AI949095	FAM83H	NM_198488	0.0320	0.665	-1.505
AF272663	GPHN	NM_001024218	0.0325	0.665	-1.504
NM_014612	FAM120A	NM_014612	0.0469	0.665	-1.504
AF084513	RAD1	NM_002853	0.0319	0.665	-1.503
NM_005842	SPRY2	NM_005842	0.0349	0.666	-1.502
BE048857	VPS13B	NM_015243	0.0084	0.666	-1.501
NM_017615	NSMCE4A	NM_017615	0.0108	0.666	-1.501
AF083105	SOX13	NM_005686	0.0098	0.666	-1.501
AA741090	CALML4	NM_001031733	0.0234	0.667	-1.500
BC013132	GDAP2	NM_017686	0.0209	0.667	-1.500
AL078459	DDAH1	NM_012137	0.0028	0.667	-1.499
BG289967	RAD21	NM_006265	0.0164	0.667	-1.499
NM_024098	CCDC86	NM_024098	0.0063	0.667	-1.499
NM_001270	CHD1	NM_001270	0.0214	0.668	-1.498
AI459274	ZFR	NM_016107	0.0436	0.668	-1.497
AW469181	TMC5	NM_001105248	0.0275	0.668	-1.497
NM_001323	CST6	NM_001323	0.0449	0.669	-1.496
AA526844	MYLK	NM_005965	0.0404	0.669	-1.494
AF161528	NIP7	NM_016101	0.0346	0.670	-1.493
NM_000698	ALOX5	NM_000698	0.0347	0.670	-1.493
AI672489			0.0365	0.670	-1.492
NM_001386	DPYSL2	NM_001386	0.0123	0.671	-1.491
AI241810			0.0266	0.671	-1.491
AI807206	ZDHHC21	NM_178566	0.0164	0.671	-1.490
AI130715	CEP152	NM_014985	0.0478	0.672	-1.489
AL832823	HS3ST3B1	NM_006041	0.0270	0.672	-1.489
AI356895	RHBDD1	NM_032276	0.0174	0.672	-1.489
AA909035	COL4A2	NM_001846	0.0145	0.672	-1.488
BE549973	UBA5	NM_024818	0.0307	0.672	-1.488
AU147713	SRRM1	NM_005839	0.0119	0.672	-1.488
NM_005808	CTDSPL	NM_001008392	0.0065	0.673	-1.486
M58596	FUT4	NM_002033	0.0205	0.673	-1.486
H37943			0.0369	0.673	-1.485
AL136782	KBTBD7	NM_032138	0.0376	0.674	-1.485
U90902	TIAM1	NM_003253	0.0233	0.674	-1.483
AF305057	ENOSF1	NM_017512	0.0151	0.674	-1.483
AF020543	PPT2	XM_005155	0.0482	0.674	-1.483
AI590926	SLC35B4	NM_032826	0.0111	0.674	-1.483
AB011100	KIAA0528	NM_014802	0.0107	0.675	-1.481
AI762884			0.0306	0.675	-1.481
NM_001821	CHML	NM_001821	0.0118	0.676	-1.480
AW151538	C21orf45	NM_018944	0.0428	0.676	-1.480
NM_004504	HRB	NM_004504	0.0029	0.676	-1.480
AW195407	C10orf30	NM_001100912	0.0378	0.676	-1.479
AL045882	PCGF5	NM_032373	0.0300	0.676	-1.479
AK027737	PRMT5	NM_001039619	0.0072	0.677	-1.477
NM_001649	SHROOM2	NM_001649	0.0074	0.677	-1.477
BC003697	KCTD20	NM_173562	0.0134	0.677	-1.477
BE328496	MBNL2	NM_144778	0.0099	0.677	-1.477
BF214358	FAM76B	NM_144664	0.0393	0.677	-1.477
NM_005544	IRS1	NM_005544	0.0195	0.678	-1.475
AI680541	LIFR	NM_002310	0.0480	0.678	-1.475
AL359939	VPS54	NM_001005739	0.0055	0.678	-1.475

AF362887	TPM4		NM_003290	0.0419	0.678	-1.474
Y11162	SNORA68		NR_000012	0.0489	0.678	-1.474
AA007367	FAM109A		NM_144671	0.0047	0.678	-1.474
AA195024	LONP2		NM_031490	0.0477	0.679	-1.474
BF439282	RAPGEF2		NM_014247	0.0371	0.679	-1.472
AV721430	TCF7L2		NM_030756	0.0119	0.680	-1.471
AU152194	LOC388720 /// RPS27A		NM_002954	0.0321	0.681	-1.468
BF217861	MT1E		NM_175617	0.0321	0.681	-1.468
AF085969				0.0255	0.682	-1.467
BF197122	KIAA0090		NM_015047	0.0128	0.682	-1.466
AI708524	LOC440552			0.0213	0.682	-1.466
BG532405	C13orf1		NM_020456	0.0163	0.682	-1.466
AI400463	CTGLF3			0.0068	0.682	-1.465
BC001161	ZNF174		NM_001032292	0.0343	0.683	-1.465
N64780	ASXL1		NM_015338	0.0242	0.683	-1.465
BE221212	COL1A1		NM_000088	0.0090	0.683	-1.465
AI554467	LOC388344 /// RPL13 /// SNORD68		NM_000977	0.0302	0.683	-1.465
AK026630	C10orf84		NM_022063	0.0212	0.683	-1.464
NM_006090	CEPT1		NM_001007794	0.0277	0.683	-1.464
NM_152484	ZNF569		NM_152484	0.0221	0.684	-1.463
NM_014942	ANKRD6		NM_014942	0.0440	0.684	-1.463
U94363	GYG2		NM_001079855	0.0482	0.684	-1.463
AK001380	ASPM		NM_018136	0.0324	0.684	-1.462
AI382123	MYH10		NM_005964	0.0071	0.684	-1.462
NM_006296	VRK2		NM_006296	0.0043	0.684	-1.462
BC004234	LONP2		NM_031490	0.0168	0.685	-1.460
AL136776	MED23		NM_004830	0.0201	0.685	-1.460
NM_000951	PRRG2		NM_000951	0.0127	0.685	-1.460
AB014560	G3BP2		NM_012297	0.0475	0.685	-1.460
NM_001943	DSG2		NM_001943	0.0323	0.685	-1.460
NM_020674	CYP20A1		NM_020674	0.0266	0.685	-1.459
BF590317	CTDSPL		NM_001008392	0.0356	0.686	-1.459
BE503981				0.0473	0.686	-1.458
NM_018127	ELAC2		NM_018127	0.0067	0.687	-1.456
AF033861	ADCY3		NM_004036	0.0405	0.687	-1.456
BF058944	SCAMP1		NM_004866	0.0276	0.687	-1.455
BF001666	FBXL14		NM_152441	0.0061	0.687	-1.455
AA121673	ZNF281		NM_012482	0.0091	0.688	-1.454
AU137607	NAV2		NM_001111018	0.0474	0.688	-1.454
BF432532	TIAL1		NM_001033925	0.0280	0.688	-1.453
NM_014873	LPGAT1		NM_014873	0.0256	0.689	-1.452
BC032942	GSTCD		NM_001031720	0.0144	0.689	-1.452
NM_003144	SSR1		NM_003144	0.0203	0.689	-1.451
NM_002184	IL6ST		NM_002184	0.0155	0.689	-1.451
AU155298	CHD1		NM_001270	0.0064	0.690	-1.449
AL117518	ASXL1		NM_015338	0.0293	0.690	-1.449
NM_173709				0.0047	0.690	-1.449
AI636233	TMEM8		NM_021259	0.0464	0.691	-1.447
AI291720	DPH5		NM_001077394	0.0236	0.691	-1.447
AK024300	MGC45800		XR_017723	0.0038	0.691	-1.447
BE621259	UBE2D2		NM_003339	0.0219	0.691	-1.447
NM_006470	TRIM16 /// TRIM16L		NM_001037330	0.0320	0.691	-1.447
NM_020380	CASC5		NM_144508	0.0449	0.692	-1.446
NM_021930	RINT1		NM_021930	0.0321	0.692	-1.445
AW271106	IQGAP3		NM_178229	0.0315	0.692	-1.444
NM_012204	GTF3C4		NM_012204	0.0363	0.693	-1.444
AI694332	ARIH1		NM_005744	0.0284	0.693	-1.443

AW188170			0.0017	0.693	-1.443
AB051513	ZC3H12C	NM_033390	0.0065	0.693	-1.443
AK027737	PRMT5	NM_001039619	0.0166	0.694	-1.442
AI912190			0.0255	0.694	-1.442
AA807529	MCM5	NM_006739	0.0174	0.694	-1.442
NM_005246	FER	NM_005246	0.0030	0.694	-1.441
BF732413	SEC22C	NM_004206	0.0476	0.694	-1.441
AL122121	PAPD1	NM_018109	0.0241	0.694	-1.441
AI650892	NSUN4	NM_199044	0.0330	0.694	-1.441
BF223021	B4GALT4	NM_003778	0.0160	0.695	-1.440
AI334297	KLHDC5	NM_020782	0.0324	0.695	-1.439
NM_004901	ENTPD4	NM_004901	0.0199	0.695	-1.439
BG026723	QSER1	NM_001076786	0.0283	0.695	-1.439
AI761110	SETD2	NM_014159	0.0500	0.695	-1.438
AK022897	RECK	NM_021111	0.0343	0.695	-1.438
BG257762	CDV3	NM_017548	0.0315	0.696	-1.438
NM_006747	SIPA1	NM_006747	0.0465	0.696	-1.438
AI769587	ARHGAP27	NM_199282	0.0002	0.696	-1.436
BE892293			0.0409	0.697	-1.436
AK000776			0.0463	0.697	-1.436
AF167343	IL1RAP	NM_002182	0.0247	0.697	-1.436
AV700030	IL6R	NM_000565	0.0484	0.697	-1.435
AB032977	NAV1	NM_020443	0.0002	0.697	-1.435
AW613203	PAIP1	NM_006451	0.0067	0.697	-1.434
NM_012230	POMZP3 /// ZP3	NM_001110354	0.0339	0.698	-1.433
NM_014924	KIAA0831	NM_014924	0.0206	0.698	-1.432
BC041487			0.0168	0.698	-1.432
AI359368	LETM1	NM_012318	0.0252	0.698	-1.432
N93774	C21orf45	NM_018944	0.0183	0.698	-1.432
AF320070	EHD4	NM_139265	0.0403	0.699	-1.431
NM_024622	FASTKD1	NM_024622	0.0160	0.699	-1.431
BC000376	ZFR	NM_016107	0.0384	0.699	-1.430
AI082078	ACTN1	NM_001102	0.0152	0.699	-1.430
AI379751			0.0364	0.700	-1.429
BG289456	USP31	NM_020718	0.0423	0.700	-1.429
NM_000268	NF2	NM_000268	0.0398	0.700	-1.429
AA664258	HNRNPC	NM_001077442	0.0104	0.701	-1.427
AK001821	GNPTAB	NM_024312	0.0128	0.702	-1.425
NM_018256	WDR12	NM_018256	0.0261	0.702	-1.424
AU157049	LOC153346		0.0488	0.702	-1.424
NM_012343	NNT	NM_012343	0.0049	0.702	-1.424
AK094809	RASGRF2	NM_006909	0.0064	0.703	-1.423
BF435773	SHANK2	NM_012309	0.0223	0.703	-1.423
AW515443	NUCKS1	NM_022731	0.0219	0.703	-1.423
AK074161	SLC46A1	NM_080669	0.0072	0.703	-1.423
AA740875	GSTCD	NM_001031720	0.0498	0.703	-1.423
BF966015	ZNF18	NM_144680	0.0150	0.703	-1.423
NM_144692	C19orf55	NM_001039887	0.0222	0.703	-1.423
AW014593	GBP1	NM_002053	0.0212	0.703	-1.422
NM_016653	ZAK	NM_016653	0.0490	0.704	-1.421
U13261	METAP2	NM_006838	0.0202	0.704	-1.420
AI391443	SRFBP1	NM_152546	0.0108	0.705	-1.418
BF444916	FNDC3B	NM_022763	0.0157	0.706	-1.417
AI830698	IGF1R	NM_000875	0.0184	0.707	-1.415
AL044018	LPP	NM_005578	0.0203	0.707	-1.415
AF212224	CLK4	NM_020666	0.0051	0.707	-1.414
NM_005195	CEBPD	NM_005195	0.0061	0.707	-1.414

AJ278245	LANCL2	NM_018697	0.0104	0.707	-1.414
AL049285			0.0241	0.707	-1.414
BC002666	GBP1	NM_002053	0.0476	0.708	-1.413
AI821787			0.0381	0.708	-1.412
AA209239	ABHD6	NM_020676	0.0214	0.708	-1.412
AL031313	EIF3J /// LOC730021	NM_003758	0.0321	0.709	-1.411
AL080111	NEK7	NM_133494	0.0272	0.709	-1.411
AI049962	ZCCHC11	NM_001009881	0.0143	0.709	-1.411
AI832363			0.0305	0.710	-1.409
AI888150	PPP1R9A	NM_017650	0.0148	0.710	-1.408
BC000212	GTF3C2	NM_001035521	0.0402	0.710	-1.408
BC000853	C2orf3	NM_003203	0.0214	0.711	-1.407
NM_017555	EGLN2	NM_017555	0.0271	0.711	-1.407
AA648913	BIRC5	NM_001012270	0.0259	0.711	-1.407
D26069	CENTB2	NM_012287	0.0185	0.712	-1.405
AW001101	KIAA0368	NM_001080398	0.0137	0.712	-1.405
AL575922	SPARC	NM_003118	0.0344	0.712	-1.404
AU157155	AMOTL1	NM_130847	0.0010	0.712	-1.404
AB044661	XAB1	NM_007266	0.0235	0.712	-1.404
AA524536	LGR6	NM_001017403	0.0133	0.713	-1.403
BC004517	MRPL9	NM_031420	0.0108	0.713	-1.403
AL359571	NIN	NM_016350	0.0288	0.713	-1.403
BG105365	SKP2	NM_005983	0.0098	0.713	-1.403
AU149225	MGA	NM_001080541	0.0150	0.714	-1.401
AW009330	C13orf1	NM_020456	0.0315	0.714	-1.401
AL045513	POFUT1	NM_015352	0.0048	0.714	-1.400
NM_024657	MORC4	NM_001085354	0.0098	0.714	-1.400
AV699857	RPE	NM_006916	0.0024	0.714	-1.400
AI431597	WDR22	NM_003861	0.0096	0.715	-1.400
AK024986	PTEN	NM_000314	0.0232	0.715	-1.399
NM_018443	ZNF302	NM_001012320	0.0089	0.715	-1.399
NM_022766	CERK	NM_022766	0.0009	0.715	-1.399
NM_006800	MSL3L1	NM_006800	0.0478	0.715	-1.399
NM_003079	SMARCE1	NM_003079	0.0359	0.715	-1.399
H95263	STX2	NM_001980	0.0431	0.715	-1.398
AI674915			0.0429	0.715	-1.398
AL575509	ETS2	NM_005239	0.0121	0.715	-1.398
NM_017688	BSPRY	NM_017688	0.0185	0.715	-1.398
NM_015198	COBL	NM_015198	0.0336	0.715	-1.398
NM_014832	TBC1D4	NM_014832	0.0346	0.716	-1.397
BF515963	WARS2	NM_015836	0.0081	0.716	-1.397
AL552001	PRKAB2	NM_005399	0.0283	0.716	-1.397
AF044286	H2AFY	NM_001040158	0.0092	0.716	-1.396
AB037732	RBM27		0.0205	0.718	-1.394
NM_012338	TSPAN12	NM_012338	0.0017	0.718	-1.394
AI800609	STX17	NM_017919	0.0414	0.718	-1.393
BC004558	RTKN	NM_001015055	0.0020	0.718	-1.392
AA528140	DDIT4L	NM_145244	0.0210	0.718	-1.392
NM_016056	TMBIM4	NM_016056	0.0191	0.719	-1.392
AI346432	MINA	NM_001042533	0.0203	0.719	-1.390
AW157070	EGFR	NM_005228	0.0409	0.720	-1.389
NM_005754	G3BP1	NM_005754	0.0285	0.720	-1.389
AL046696	BMPR2	NM_001204	0.0414	0.720	-1.388
NM_001450	FHL2	NM_001039492	0.0499	0.720	-1.388
AL117643	ACVR1B	NM_004302	0.0067	0.720	-1.388
NM_005154	USP8	NM_005154	0.0150	0.721	-1.388
AK022530	DNAJC16	NM_015291	0.0440	0.721	-1.387

BC005107	C21orf105			0.0334	0.722	-1.385
NM_003630	PEX3		NM_003630	0.0184	0.724	-1.382
AU151801	C1QBP		NM_001212	0.0437	0.724	-1.382
BG168720	ZDHHC18		NM_032283	0.0030	0.724	-1.381
AV724783	PRDM2		NM_001007257	0.0376	0.724	-1.381
AL390164	GATAD2A		NM_017660	0.0303	0.725	-1.380
W93584	POLR1A		NM_015425	0.0470	0.725	-1.380
AA235202	WDR36		NM_139281	0.0419	0.725	-1.380
AA521508	ZMYM4		NM_005095	0.0172	0.725	-1.380
AA825925				0.0371	0.725	-1.379
AI935647	ARHGAP28		NM_001010000	0.0230	0.726	-1.378
AK002205	VPS54		NM_001005739	0.0212	0.726	-1.377
BC003525	MAX		NM_002382	0.0179	0.726	-1.377
BC001745	D4S234E		NM_001040101	0.0067	0.727	-1.376
N90719				0.0123	0.727	-1.376
AI167592				0.0437	0.727	-1.375
NM_005463	HNRPDL		NM_005463	0.0421	0.728	-1.375
AI160440	USP7		NM_003470	0.0088	0.729	-1.373
AA126793	HNRNPC		NM_001077442	0.0259	0.729	-1.372
BC004862	UBE2R2		NM_017811	0.0433	0.729	-1.372
AU150752	ZNF281		NM_012482	0.0117	0.730	-1.370
NM_003746	DYNLL1		NM_001037494	0.0313	0.730	-1.370
NM_016265	ZNF12		NM_006956	0.0049	0.730	-1.370
AU144413	SP3		NM_001017371	0.0326	0.730	-1.370
AA251906	METT5D1		NM_152636	0.0208	0.731	-1.369
NM_025103	IFT74		NM_001099222	0.0122	0.731	-1.368
AI707721				0.0175	0.731	-1.368
BF678497	LIN54		NM_194282	0.0115	0.731	-1.368
AI672159				0.0011	0.731	-1.368
AV700302	ZNF641		NM_152320	0.0496	0.731	-1.368
AB023215	TTLL5		NM_015072	0.0406	0.731	-1.367
NM_002398	MEIS1		NM_002398	0.0214	0.731	-1.367
NM_002533	NVL		NM_002533	0.0142	0.732	-1.366
AB007930	POGZ		NM_015100	0.0368	0.732	-1.366
AL136736	KIAA1549		NM_020910	0.0475	0.732	-1.366
NM_005077	TLE1		NM_005077	0.0240	0.733	-1.364
AI088843	C7orf30		NM_138446	0.0322	0.733	-1.364
T53175	C7orf38		NM_145111	0.0241	0.733	-1.364
BE856541	CXorf39		NM_207318	0.0081	0.733	-1.364
AW467472	APPL1		NM_012096	0.0414	0.733	-1.364
NM_016229	CYB5R2		NM_016229	0.0460	0.733	-1.364
BC004902	KIAA0947		NM_015325	0.0468	0.734	-1.363
NM_005012	ROR1		NM_001083592	0.0375	0.734	-1.363
BC004183	C10orf119		NM_024834	0.0369	0.734	-1.362
AF179221	FBXL11		NM_012308	0.0222	0.734	-1.362
BE670307				0.0286	0.735	-1.361
AJ278112	DEPDC1		NM_017779	0.0138	0.735	-1.360
BF059159	ROBO1		NM_002941	0.0128	0.736	-1.360
AU116818	FAM120A		NM_014612	0.0134	0.736	-1.359
AB051499	KIAA1712		NM_001040157	0.0356	0.736	-1.359
AA495988	C9orf5		NM_001099734	0.0381	0.736	-1.359
AI350995				0.0244	0.736	-1.359
BE620258				0.0436	0.736	-1.359
AB024703	RNF11		NM_014372	0.0389	0.737	-1.358
NM_018229	C14orf108		NM_018229	0.0209	0.737	-1.357
AU147399	CAV1		NM_001753	0.0441	0.737	-1.357
AI936976	KIAA0562		NM_014704	0.0037	0.737	-1.357

AI765051	DARS2		NM_018122	0.0320	0.737	-1.357
BF978647	GFM1		NM_024996	0.0364	0.738	-1.356
U30894	SGSH		NM_000199	0.0299	0.739	-1.354
AI571166				0.0249	0.739	-1.353
AF059318	USP47		NM_017944	0.0441	0.740	-1.352
AW204564	CREBZF		NM_001039618	0.0259	0.740	-1.352
AV724508	SDCCAG1		NM_004713	0.0491	0.741	-1.350
NM_003592	CUL1		NM_003592	0.0196	0.741	-1.349
N38985	C3orf63		NM_001112736	0.0362	0.741	-1.349
NM_006965	ZNF24		NM_006965	0.0190	0.741	-1.349
AY137580	CDC25A		NM_001789	0.0170	0.742	-1.348
BF056507	NSMAF		NM_003580	0.0202	0.742	-1.348
AI763123	ADD3		NM_001121	0.0426	0.743	-1.346
AF131850	EI24		NM_001007277	0.0191	0.743	-1.346
BF435513	RASAL2		NM_004841	0.0209	0.743	-1.346
NM_014669	NUP93		NM_014669	0.0104	0.743	-1.346
AK002054	COBLL1		NM_014900	0.0265	0.744	-1.344
BF843343				0.0281	0.745	-1.343
AK027184	BPTF		NM_004459	0.0049	0.745	-1.342
AA456955	ANKRD38		NM_181712	0.0464	0.745	-1.342
NM_019005	FLJ20323		NM_019005	0.0241	0.746	-1.341
BC038440	GALNT1		NM_020474	0.0388	0.746	-1.341
NM_004713	SDCCAG1		NM_004713	0.0136	0.746	-1.340
AK023637	AMMECR1		NM_001025580	0.0234	0.747	-1.340
NM_002901	RCN1		NM_002901	0.0029	0.747	-1.339
BC001002	TUBB		NM_178014	0.0345	0.747	-1.339
BE999967				0.0023	0.747	-1.339
BC013009	ZMYM3		NM_005096	0.0354	0.748	-1.338
BE672408				0.0332	0.748	-1.337
AI339586	ZNF420		NM_144689	0.0462	0.748	-1.337
NM_006825	CKAP4		NM_006825	0.0062	0.748	-1.337
NM_017810	ZNF434		NM_017810	0.0264	0.748	-1.337
NM_021078	GCN5L2		NM_021078	0.0249	0.748	-1.337
NM_006307	SRPX		NM_006307	0.0207	0.748	-1.337
AI742925	RAD1		NM_002853	0.0439	0.749	-1.336
BE737620	PPP1R12A		NM_002480	0.0036	0.750	-1.334
AF262027	RAD23B		NM_002874	0.0139	0.751	-1.332
AL561281	MAP4K4		NM_004834	0.0473	0.751	-1.332
AV707142	KCTD20		NM_173562	0.0244	0.751	-1.332
AI277617	FGD4		NM_139241	0.0212	0.751	-1.332
BE858199	RPL7L1		NM_198486	0.0053	0.751	-1.331
AI803633	TSR1		NM_018128	0.0159	0.751	-1.331
AI652872	EPB41L5		NM_020909	0.0068	0.752	-1.330
NM_017681	NUP62CL		NM_017681	0.0239	0.752	-1.329
D84109	RBPMS		NM_001008710	0.0423	0.752	-1.329
BC041481	FLJ35848		NM_001033659	0.0328	0.752	-1.329
AU157441	WDR32		NM_024345	0.0303	0.753	-1.328
BF062139	POLR3G		NM_006467	0.0278	0.754	-1.327
AI651265	CRKRS		NM_015083	0.0295	0.754	-1.327
AL514547	RBM12		NM_006047	0.0198	0.754	-1.327
BQ022804	LAYN		NM_178834	0.0262	0.754	-1.327
AI150690				0.0172	0.754	-1.327
AK025482	TMEM168		NM_022484	0.0433	0.754	-1.326
AK023184	KIF1B		NM_015074	0.0464	0.754	-1.326
AI744451				0.0264	0.755	-1.325
U49844	ATR		NM_001184	0.0131	0.755	-1.325
AA541758	CPNE3		NM_003909	0.0442	0.755	-1.324

H48840	FXR1	NM_001013438	0.0491	0.756	-1.323
AB020712	SEC31A	NM_001077206	0.0277	0.756	-1.322
BE503800	DDX31		0.0460	0.756	-1.322
AA973551			0.0071	0.757	-1.321
AL136872	COMMD4	NM_017828	0.0174	0.757	-1.321
U62325	APBB2	NM_173075	0.0288	0.757	-1.321
AA448956	CAMK2D	NM_001221	0.0279	0.757	-1.321
NM_004390	CTSH	NM_004390	0.0045	0.757	-1.321
NM_005134	PPP4R1	NM_001042388	0.0160	0.757	-1.321
W84421	LOC647121	NR_003955	0.0215	0.758	-1.320
AA479290			0.0355	0.758	-1.319
AB049740	FUT8	NM_004480	0.0380	0.759	-1.318
AI796010	RAD1	NM_002853	0.0095	0.759	-1.318
NM_003685	KHSRP	NM_003685	0.0360	0.759	-1.317
NM_002874	RAD23B	NM_002874	0.0080	0.759	-1.317
N24868	PIAS1	NM_016166	0.0040	0.760	-1.316
BG025078	FXR1	NM_001013438	0.0377	0.760	-1.316
AF272898	PRDM6	XM_927647	0.0128	0.760	-1.316
AB018284	EIF5B	NM_015904	0.0124	0.761	-1.314
NM_017735	TTC27	NM_017735	0.0001	0.761	-1.314
AA026388			0.0128	0.761	-1.314
AI828221	SHPRH	NM_001042683	0.0362	0.761	-1.314
AI340241	DKFZp686E2433	XM_293828	0.0488	0.762	-1.312
BF966540	PPP1R2	NM_006241	0.0337	0.762	-1.312
AA594937	COBL	NM_015198	0.0040	0.763	-1.310
NM_018844	BCAP29	NM_001008405	0.0365	0.764	-1.310
D84109	RBPMS	NM_001008710	0.0053	0.764	-1.309
BG403361			0.0138	0.764	-1.309
AI300168	ZNF746	NM_152557	0.0386	0.764	-1.309
BG341906	ARF3	NM_001659	0.0111	0.765	-1.308
AL548941	KDELC2	NM_153705	0.0123	0.765	-1.307
NM_024615	PARP8	NM_024615	0.0095	0.765	-1.307
NM_012482	ZNF281	NM_012482	0.0053	0.765	-1.307
AF268193	TBL1XR1	NM_024665	0.0255	0.766	-1.306
AV712577	ANP32B	NM_006401	0.0122	0.767	-1.304
BE250417	ZMYND11	NM_006624	0.0283	0.767	-1.304
AA551784	CARM1	NM_199141	0.0296	0.767	-1.304
AW026194	PDCD11	NM_014976	0.0385	0.768	-1.302
AF054589	MDFIC	NM_199072	0.0000	0.769	-1.301
AL136770	CLDN12	NM_012129	0.0329	0.769	-1.300
NM_006048	UBE4B	NM_001105562	0.0242	1.301	1.301
AA573502	TAP2	NM_000544	0.0024	1.303	1.303
AL527334			0.0442	1.303	1.303
AV727934			0.0255	1.304	1.304
AL117612	MAL2	NM_052886	0.0396	1.304	1.304
AL080220	C2CD3	NM_015531	0.0268	1.308	1.308
NM_001033	RRM1	NM_001033	0.0392	1.310	1.310
NM_022067	C14orf133	NM_022067	0.0408	1.311	1.311
AU145019	FRMD4B	NM_015123	0.0167	1.311	1.311
NM_000057	BLM	NM_000057	0.0047	1.314	1.314
D89678	HNRPDL	NM_005463	0.0280	1.314	1.314
AW296028			0.0197	1.314	1.314
AW270158			0.0072	1.315	1.315
AJ131244	SEC24A	NM_021982	0.0398	1.316	1.316
NM_018062	FANCL	NM_018062	0.0386	1.316	1.316
AI587307	MANEA	NM_024641	0.0002	1.318	1.318
AL573951	LOC732402 /// PTPLAD1	NM_016395	0.0075	1.318	1.318

NM_004969	IDE		NM_004969	0.0055	1.319	1.319
NM_022969	FGFR2		NM_000141	0.0115	1.320	1.320
NM_003136	SRP54		NM_003136	0.0249	1.320	1.320
BF033242	CES2		NM_003869	0.0489	1.320	1.320
NM_005667	RNF103		NM_005667	0.0174	1.321	1.321
AF052094	EPAS1		NM_001430	0.0101	1.321	1.321
NM_021140	UTX		NM_021140	0.0251	1.322	1.322
AL047650	ACBD5		NM_001042473	0.0084	1.322	1.322
NM_022445	TPK1		NM_001042482	0.0336	1.323	1.323
NM_005038	PPID		NM_005038	0.0019	1.323	1.323
AA206016				0.0406	1.325	1.325
BE503392				0.0268	1.325	1.325
BC002447	PHTF1		NM_006608	0.0281	1.326	1.326
NM_002945	RPA1		NM_002945	0.0285	1.326	1.326
AF112216	CMPK		NM_016308	0.0311	1.326	1.326
D83485	PDIA3		NM_005313	0.0338	1.326	1.326
AI624156				0.0439	1.327	1.327
AA227879				0.0405	1.327	1.327
BF055171	ACOX3		NM_001101667	0.0454	1.329	1.329
BG054844	RND3		NM_005168	0.0012	1.331	1.331
AK055438				0.0363	1.332	1.332
BG548811	ZRANB3		NM_032143	0.0133	1.333	1.333
NM_000161	GCH1		NM_000161	0.0206	1.333	1.333
AI478300	NFATC2IP		NM_032815	0.0173	1.334	1.334
NM_018318	CCDC91		NM_018318	0.0425	1.334	1.334
AV734793	ZDBF2		NM_020923	0.0192	1.336	1.336
AI889160	CABLES1		NM_001100619	0.0314	1.337	1.337
M87771	FGFR2		NM_000141	0.0310	1.338	1.338
AA886888				0.0376	1.338	1.338
AF210057	C3orf1		NM_016589	0.0272	1.338	1.338
BG501219	TMEM167		NM_174909	0.0331	1.338	1.338
AA779684	BRMS1L		NM_032352	0.0122	1.339	1.339
NM_022735	ACBD3		NM_022735	0.0229	1.340	1.340
NM_002013	FKBP3		NM_002013	0.0290	1.341	1.341
AK025872	TNRC8			0.0498	1.341	1.341
AI990326	MPHOSPH9		NM_022782	0.0230	1.344	1.344
AA634272	STAT3		NM_003150	0.0228	1.345	1.345
X14174	ALPL		NM_000478	0.0098	1.345	1.345
W93554	SH3PXD2A		NM_014631	0.0347	1.346	1.346
AA129773	MAPK1		NM_002745	0.0063	1.348	1.348
NM_003330	TXNRD1		NM_001093771	0.0012	1.348	1.348
X57348	SFN		NM_006142	0.0375	1.348	1.348
BF223370				0.0357	1.349	1.349
BF516305				0.0404	1.350	1.350
BC036200	C1orf71		NM_152609	0.0171	1.350	1.350
AA843238	SLU7		NM_006425	0.0043	1.350	1.350
AF072098	TPT1		NM_003295	0.0215	1.351	1.351
NM_015542	UPF2		NM_015542	0.0411	1.352	1.352
AL110136	LOC440944		XR_017845	0.0285	1.352	1.352
NM_014711	CP110		NM_014711	0.0047	1.352	1.352
AL133267	LOC442175		XM_001130492	0.0242	1.353	1.353
NM_015986	CRLF3		NM_015986	0.0405	1.353	1.353
NM_003133	SRP9		NM_003133	0.0063	1.353	1.353
AI927993	OSBP		NM_002556	0.0117	1.355	1.355
NM_018023	YEATS2		NM_018023	0.0064	1.356	1.356
BF114745				0.0437	1.356	1.356
BG109855	SEMA5A		NM_003966	0.0322	1.356	1.356

BC001393	C2orf24	NM_015680	0.0271	1.358	1.358
H40020			0.0395	1.360	1.360
AI991996	KIAA1211	NM_020722	0.0403	1.360	1.360
AU145642	C16orf52	NM_173501	0.0468	1.361	1.361
AL031295	hCG_2003956 /// LYPLA2 /// LYPLA2P1	NM_007260	0.0395	1.362	1.362
NM_016399	TRIAP1	NM_016399	0.0480	1.362	1.362
NM_006353	HMGN4	NM_006353	0.0060	1.364	1.364
AW006290	RIOK3	NM_003831	0.0014	1.364	1.364
BE677844			0.0283	1.366	1.366
AA975427			0.0384	1.367	1.367
H09470	FLJ31958		0.0368	1.367	1.367
BC005176	TM7SF3	NM_016551	0.0075	1.368	1.368
NM_025201	PLEKHO2	NM_025201	0.0089	1.368	1.368
BG104860	CSNK1G1	NM_022048	0.0252	1.368	1.368
BG496998	FAM33A	NM_001100595	0.0138	1.369	1.369
AI949179	BCL2L11	NM_006538	0.0113	1.370	1.370
NM_017998	C9orf40	NM_017998	0.0040	1.370	1.370
NM_030801	MAGED4 /// MAGED4B	NM_001098800	0.0373	1.371	1.371
NM_006810	PDIA5	NM_006810	0.0453	1.371	1.371
NM_002318	LOXL2	NM_002318	0.0278	1.372	1.372
AI378406	EGLN3	NM_022073	0.0097	1.372	1.372
AW188940	B2M	NM_004048	0.0314	1.374	1.374
BF666293	FVT1	NM_002035	0.0106	1.374	1.374
BC001362	CNP	NM_033133	0.0205	1.375	1.375
NM_021947	SRR	NM_021947	0.0395	1.375	1.375
NM_005475	SH2B3	NM_005475	0.0243	1.376	1.376
AL542358	SLC36A4	NM_152313	0.0134	1.377	1.377
AI674647	SPPL2A	NM_032802	0.0300	1.377	1.377
BE890365	WWC2	NM_024949	0.0284	1.378	1.378
AI190287	ZNF788	XR_015208	0.0477	1.380	1.380
AK057473	LOC339260		0.0263	1.382	1.382
U62317	LMF2	NM_033200	0.0401	1.382	1.382
NM_014736	KIAA0101	NM_001029989	0.0035	1.383	1.383
AB007899	NEDD4L	NM_015277	0.0310	1.384	1.384
NM_022471	GMCL1	NM_178439	0.0426	1.384	1.384
AI807211			0.0043	1.385	1.385
NM_018639	WSB2	NM_018639	0.0146	1.385	1.385
BF540749			0.0300	1.386	1.386
BG391282			0.0257	1.387	1.387
N51717			0.0329	1.387	1.387
NM_015710	GLTSCR2	NM_015710	0.0036	1.388	1.388
NM_013257	SGK3	NM_001033578	0.0482	1.388	1.388
BE897866	ACADSB	NM_001609	0.0033	1.388	1.388
AI354864	GPC1	NM_002081	0.0299	1.388	1.388
BG537190	FTL	NM_000146	0.0001	1.393	1.393
BC005997	C1orf97	NM_032705	0.0280	1.393	1.393
NM_003610	RAE1	NM_001015885	0.0025	1.393	1.393
AI701170			0.0198	1.395	1.395
BE645144	FAM73A	NM_198549	0.0181	1.395	1.395
AV758242	CCDC111	NM_152683	0.0400	1.395	1.395
AI816243	STX12	NM_177424	0.0129	1.396	1.396
NM_016371	HSD17B7 /// HSD17B7P2 /// LOC730412	NM_016371	0.0379	1.396	1.396
AI749451	CISD2	NM_001008388	0.0382	1.396	1.396
AI831738	DDX59	NM_001031725	0.0232	1.396	1.396
BC000873	GNB4	NM_021629	0.0448	1.396	1.396
AL519710	CADM1	NM_001098517	0.0100	1.396	1.396
AB020681	ANKRD12	NM_001083625	0.0212	1.397	1.397

AF072506	ERVWE1		NM_014590	0.0172	1.400	1.400
AI032786	EDG5		NM_004230	0.0075	1.401	1.401
BU846215				0.0242	1.401	1.401
NM_012382	TTC33		NM_012382	0.0031	1.402	1.402
AI754404	PLOD2		NM_000935	0.0097	1.402	1.402
AI744083	MOSPD2		NM_152581	0.0438	1.402	1.402
AI760772	RFFL		NM_001017368	0.0233	1.403	1.403
NM_019114	EPB41L4B		NM_018424	0.0082	1.405	1.405
D85181	SC5DL		NM_001024956	0.0306	1.407	1.407
R43205	GUSBL2		NM_206908	0.0250	1.408	1.408
BC000268	PSMB2		NM_002794	0.0029	1.408	1.408
AL513583	GM2A		NM_000405	0.0359	1.408	1.408
NM_013229	APAF1		NM_001160	0.0407	1.409	1.409
AV683529	C2orf49			0.0349	1.411	1.411
BF185904	GRPEL2		NM_152407	0.0005	1.411	1.411
AI627666	FCHO2		NM_138782	0.0242	1.411	1.411
BC011119	SPIRE2		NM_032451	0.0136	1.412	1.412
AW504458	GNB4		NM_021629	0.0433	1.412	1.412
N51405	DXS542			0.0217	1.413	1.413
BC004185	C16orf35		NM_001039476	0.0145	1.413	1.413
NM_023948	MOSPD3		NM_001040097	0.0116	1.413	1.413
NM_024310	PLEKHF1		NM_024310	0.0226	1.415	1.415
BG284827				0.0420	1.415	1.415
AL136827	WDR37		NM_014023	0.0216	1.417	1.417
AB037793	USP35		NM_020798	0.0255	1.417	1.417
AV704232				0.0090	1.418	1.418
N51263	PHCA		NM_018367	0.0385	1.419	1.419
AB033058	DLG3		NM_020730	0.0326	1.420	1.420
BC039551				0.0473	1.422	1.422
AI307586				0.0177	1.423	1.423
D83243	NPAT		NM_002519	0.0123	1.423	1.423
M31659	SLC25A16		NM_152707	0.0319	1.428	1.428
AI355709	ZNF789		NM_001013258	0.0070	1.428	1.428
AV702692				0.0113	1.429	1.429
AF158185	POLH		NM_006502	0.0256	1.429	1.429
BF038366	TMEM97		NM_014573	0.0137	1.429	1.429
NM_152327	AK7		NM_152327	0.0362	1.430	1.430
AK001393	EFCAB2		NM_032328	0.0460	1.431	1.431
BF219240	ZNF655		NM_001009956	0.0147	1.432	1.432
NM_001755	CBFB		NM_001755	0.0022	1.433	1.433
BE256900	JMJD2B		NM_015015	0.0320	1.435	1.435
NM_001294	CLPTM1		NM_001294	0.0214	1.435	1.435
AW150236	SNX16		NM_022133	0.0151	1.437	1.437
BG035985	HMGCS1		NM_001098272	0.0166	1.438	1.438
AI341146	E2F7		NM_203394	0.0066	1.439	1.439
NM_003422	MZF1		NM_003422	0.0319	1.439	1.439
AW237290				0.0032	1.440	1.440
BC000143	ELMO2		NM_133171	0.0342	1.440	1.440
NM_004855	PIGB		NM_004855	0.0397	1.441	1.441
NM_023923	PHACTR4		NM_001048183	0.0026	1.441	1.441
NM_000617	SLC11A2		NM_000617	0.0422	1.441	1.441
AA453163	PCMTD1		NM_052937	0.0040	1.442	1.442
BF979497	SQLE		NM_003129	0.0485	1.442	1.442
NM_006564	CXCR6		NM_006564	0.0344	1.443	1.443
NM_024899	CEP76		NM_024899	0.0243	1.445	1.445
AI659800	C13orf31		NM_153218	0.0127	1.445	1.445
NM_005561	LAMP1		NM_005561	0.0024	1.446	1.446

AA653638			0.0404	1.446	1.446
BG393032	LOC641845 /// LOC647087 /// SLC13A4	NM_012450	0.0075	1.446	1.446
AL049452	LOC144874		0.0485	1.447	1.447
AV690866	SGK3	NM_001033578	0.0203	1.448	1.448
AW291187	C1orf71	NM_152609	0.0151	1.448	1.448
AW611729	CEP27	NM_018097	0.0071	1.448	1.448
NM_006493	CLN5	NM_006493	0.0309	1.449	1.449
AI148567	USP32	NM_032582	0.0186	1.449	1.449
AL534095	GPR177	NM_001002292	0.0309	1.451	1.451
AI796222			0.0476	1.457	1.457
BF223300	ENAH	NM_001008493	0.0115	1.457	1.457
BC004162	PPARA	NM_001001928	0.0384	1.457	1.457
AL534095	GPR177	NM_001002292	0.0303	1.458	1.458
AL569476	ANKRD13A	NM_033121	0.0369	1.458	1.458
AK023732	RBM41	NM_018301	0.0311	1.459	1.459
NM_018986	SH3TC1	NM_018986	0.0459	1.460	1.460
AI890529			0.0484	1.461	1.461
NM_024854	PYROXD1	NM_024854	0.0036	1.461	1.461
Y16521	CDS2	NM_003818	0.0360	1.462	1.462
AL037450	RIT1	NM_006912	0.0328	1.463	1.463
AI539710	ABCC1	NM_004996	0.0068	1.463	1.463
BC005127	ADFP	NM_001122	0.0116	1.464	1.464
AA514384	PHPT1	NM_014172	0.0295	1.465	1.465
AB050049	MCCC2	NM_022132	0.0198	1.466	1.466
AF272036	RRAGD	NM_021244	0.0220	1.467	1.467
NM_031296	RAB33B	NM_031296	0.0277	1.469	1.469
AI675308			0.0138	1.469	1.469
AA574240	LOC90826	NM_138364	0.0065	1.470	1.470
BG285017	HDGFRP3	NM_016073	0.0049	1.471	1.471
AB032261	SCD	NM_005063	0.0003	1.471	1.471
N38751	KLHL22	NM_032775	0.0230	1.471	1.471
AW084510	LSS	NM_001001438	0.0303	1.472	1.472
AF225425	SEMA6A	NM_020796	0.0008	1.472	1.472
AW444944			0.0465	1.473	1.473
AI761250	MBOAT2	NM_138799	0.0383	1.473	1.473
AK098125	RETSAT	NM_017750	0.0428	1.473	1.473
AI246590	IRAK2	NM_001570	0.0249	1.474	1.474
NM_021183	RAP2C	NM_021183	0.0213	1.475	1.475
AI140985			0.0127	1.475	1.475
NM_021729	VPS11	NM_021729	0.0460	1.476	1.476
NM_014959	CARD8	NM_014959	0.0032	1.477	1.477
NM_004688	NMI	NM_004688	0.0430	1.477	1.477
AF021834	TFPI	NM_001032281	0.0292	1.477	1.477
BC005979	UBE2B	NM_003337	0.0261	1.477	1.477
X57348	SFN	NM_006142	0.0012	1.480	1.480
AA743462			0.0114	1.480	1.480
NM_016325	ZNF274	NM_016324	0.0353	1.481	1.481
NM_001673	ASNS	NM_001673	0.0238	1.482	1.482
AB028951	CDC2L6	NM_015076	0.0399	1.485	1.485
NM_017911	FAM118A	NM_001104595	0.0013	1.485	1.485
BE645154			0.0435	1.486	1.486
AI684281	P15RS	NM_018170	0.0148	1.487	1.487
AI910842			0.0415	1.487	1.487
AA219354	HPS3	NM_032383	0.0153	1.488	1.488
BE962615	SNX3	NM_003795	0.0382	1.489	1.489
BC004419	VPS24	NM_001005753	0.0246	1.489	1.489
AI339606	C10orf88	NM_024942	0.0011	1.489	1.489

BC001282	HMGN4		NM_006353	0.0101	1.490	1.490
NM_080867	SOCS4		NM_080867	0.0093	1.492	1.492
NM_014905	GLS		NM_014905	0.0092	1.492	1.492
AW575737	CCDC32		NM_001080791	0.0477	1.493	1.493
AL049942	ZNF337		NM_015655	0.0331	1.494	1.494
NM_003692	TMEFF1		NM_003692	0.0303	1.494	1.494
AI635131	C1orf136			0.0087	1.495	1.495
AW276572	SBF2		NM_030962	0.0038	1.495	1.495
AF126181	MAGED2		NM_014599	0.0172	1.497	1.497
AF088033	VCPIP1			0.0090	1.498	1.498
BF000047				0.0234	1.498	1.498
BC000282	TMEM116		NM_138341	0.0032	1.498	1.498
NM_016061	YPEL5		NM_016061	0.0123	1.499	1.499
NM_024942	C10orf88		NM_024942	0.0311	1.500	1.500
AA460299	MLF1IP		NM_024629	0.0287	1.500	1.500
NM_007034	DNAJB4		NM_007034	0.0230	1.501	1.501
AL564683	CEBPB		NM_005194	0.0388	1.502	1.502
NM_002032	FTH1		NM_002032	0.0157	1.505	1.505
AI339732	CIAO1		NM_004804	0.0364	1.506	1.506
AI766279				0.0145	1.506	1.506
BF115203	MPP5		NM_022474	0.0123	1.506	1.506
NM_000259	MYO5A		NM_000259	0.0120	1.507	1.507
AA777752	ELOVL6			0.0049	1.511	1.511
AW993257				0.0210	1.512	1.512
AI742358	SVIP		NM_148893	0.0095	1.513	1.513
AW136032				0.0160	1.513	1.513
BG028765	LIN52		NM_001024674	0.0197	1.515	1.515
AB033024	ZNF490		NM_020714	0.0322	1.518	1.518
J04755	FTHP1			0.0034	1.519	1.519
AF016266	TNFRSF10B		NM_003842	0.0069	1.519	1.519
AL122088	LYSMD1		NM_212551	0.0462	1.519	1.519
AK092760	ZNF564		NM_144976	0.0085	1.520	1.520
NM_024498	ZNF117		NM_015852	0.0305	1.522	1.522
AF288392	C1orf26		NM_001105518	0.0397	1.522	1.522
NM_002946	RPA2		NM_002946	0.0438	1.525	1.525
AI768723	UBE2B		NM_003337	0.0091	1.526	1.526
AI800025				0.0102	1.526	1.526
AA648506	FAM149B1			0.0055	1.527	1.527
AW299507	GGPS1		NM_001037277	0.0188	1.528	1.528
AI458208				0.0228	1.530	1.530
AW592266	MYBL1		NM_001080416	0.0076	1.532	1.532
NM_004294	MTRF1		NM_004294	0.0098	1.533	1.533
NM_014665	LRRC14		NM_014665	0.0448	1.534	1.534
NM_018456	EAF2		NM_018456	0.0211	1.534	1.534
BM980001	APOL6		NM_030641	0.0447	1.534	1.534
AI625741	UBE2W		NM_001001481	0.0382	1.535	1.535
BC043596	FANCB		NM_001018113	0.0081	1.536	1.536
AW131553	C21orf86		NM_153454	0.0340	1.536	1.536
BE674103	CROT		NM_021151	0.0290	1.536	1.536
AW612407	PHF20L1		NM_016018	0.0014	1.538	1.538
NM_001935	DPP4		NM_001935	0.0203	1.538	1.538
AF098865	SQLE		NM_003129	0.0173	1.540	1.540
BE857704				0.0485	1.540	1.540
AF070448	CTSL2		NM_001333	0.0348	1.541	1.541
AI090331	PPP1R7			0.0168	1.542	1.542
BF593252	ADSSL1		NM_152328	0.0369	1.542	1.542
AW295547	WIPF2		NM_133264	0.0227	1.542	1.542

AV734646	FAM26F	NM_001010919	0.0409	1.543	1.543
AF111804	CAMTA1	NM_015215	0.0143	1.544	1.544
BE856302			0.0429	1.546	1.546
AA553722	SPIRE2	NM_032451	0.0061	1.547	1.547
NM_004260	RECQL4	NM_004260	0.0436	1.549	1.549
NM_003563	SPOP	NM_001007226	0.0430	1.550	1.550
NM_024610	HSPBAP1	NM_024610	0.0160	1.554	1.554
AW024656			0.0321	1.556	1.556
BE620598	LOC201725	NM_001008393	0.0057	1.557	1.557
AB051515	TANC1	NM_033394	0.0278	1.559	1.559
AA744682	LOC653256 /// RABL3	NM_173825	0.0077	1.561	1.561
NM_005044	PRKX	NM_005044	0.0465	1.562	1.562
NM_004431	EPHA2	NM_004431	0.0081	1.564	1.564
AI765445	BTG3	NM_006806	0.0331	1.564	1.564
AW070229	IQCK	NM_153208	0.0043	1.566	1.566
NM_005213	CSTA	NM_005213	0.0453	1.567	1.567
NM_000235	LIPA	NM_000235	0.0431	1.568	1.568
AL577866	ZNF615	NM_198480	0.0341	1.569	1.569
NM_003408	ZFP37	NM_003408	0.0209	1.570	1.570
NM_014872	ZBTB5	NM_014872	0.0180	1.570	1.570
AL365375	SIRT6	NM_016539	0.0487	1.572	1.572
AA460299	MLF1IP	NM_024629	0.0401	1.572	1.572
NM_000950	PRRG1	NM_000950	0.0123	1.574	1.574
NM_018656	SLC35E3	NM_018656	0.0262	1.575	1.575
AL133609	CCDC21	NM_022778	0.0262	1.575	1.575
AW162758			0.0261	1.575	1.575
BC038383	TMEM80	NM_001042463	0.0348	1.579	1.579
AI760332			0.0361	1.581	1.581
AK026921	SLC17A5	NM_012434	0.0206	1.583	1.583
BE217882	JHDM1D	NM_030647	0.0241	1.583	1.583
AK056852	LOC144571		0.0027	1.584	1.584
NM_000935	PLOD2	NM_000935	0.0035	1.584	1.584
BF131886	SESN2	NM_031459	0.0070	1.584	1.584
AW449169	SPOP	NM_001007226	0.0437	1.585	1.585
AF022375	VEGFA	NM_001025366	0.0087	1.587	1.587
AB041261	PNPLA8	NM_015723	0.0215	1.588	1.588
AA417878	RIT1	NM_006912	0.0175	1.589	1.589
AW188087	FLJ30428 /// LOC730024	XM_496597	0.0494	1.589	1.589
NM_014399	TSPAN13	NM_014399	0.0153	1.591	1.591
AI761561	HK2	NM_000189	0.0189	1.591	1.591
X16354	CEACAM1	NM_001024912	0.0232	1.592	1.592
NM_024810	CXorf45	NM_001039210	0.0456	1.592	1.592
AI433712	MUT	NM_000255	0.0240	1.595	1.595
AF217519	PNPLA8	NM_015723	0.0320	1.597	1.597
NM_022168	IFIH1	NM_022168	0.0305	1.597	1.597
NM_016508	CDKL3	NM_016508	0.0182	1.599	1.599
NM_004779	CNOT8	NM_004779	0.0372	1.600	1.600
AI633652			0.0475	1.600	1.600
AI962276	PCMTD1	NM_052937	0.0245	1.600	1.600
AA488687	SLC7A11	NM_014331	0.0299	1.601	1.601
NM_001107	ACYP1	NM_001107	0.0304	1.602	1.602
NM_014314	DDX58	NM_014314	0.0034	1.602	1.602
NM_021249	SNX6	NM_021249	0.0374	1.603	1.603
AI934828			0.0484	1.603	1.603
AI819043	CREB5	NM_001011666	0.0475	1.604	1.604
AW263542			0.0078	1.614	1.614
AV734646	FAM26F	NM_001010919	0.0212	1.616	1.616

AW189097			0.0073	1.616	1.616
AI335509			0.0439	1.621	1.621
AF059274	CSPG5	NM_006574	0.0361	1.622	1.622
U80737	NCOA3	NM_006534	0.0228	1.622	1.622
BG432350	C20orf108	NM_080821	0.0016	1.622	1.622
AA166617	WDR37	NM_014023	0.0202	1.623	1.623
AA992936			0.0089	1.624	1.624
NM_003447	ZNF165	NM_003447	0.0240	1.626	1.626
BC005832	KIAA0101	NM_001029989	0.0059	1.626	1.626
BC004973	STAT6	NM_003153	0.0232	1.627	1.627
AA812232	TXNIP	NM_006472	0.0305	1.627	1.627
NM_032763	MGC16142		0.0149	1.627	1.627
AL121936	BTN2A1	NM_007049	0.0500	1.627	1.627
AI928037	RUNDC3B	NM_138290	0.0134	1.630	1.630
BE562742			0.0027	1.631	1.631
N48315	PPARA	NM_001001928	0.0029	1.631	1.631
AB040883	KIAA1450	NM_020840	0.0027	1.631	1.631
NM_022840	METTL4	NM_022840	0.0150	1.632	1.632
AI263909	RHOB	NM_004040	0.0401	1.633	1.633
AL080081	DNAJB9	NM_012328	0.0060	1.633	1.633
AL031714	UBE2I	NM_003345	0.0257	1.633	1.633
AB047006	PCGF6	NM_001011663	0.0161	1.637	1.637
NM_016217	HECA	NM_016217	0.0380	1.638	1.638
AW242220	EIF4E2	NM_004846	0.0370	1.639	1.639
AW515645	FRMD4A	NM_018027	0.0088	1.639	1.639
NM_018665	DDX43	NM_018665	0.0413	1.640	1.640
NM_017917	PPP2R3C	NM_017917	0.0091	1.643	1.643
D80480	TMTC4	NM_001079669	0.0139	1.645	1.645
AI979261	LOC202451	XM_928403	0.0069	1.645	1.645
AL136944	SLC40A1	NM_014585	0.0288	1.647	1.647
NM_018336			0.0128	1.648	1.648
BE439987	GAS7	NM_003644	0.0239	1.649	1.649
AA160474	C20orf111	NM_016470	0.0140	1.650	1.650
NM_014278	HSPA4L	NM_014278	0.0364	1.650	1.650
BC001188	TFRC	NM_003234	0.0041	1.653	1.653
AF115515	C3orf33	NM_173657	0.0344	1.654	1.654
N51479	ATXN3	NM_001024631	0.0340	1.655	1.655
AB051511	SELI	NM_033505	0.0058	1.656	1.656
AU144102	SNRPE	NM_003094	0.0337	1.657	1.657
AB037741	HACE1	NM_020771	0.0013	1.658	1.658
AI335267			0.0216	1.658	1.658
AW511135	NUDT4	NM_019094	0.0245	1.658	1.658
BE880245	GNS	NM_002076	0.0286	1.659	1.659
AF060922	BNIP3L	NM_004331	0.0240	1.660	1.660
AI652845	LRRC51	NM_145309	0.0389	1.667	1.667
BE855799	KIAA1211	NM_020722	0.0292	1.668	1.668
AI978623	OBSL1	NM_015311	0.0433	1.669	1.669
AI797063	KIAA1377	NM_020802	0.0051	1.671	1.671
M80536	DPP4	NM_001935	0.0138	1.674	1.674
BF970855	MED12L	NM_053002	0.0389	1.676	1.676
AA764787	METTL4	NM_022840	0.0197	1.676	1.676
AV727336	LOC401152	NM_001001701	0.0296	1.678	1.678
AF126163	HHLA3	NM_001031693	0.0068	1.678	1.678
BC000586	SCLY	NM_016510	0.0336	1.678	1.678
NM_014762	DHCR24	NM_014762	0.0345	1.679	1.679
AW080025			0.0221	1.679	1.679
AU146105	ATXN3	NM_001024631	0.0234	1.679	1.679

AA573449	MTRF1		NM_004294	0.0230	1.682	1.682
BG028320				0.0019	1.682	1.682
D83768	UBXD6		NM_005671	0.0419	1.682	1.682
AV704962	SC4MOL		NM_001017369	0.0392	1.684	1.684
NM_006536	CLCA2		NM_006536	0.0175	1.685	1.685
BC001305	ELOVL6		NM_024090	0.0024	1.686	1.686
AA708470				0.0408	1.687	1.687
BC005247	IDI1		NM_004508	0.0015	1.688	1.688
BC034316				0.0493	1.693	1.693
AW298070				0.0297	1.695	1.695
NM_002130	HMGCS1		NM_001098272	0.0067	1.696	1.696
BC034248	NBR2		NM_005821	0.0048	1.699	1.699
NM_173503	EFCAB3		NM_173503	0.0493	1.699	1.699
AL136597	KLHL7		NM_001031710	0.0243	1.700	1.700
AA779795	TEF		NM_003216	0.0235	1.702	1.702
BE645222	ZSWIM7		NM_001042697	0.0463	1.702	1.702
NM_005896	IDH1		NM_005896	0.0263	1.702	1.702
AA083483	FTH1		NM_002032	0.0124	1.702	1.702
NM_005044	PRKX /// PRKY		NM_002760	0.0147	1.703	1.703
NM_022157	RRAGC		NM_022157	0.0063	1.704	1.704
AI972146	LOC401577		XM_379694	0.0440	1.705	1.705
NM_005346	HSPA1B		NM_005346	0.0397	1.705	1.705
NM_024589	ROGDI		NM_024589	0.0443	1.708	1.708
L14611	RORA		NM_002943	0.0062	1.709	1.709
AA628398	STARD4		NM_139164	0.0394	1.709	1.709
AF112204	ATP6V1H		NM_015941	0.0223	1.712	1.712
BC001727	ANKRD10		NM_017664	0.0275	1.713	1.713
W93847	MUC15		NM_145650	0.0454	1.713	1.713
NM_022912	REEP1		NM_022912	0.0006	1.716	1.716
NM_003620	PPM1D		NM_003620	0.0300	1.716	1.716
AA886870	ANKRD37		NM_181726	0.0444	1.718	1.718
AL359652	LOC92497		XM_931850	0.0187	1.718	1.718
NM_144707	PROM2		NM_144707	0.0109	1.719	1.719
CA313430				0.0239	1.723	1.723
Y13786	ADAM19		NM_023038	0.0246	1.723	1.723
AA284532	C9orf19		NM_022343	0.0268	1.723	1.723
AI439556	TXNIP		NM_006472	0.0024	1.725	1.725
AV686514	EMP2		NM_001424	0.0176	1.726	1.726
AW138827	TAF5		NM_006951	0.0122	1.726	1.726
NM_006350	FST		NM_006350	0.0146	1.727	1.727
NM_024094	DCC1		NM_024094	0.0079	1.728	1.728
AI863954				0.0142	1.730	1.730
AF216962	CNNM2		NM_017649	0.0478	1.733	1.733
BE550599	CACNA1D		NM_000720	0.0163	1.735	1.735
AI305170	SLC25A16		NM_152707	0.0394	1.740	1.740
AB037791	KIAA1370		NM_019600	0.0008	1.741	1.741
AI923944				0.0119	1.741	1.741
AW241813	H2AFJ		NM_018267	0.0220	1.744	1.744
AA770596	MARCKS		NM_002356	0.0297	1.746	1.746
AI273692				0.0378	1.746	1.746
AI671172	TMEM68		NM_152417	0.0270	1.746	1.746
NM_003864	SAP30		NM_003864	0.0079	1.747	1.747
AF116709	GAPDH			0.0405	1.749	1.749
AI932618				0.0490	1.752	1.752
AL049215	DST		NM_001723	0.0486	1.752	1.752
AI810767				0.0320	1.754	1.754
AI361034				0.0243	1.755	1.755

BF589251			0.0178	1.755	1.755
AI122770	FBXL20	NM_032875	0.0255	1.756	1.756
NM_001458	FLNC	NM_001458	0.0155	1.763	1.763
AL524643	TMEM198	NM_001005209	0.0180	1.763	1.763
AK002152	STAU2	NM_014393	0.0053	1.769	1.769
NM_024578	OCEL1	NM_024578	0.0011	1.773	1.773
AI925316			0.0327	1.774	1.774
NM_017729	EPS8L1	NM_017729	0.0066	1.779	1.779
AI632214			0.0190	1.779	1.779
NM_017818	WDR8	NM_017818	0.0492	1.780	1.780
AL138431	MTHFR	NM_005957	0.0210	1.780	1.780
AK023754	HES2	NM_019089	0.0414	1.784	1.784
AU145356	AGPAT5	NM_018361	0.0261	1.785	1.785
AI146450	NANP	NM_152667	0.0083	1.792	1.792
AI817041	CXCR7	NM_020311	0.0477	1.797	1.797
BC001282	HMGN4	NM_006353	0.0042	1.800	1.800
AI743092			0.0068	1.801	1.801
AI141670	FAM131A	NM_144635	0.0022	1.803	1.803
AI810669			0.0191	1.805	1.805
NM_018370	DRAM	NM_018370	0.0067	1.809	1.809
M68956	MARCKS	NM_002356	0.0457	1.814	1.814
NM_019081	KIAA0430	NM_014647	0.0222	1.815	1.815
AA649070	DKFZp667E0512		0.0266	1.820	1.820
NM_004403	DFNA5	NM_004403	0.0005	1.822	1.822
AA551090	AP1S2	NM_003916	0.0004	1.825	1.825
AL136820	FAM135A	NM_001105531	0.0089	1.826	1.826
AB040875	SLC7A11	NM_014331	0.0195	1.827	1.827
AI028528			0.0485	1.828	1.828
AF251050	TIGD7	NM_033208	0.0259	1.829	1.829
BF516341			0.0002	1.833	1.833
AA702248	UCA1		0.0285	1.837	1.837
NM_014454	SESN1	NM_014454	0.0196	1.841	1.841
NM_015385	SORBS1	NM_001034954	0.0446	1.842	1.842
NM_004772	C5orf13	NM_004772	0.0345	1.845	1.845
NM_018267	H2AFJ	NM_018267	0.0263	1.846	1.846
BC016828	ASAH1	NM_004315	0.0222	1.848	1.848
BC043594	TCTE3	NM_174910	0.0111	1.850	1.850
AI991328	CHKA	NM_001277	0.0023	1.851	1.851
BC005202	NIPSNAP3B	NM_018376	0.0488	1.852	1.852
AA573901	CCDC57 /// LOC732476	NM_198082	0.0211	1.854	1.854
NM_015515	KRT23	NM_015515	0.0106	1.855	1.855
AL132665	BNIP3L	NM_004331	0.0221	1.859	1.859
BC003073	ARHGEF10L	NM_001011722	0.0013	1.859	1.859
AV703731			0.0045	1.864	1.864
AV648364	CBX7	NM_175709	0.0482	1.872	1.872
AL558164	TMEM143	NM_018273	0.0417	1.872	1.872
AI803010			0.0062	1.875	1.875
AI014470	LOC728485	XM_001130518	0.0015	1.876	1.876
NM_005689	ABCB6	NM_005689	0.0020	1.876	1.876
NM_024090	ELOVL6	NM_024090	0.0218	1.877	1.877
AI761748	NCOA3	NM_006534	0.0002	1.881	1.881
BE858194			0.0198	1.883	1.883
AI538394	NSUN7	NM_024677	0.0067	1.889	1.889
NM_014155	ZBTB44	NM_014155	0.0420	1.890	1.890
NM_004508	IDI1	NM_004508	0.0061	1.891	1.891
AK001947	RP5-1022P6.2	NM_019593	0.0041	1.894	1.894
AF019214	HBP1	NM_012257	0.0039	1.906	1.906

NM_000389	CDKN1A	NM_000389	0.0138	1.906	1.906
H27948	MGC33894	NM_152914	0.0040	1.907	1.907
BF569051	H19	NR_002196	0.0146	1.911	1.911
NM_004849	ATG5	NM_004849	0.0373	1.913	1.913
AW241910	COL22A1	NM_152888	0.0304	1.915	1.915
NM_006763	BTG2	NM_006763	0.0101	1.917	1.917
AA401492	GNAS	NM_000516	0.0268	1.917	1.917
NM_024702	ZNF750	NM_024702	0.0135	1.921	1.921
AA776810	ZNF610	NM_173530	0.0027	1.926	1.926
AI758317			0.0149	1.926	1.926
AI817264	SP6	NM_199262	0.0056	1.931	1.931
AI242583	MYCT1	NM_025107	0.0164	1.931	1.931
BC039154	C16orf79	NM_182563	0.0281	1.932	1.932
AI817388	GNPDA2	NM_138335	0.0288	1.935	1.935
NM_018593	SLC16A10	NM_018593	0.0195	1.935	1.935
AF147782	ETV7	NM_016135	0.0035	1.937	1.937
BC024748			0.0258	1.937	1.937
AL133001	SULF2	NM_018837	0.0050	1.938	1.938
BG031897	AMN1	NM_207337	0.0221	1.938	1.938
AI553933	SLC30A1	NM_021194	0.0173	1.940	1.940
BC003177	CALCOCO1	NM_020898	0.0442	1.947	1.947
AI738556	TNFRSF10D	NM_003840	0.0050	1.947	1.947
AW006935	ATP10B	NM_025153	0.0351	1.948	1.948
AI188653	MXD1	NM_002357	0.0066	1.952	1.952
H63435	C11orf54	NM_014039	0.0094	1.959	1.959
AW235548	MYO5A	NM_000259	0.0073	1.963	1.963
NM_003234	TFRC	NM_003234	0.0001	1.964	1.964
AA502768	C5orf34	NM_198566	0.0284	1.968	1.968
BE540552	FADS1	NM_013402	0.0037	1.975	1.975
NM_018050	MANSC1	NM_018050	0.0125	1.979	1.979
NM_003151	STAT4	NM_003151	0.0167	1.986	1.986
AA669336	COCH	NM_004086	0.0074	1.989	1.989
NM_014398	LAMP3	NM_014398	0.0242	2.002	2.002
BF001786	SCML1	NM_001037535	0.0306	2.004	2.004
BF438173	FST	NM_006350	0.0180	2.009	2.009
AA811371			0.0441	2.014	2.014
NM_025001	MTHFD2L	NM_001004346	0.0021	2.016	2.016
BC040700			0.0292	2.020	2.020
AL042588	PEG3	NM_006210	0.0207	2.022	2.022
AI440495	LOC284702		0.0492	2.023	2.023
AI934569	ASAH1	NM_004315	0.0110	2.025	2.025
BE513006	PROM2	NM_144707	0.0115	2.026	2.026
M76742	CEACAM1	NM_001024912	0.0088	2.026	2.026
AL571684	LOC401152	NM_001001701	0.0158	2.029	2.029
AK096683	ZNF33B	NM_006955	0.0035	2.036	2.036
AL136680	GBP3	NM_018284	0.0265	2.040	2.040
AA135522	GPD1L	NM_015141	0.0063	2.045	2.045
BF970044			0.0035	2.047	2.047
U47674	ASAH1	NM_004315	0.0424	2.051	2.051
BG165833	FADS1	NM_013402	0.0002	2.052	2.052
AA088177	TMEM200A	NM_052913	0.0111	2.052	2.052
BF063271	GALNT3	NM_004482	0.0028	2.058	2.058
AI075407	IFIT3	NM_001031683	0.0080	2.060	2.060
AI004453	TRIML1	NM_178556	0.0385	2.062	2.062
NM_024519	FAM65A	NM_024519	0.0264	2.062	2.062
AK095151	UBR5	NM_015902	0.0068	2.065	2.065
N49935	RASSF4	NM_032023	0.0143	2.067	2.067

AF070673	SNN	NM_003498	0.0088	2.068	2.068
AI432195			0.0059	2.069	2.069
AK026736	ITGB6		0.0014	2.072	2.072
AF131801	SPG3A	NM_015915	0.0057	2.077	2.077
AB051846	RAP1A	NM_001010935	0.0397	2.080	2.080
NM_016323	HERC5	NM_016323	0.0007	2.083	2.083
AW237462	MAP7D2	NM_152780	0.0325	2.089	2.089
N21320	SLC12A6	NM_001042494	0.0293	2.089	2.089
N74607	AQP3	NM_004925	0.0333	2.089	2.089
AB037810	SIPA1L2	NM_020808	0.0017	2.094	2.094
AI650582	FAM118A	NM_001104595	0.0204	2.105	2.105
AA946876			0.0363	2.109	2.109
NM_003823	RTEL1 /// TNFRSF6B	NM_003823	0.0476	2.109	2.109
BC032952	MEX3C	NM_016626	0.0319	2.111	2.111
AL574184	HPGD	NM_000860	0.0446	2.112	2.112
AF280094	SP110	NM_004509	0.0318	2.113	2.113
BC004907	EPS8L1	NM_017729	0.0199	2.115	2.115
AA166895	NHLH2	NM_001111061	0.0005	2.126	2.126
AB037797	ARRDC3	NM_020801	0.0161	2.129	2.129
AW511227	MIB2	NM_080875	0.0425	2.131	2.131
S69232	ETFDH	NM_004453	0.0349	2.134	2.134
N22849			0.0074	2.140	2.140
AW611550	MFSD8	NM_152778	0.0030	2.145	2.145
AI884906	RNF182	NM_152737	0.0041	2.146	2.146
AI743534	ARHGAP24	NM_001025616	0.0074	2.154	2.154
AL117607	LOC203274		0.0165	2.155	2.155
NM_001277	CHKA /// LOC650122	NM_001277	0.0192	2.157	2.157
BC020812	LOC389072	NM_001080475	0.0197	2.160	2.160
NM_005410	SEPP1	NM_001085486	0.0145	2.163	2.163
U46006	CSRP2	NM_001321	0.0215	2.170	2.170
AL120021	KLHL24	NM_017644	0.0190	2.175	2.175
BF512388	C10orf58	NM_032333	0.0004	2.176	2.176
NM_024581	C6orf60	NM_001100411	0.0016	2.193	2.193
NM_017786	GOLSYN	NM_001099743	0.0069	2.193	2.193
NM_013409	FST	NM_006350	0.0341	2.195	2.195
R12665	PATL2	XR_015470	0.0163	2.197	2.197
AL109698			0.0190	2.204	2.204
AW402635	POLR2J2 /// POLR2J3 /// POLR2J4	NM_001015884	0.0271	2.206	2.206
U77914	JAG1	NM_000214	0.0077	2.207	2.207
AL512760	FADS1	NM_013402	0.0121	2.214	2.214
AW071793	MXD1	NM_002357	0.0104	2.220	2.220
NM_004509	SP110	NM_004509	0.0068	2.223	2.223
BC030754			0.0255	2.228	2.228
AI435399	SLFN5	NM_144975	0.0187	2.229	2.229
AW204518	ZNF341	NM_032819	0.0229	2.237	2.237
NM_020632	ATP6V0A4	NM_020632	0.0251	2.255	2.255
W73230	C7orf41	NM_152793	0.0143	2.262	2.262
AI991103	C5orf39	NM_001014279	0.0081	2.279	2.279
AK022852	SIPA1L2	NM_020808	0.0001	2.280	2.280
AA860341	MORN3	NM_173855	0.0308	2.284	2.284
BF109592	C11orf54	NM_014039	0.0245	2.286	2.286
BC006472	DCAKD	NM_024819	0.0351	2.293	2.293
NM_003813	ADAM21	NM_003813	0.0198	2.305	2.305
AU157271	LOC731450	XM_001133142	0.0057	2.315	2.315
U73936	JAG1	NM_000214	0.0101	2.319	2.319
AJ247087	MLCK	NM_182493	0.0061	2.321	2.321
BC005871	C10orf58	NM_032333	0.0113	2.327	2.327

AW301218	THAP9		NM_024672	0.0067	2.336	2.336
AI822125	DUSP27		NM_001080426	0.0013	2.343	2.343
NM_001321	CSRP2		NM_001321	0.0127	2.347	2.347
AA565499	NLRP7		NM_139176	0.0151	2.347	2.347
AW162015	ZNF143		NM_003442	0.0204	2.352	2.352
AW134535	CCNG2		NM_004354	0.0120	2.357	2.357
AA543084				0.0263	2.357	2.357
AL575306	H19		NR_002196	0.0296	2.400	2.400
N47725	IFIT5		NM_012420	0.0407	2.429	2.429
NM_006536	CLCA2		NM_006536	0.0276	2.450	2.450
AA400206	FAM65A		NM_024519	0.0033	2.454	2.454
AA131041	IFIT2		NM_001547	0.0418	2.456	2.456
AW293316				0.0081	2.469	2.469
AB046817	SYTL2		NM_032379	0.0114	2.469	2.469
AV716964	ATF7IP2		NM_024997	0.0262	2.484	2.484
NM_002356	MARCKS		NM_002356	0.0089	2.492	2.492
AA485440	SPHK2		NM_020126	0.0334	2.506	2.506
AI827820	MBD2		NM_003927	0.0034	2.525	2.525
W57613				0.0318	2.532	2.532
Z98884	CAMTA1		NM_015215	0.0026	2.542	2.542
AI890761	TMEM68		NM_152417	0.0012	2.552	2.552
NM_052889	CASP1 /// COP1		NM_001017534	0.0360	2.580	2.580
AI686890				0.0042	2.604	2.604
AW341649	TP53INP1		NM_033285	0.0189	2.610	2.610
AB051846	RAP1A		NM_001010935	0.0383	2.616	2.616
BE552414	TMEM52		NM_178545	0.0152	2.633	2.633
AI826268	SLC25A29		NM_001039355	0.0037	2.636	2.636
NM_006472	TXNIP		NM_006472	0.0087	2.636	2.636
AA911561				0.0292	2.649	2.649
BF002104	GDAP1		NM_001040875	0.0166	2.669	2.669
AI928764	LOC154761			0.0161	2.687	2.687
NM_018095	KBTBD4 /// PTPMT1		NM_016506	0.0003	2.698	2.698
BC005286	EPM2A		NM_001018041	0.0158	2.723	2.723
NM_004354	CCNG2		NM_004354	0.0359	2.762	2.762
AI572938				0.0184	2.792	2.792
NM_004780	TCEAL1		NM_001006639	0.0229	2.810	2.810
AI827820	MBD2		NM_003927	0.0066	2.824	2.824
AW474434	TNFSF10		NM_003810	0.0070	2.838	2.838
NM_024786	ZDHHC11		NM_024786	0.0054	2.851	2.851
D63807	LSS		NM_001001438	0.0037	2.891	2.891
AI348159	REEP6		NM_138393	0.0035	2.897	2.897
AI446414	KITLG		NM_000899	0.0126	2.929	2.929
AL117598				0.0244	2.957	2.957
BE268538	DENND4A		NM_005848	0.0268	2.987	2.987
NM_006746	SCML1		NM_001037535	0.0211	3.009	3.009
NM_003810	TNFSF10		NM_003810	0.0005	3.048	3.048
AI709406	MARCKS		NM_002356	0.0011	3.101	3.101
BF114815	MLCK		NM_182493	0.0008	3.112	3.112
NM_025155	PAAF1		NM_025155	0.0481	3.244	3.244
L49506	CCNG2		NM_004354	0.0033	3.344	3.344
AV720803				0.0125	3.346	3.346
NM_005670	EPM2A		NM_001018041	0.0017	3.372	3.372
BC035640	AP3B2		NM_004644	0.0010	3.401	3.401
AU156189				0.0037	3.580	3.580
AF003934	GDF15		NM_004864	0.0073	3.594	3.594
NM_024626	VTCN1		NM_024626	0.0000	3.603	3.603
AI286239	LOC440731		XM_933693	0.0000	3.699	3.699

NM_001717	BNC1	NM_001717	0.0480	3.836	3.836
NM_024703	SMPD3	NM_018667	0.0133	4.093	4.093
AI376549	MLCK	NM_182493	0.0090	4.153	4.153
AF007162	CRYAB	NM_001885	0.0043	4.560	4.560
AF267859	ZDHHC11	NM_024786	0.0242	4.590	4.590
R99291	IHPK3	NM_054111	0.0001	4.665	4.665

Supplemental Table 2. Primers used for qPCR analysis.
Table shows amplicon size and annealing temperature used for each gene in real-time quantitative RT-PCR.

	Gene	Accession Number	Forward (5'-->3')	Reverse (5'-->3')	Size (bp)	T_a (°C)
Human	CCDC88A	NM_001135597	CTC TGC CAG AAT GTA CCG AGA	ATT TAT CAG AAC GAG CAC GAG T	221	57
	CCND1	NM_053056	ACG AAG GTC TGC GCG TGT T	CCG CTG GCC ATG AAC TAC CT	320	58
	CCNG2	NM_004354	GAG CTG CCA ACG ATA CCT G	TCT AAG ATG GAA AGC ACA GTG	172	58
	CDK6	NM_001145306	CGA GTA GTG CAT CGC GAT CTA A	GGT CTT TGC CTA GTT CAT CGA T	407	58
	CDKN1A	NM_000389	CGA AGT CAG TTC CTT GTG GAG	CAT GGG TTC TGA CGG ACA T	111	57
	CRYAB	NM_001885	CAC CCA GCT GGT TTG ACA CT	TGA CAG AGA ACC TGT CCT TCT	63	57
	GDF15	NM_004864	CCG GAT ACT CAC GCC AGA	AGA GAT ACG CAG GTG CAG	63	58
	IGF1R	NM_000875	CTC AAA AGT TAT CTC CGG TCT	TTT GAC TGT GAA ATC TTC GGC TA	192	57
	IGFBP3	NM_000598	CAT CAT CAA GAA AGG GCA T	GCT GCC CAT ACT TAT CCA C	293	57
	JAG1	NM_000214	CAA ACC TTG TGT AAA CGC CAA	ACC ATT AAC CAA ATC CGG ACA	157	58
	LIFR	NM_001127671	CCC CAA CAT GAC TTG CGA CT	CTG TAT AGG CTC GCA AGA CCA	497	58
	MCAM	NM_006500	TCA AGG AGA GGA AGG TGT GG	ACT CGC TGT GGA TCT TGG TC	136	58
	MXD1	NM_001202513	GAC AGA AAA GCC GTT CAC C	CTC GTC AGA GTC GCT CAC A	228	57
	MYC	NM_002467	CCT ACC CTC TCA ACG ACA GC	CTC TGA CCT TTT GCC AGG AG	247	58
	OVOL2	NM_021220	CAC CTC AAG TGC CAC AAC CAG	TGT AGC CGC AAT CCT CGC AGA	256	58
	PTEN	NM_000314	CAC CGC CAA ATT AA TTG CAG	CCC CGA TGT AAT AAA TAT GCA CA	198	57
	PXN	NM_001080855	CTG AGC CTT CAC CCA CCG TA	CCG CTT AGG CTT CTC TTT CGT	233	58
	RPS15	NM_001018	TTC CGC AAG TTC ACC TAC C	CGG CCC GGC CAT GCT TTA CG	361	60
	SOCS2	NM_003877	TCT CTG CCA CCA TTT CGG ACA	GTC CAA TCT GAA TTT TCC GTC T	452	58
	TFPI2	NM_006528	TCT GCC AAT GTG ACT CGC TA	ATT CTA CTG GCA AAG CGA AG	179	58
	TNFSF10	NM_001190942	TAC GTG TAC TTT ACC AAC GAG	GAG TTG CCA CTT GAC TTG C	150	60
	TWIST1	NM_000474	TCA GCT ACG CCT TCT CGG TC	AGA AAG TCC ATA GTG ATG CCT T	473	58
Ovine	GAPDH	NM_001190390	TAC TGG CAA AGT GGA CAT CGT T	TTG ATG ACG AGC TTC CCG TTC	138	58
	GDF15	NM_001206298	CCG GCA GCA CCA CAT CGC TCT	TCC CAC GAG CTC CAC GCC TTC	398	60

163